Chemical Study of the Ghanaian Parasitic Plant *Thonningia sanguinea* Vahl

（ガーナ産寄生植物 *Thonningia sanguinea* Vahl の 成分に関する化学的研究）

A thesis
submitted in fulfilment of the requirements for the degree of
DOCTOR OF PHILOSOPHY

by

THOMFORD, AMA KYERAA

GRADUATE SCHOOL OF BIOMEDICAL SCIENCES
NAGASAKI UNIVERSITY, JAPAN

September, 2018

Chemical Study of the Ghanaian Parasitic Plant *Thonningia sanguinea* Vahl

（ガーナ産寄生植物 *Thonningia sanguinea* Vahl の成分に関する化学的研究）

A thesis
submitted in fulfilment of the requirements for the degree of
DOCTOR OF PHILOSOPHY
(NATURAL PRODUCT CHEMISTRY)

by

THOMFORD, AMA KYERAA

Under the Supervision of
Professor KOJI YAMADA

GRADUATE SCHOOL OF BIOMEDICAL SCIENCES
NAGASAKI UNIVERSITY, JAPAN

September, 2018

TABLE OF CONTENTS

LIST OF TABLES

LIST OF FIGURES

LIST OF ABBREVIATIONS

AP-1	Activator protein 1
br. s.	Broad singlet
cAMP	Cyclic adenosine monophosphate
cGMP	cyclic guanosine monophosphate
^{13}C NMR	Carbon-13 Nuclear magnetic resonance
C_5D_5N	Deuterated pyridine
CD_3OD	Deuterated methanol
$CDCl_3$	Deuterated chloroform
CNS	Central nervous system
COX	Cyclooxygenase
d	Doublet
dd	Doublet of doublet
DEPT	Distortion-less Enhancement by Polarization Transfer
DMSO	Dimethyl Sulfoxide
EGF	Epidermal growth factor
eNOS	Endothelial nitric oxide synthase
EtOAc	Ethyl acetate
FAB-MS	Fast atom bombardment –mass spectroscopy
FAMEs	Fatty acid methyl esters
hGSTP1-1	Human glutathione S-transferase polymorphism 1-1
^{1}H NMR	Proton-1 Nuclear magnetic resonance
HPLC	High Performance Liquid Chromatography
HSV-1	Herpes Simplex Virus Type 1
IGF-I	Insulin-like growth factor 1
iNOS	Inducible nitric oxide synthase
IR	Infrared
IL-	Interleukin

J	Coupling constant
LCB	Long chain base
LOX	Lectin-type oxidized LDL receptor
m/z	Mass to charge ratio
M	Multiplicity
m	Multiplet
MAPK	Mitogen-activated protein kinases
MeCN	Acetonitrile
MHz	Mega hertz
n	Normal
n-BuOH	*n*-butanol
NFκB	nuclear factor kappa-light-chain-enhancer of activated B cells
PPAR	Peroxisome proliferator-activated receptor
ppm	Part per million
RI	Refractive Index
RP	Reversed phase
t_R	Retention time
s	Singlet
SIRT1	Sirtuin 1 gene
t	Triplet
TLC	Thin Layer Chromatography
TNF-α	Tumour necrosis factor- α
TRPV1	Transient receptor potential cation channel subfamily V member 1
VEGF	Vascular endothelial growth factor
WHO	World Health Organisation

Chapter 1

INTRODUCTION

1.1 General Introduction

The earth is endowed with natural resources that provide us with the essentials needed for the sustenance and perpetuation of all species. For man, these resources supply the important elements, the foods we eat, and numerous traditional medical products derived from plants, animals, microbes and mineral sources used in the prevention and treatment of diseases.[1)]

The tropics and the African continent in general remain an abundant source of several plant species with medicinal properties that have been employed in the treatment of ailments for centuries. These resources have therefore become an important source of bioprospecting. Examples exists for compounds such as artemisinine, quinidine and vincristine which have parent molecules of plant origin. In the drug discovery process today, medicinal plants are essential materials in the search for newer moieties with beneficial biological actions.

Despite the widespread interest in plant resources in the search for lead molecules towards the development of newer medicines, many developing countries still rely on the crude to minimally processed products from plants. Thus, herbal and other traditional therapies are still the most accessible form of primary healthcare for majority of the population in these parts of the world.[4,5)] The relevance of such traditional knowledge in the modern drug discovery process cannot be under-emphasised.

The increasing reliance and incorporation of traditional knowledge in the drug discovery process is known to improve the lead to hit. It is known that the potential of finding a bioactive compound through random search is 1 in 10000 with 1 in 4 chances of such moieties reaching a marketable product. The odds are greatly improved in selective screening that involves some traditional knowledge on the use of the material.[6)] There is hence a growing interest in traditional knowledge and associated genetic resources, especially for global problems such as Human Immune-deficiency Virus (HIV), malaria and cancers.

Plant-based health systems will continue to play an essential role in healthcare, and their use by different cultures will evolve and expand as healthcare becomes less paternalistic and the need to provide more candidate drugs becomes more pressing.[7-9)]

1.2 Ethnoknowledge and the Drug Discovery Process

For centuries, mankind has evolved in the use of natural resources to ensure the continuity of his species. Written documents and/or oral transmission in many cultures and past civilizations on the concept of disease, well-being and general health are available. Such knowledge has been built mainly on the gradual refinement of traditional healing practices, which utilise the natural resources present in their various geographical locations for healing and disease prevention.[10)]

The unique flora of plants across the earth, and the different traditional systems of health means there is a rich source of information on the traditional uses of medicinal plants, either alone or together with other plants, animal, microbes or minerals.[11)] Ethnobotanical and ethnopharmacological knowledge of traditional herbs are a great source of information to chemists, providing lead compounds to address the various challenges in drug discovery, and as well as offering new biological targets to be exploited in drug discovery.[12)]

Well-documented ethnopharmacological information can predict compounds which are therapeutically effective in humans. For instance, it has been reported that about 80% of the 122 plant-derived compounds used as pharmaceutical drugs worldwide originate from plants with ethnomedical use similar or related to the indications for which the individual pure compounds are prescribed.[13-15)]

Medicinal plants have contributed immensely to the growing field of natural product chemistry. The numerous discoveries from natural products has also led to its acceptance as an important tool in meeting the healthcare needs of numerous societies. Hence, natural products are part of modern and effective tools for the development of new drugs as well as serving as a bank for drug templates.[16-19)] Important areas of contribution of medicinal plants include antimicrobial,[20)] antiinflammatory,[21)] antihelminthic,[22-23)] antidiabetic,[24)] and anticancer activity.[25,26)]

1.3 Medicinal Plants as Sources of Bioactive Compounds

The medicinal importance and contribution of plants to healthcare has been increasing along with the prospects and promise of isolating lead novel phytochemicals. Plants remain the dominant source of natural medicine, due to their chemical and structural diversity and their biodiversity. Several compounds have been isolated from various plant sources, from diverse geographical locations and from different parts of the plants (seeds, fruits, leaves, roots, barks, twigs etc.). These compounds have been screened for various biological activities, *in vitro* and in *vivo*, with various end points to characterise them and develop them for clinical use.[27,28)]

Many successful drugs used worldwide in clinical practice are either natural products or their derivatives. Hence, medicinal plants will continue to be a great source of new drugs or templates for enhanced biologically effective drugs in the treatment of many life-threatening diseases such as cancers, neurodegenerative diseases like Alzheimer's disease and Parkinson's disease, protozoan diseases like malaria, inflammatory and pain related diseases like rheumatoid arthritis, bronchial asthma etc.[28)]

Important examples of such drugs derived from plants include morphine, an opioid analgesic from the opium poppy *Papaver somniferum*,[29)] salicylic acid, an antiinflammatory drug from willow tree bark *Salix alba*,[30)] artemisinin, an antimalarial drug from *Artemisia annua*,[31)] digoxin, a cardiac glycoside from the leaves of *Digitalis lanata*,[32)] and reserpine, an antihypertensive drug from *Rauwolfia serpentina*.[17,33)]

1.3.1 Anticancer Agents from Plants

Cancer refers to a diverse group of diseases in which there is uncontrolled proliferation of cells as a result of the disregard for normal rules of cell division. This degree of autonomy from normal control signals leads to cancer cells developing into tumour tissues, which may eventually spread to other organs in a process referred to as metastasis. About 90% of deaths from cancer arises from metastases.[34,35)] The importance of identifying newer chemotherapeutic agents capable of use in cancer therapy is therefore paramount.

1.3.1.1 Vinca alkaloids

The vinca alkaloids: vincristine and vinblastine (Figure 1.1) originally derived from the Madagascar periwinkle *Catharanthus roseus* (Apocynaceae) as well as the vinblastine analogues: vindesine and vinorelbine are well known for their potent anticancer properties. The major importance of vinblastine and its analogues are an important part of the combinatory treatment for testicular carcinoma, Hodgkin and non-Hodgkin lymphomas, breast cancer, germ cell tumours and Kaposi sarcomas.[36,37)] The main mechanisms of vinca alkaloid cytotoxicity is reported to be due to their interactions with tubulin and disruption of microtubule function, particularly of microtubules comprising the mitotic spindle apparatus, directly causing metaphase arrest.[38)] Vincristine is also used in combinatory chemotherapy of acute lymphoblastic leukaemia's and lymphomas has been approved to treat acute leukaemia, rhabdomyosarcoma, neuroblastoma, Wilm's tumour, Hodgkin's disease and other lymphomas. It has been reported to be used in treating several non-malignant hematologic disorders such as refractory autoimmune thrombocytopenia, haemolytic uremic syndrome and thrombotic thrombocytopenia purpura.[34,37,39,40)]

1.3.1.2 Homoharringtonine

Homoharringtonine (HHT) is a natural plant alkaloid derived from *Cephalotoxus fortunei* (Figure 1.1) and has been identified by Chinese researchers as an active anticancer agent in acute myeloid leukaemia (AML), chronic myeloid leukaemia (CML), myelodysplastic syndrome (MDS), acute promyelocytic leukaemia (APL), polycythaemia vera, and as intrathecal therapy for central nervous system (CNS) leukaemia.[41,42)] HHT has a unique mechanism of action by preventing the initial elongation step of protein synthesis via an interaction with the ribosomal A-site.[43,44)] Omacetaxine mepesuccinate, a cephalotaxine ester is a semisynthetic form of HHT with excellent bioavailability by the subcutaneous route recently been approved by FDA of the United States for the treatment of CML refractory to tyrosine kinase inhibitors.[45)]

1.3.1.3 Taxol

Taxol from *Taxus brevifolia* is another drug derived from a natural product and marketed as Paclitaxel® (Figure 1.1). The product is currently used as chemotherapeutic medication for many

cancers such as the ovarian cancers, breast cancers, pancreatic cancers, non-small cell lung cancers, AIDS- related Kaposi sarcomas, cervical cancers, and pancreatic cancers. The product is also listed in the WHO's List of Essential Medicines of cytotoxic drugs.[37,46)] The antileukemic and tumour inhibitory properties of paclitaxel has been reported as inhibiting cell mitosis.[47,48)] Paclitaxel also inhibits the depolymerization of microtubules, a process necessary for normal cell division. Specifically, microtubule stabilisation by paclitaxel blocks cells in G2 and M phases of the cell cycle resulting in cell death.[49)]

1.3.1.4 Camptothecin and its Derivatives

Camptothecin is a quinoline alkaloid isolated from the bark and stems of *Camptotheca acuminata*. Its derivatives, topotecan and irinotecan are topoisomerase I inhibitors currently extensively used chemotherapy. Topotecan is used as a second-line therapy for ovarian cancer and small-cell lung cancer, while irinotecan for the treatment of including carcinomas (colon, stomach, lung, ovary, cervix), lymphomas and different childhood tumours. Their mode of action is that of binding to topoisomerase I-DNA complex, which thus prevents DNA re-ligation resulting in apoptosis via DNA damage.[50,51)]

Etoposide and teniposide (Figure 1.1) are synthetic derivatives of epipodophyllotoxins, an important class of anticancer agents occurring in the roots of *Podophyllum peltatum*. They are currently used as chemotherapy for various types of cancer, including small cell lung cancer, testicular carcinoma, lymphoma and Kaposi's sarcoma. Both derivatives work differently by inhibiting the enzyme topoisomerase II to block DNA synthesis and replication in dividing tumour cells.[37,52-54)]

1.3.2 Antiinflammatory Compounds from Plants

The use of plants for their antiinflammatory actions is one of the widest application, and one of the most explored in natural drug research. Plant derived metabolites with potent antiinflammatory properties are known to interfere directly or indirectly with the various inflammatory mediators such as the arachidonic acid metabolites, peptides, cytokines and the excitatory amino acids. These agents also inhibit the production and/or action of second messengers: cGMP, cAMP, various protein kinases, and calcium. The expression of transcription factors such as AP-1, NFκB, and

proto-oncogenes (*c-jun*, *c-fos*, and *c-myc*) is also known to be inhibited by antiinflammatory agents from plants. Aside these pathways, the expression of key pro-inflammatory molecules such as inducible NO synthase (iNOS), cyclooxygenase (COX-2), cytokines (IL-1β, TNF-α, etc.), neuropeptides and proteases are also limited by such natural products.[55,56)]

1.3.2.1 Curcumin

Curcumin (diferuloylmethane), a yellow pigment is the main ingredient of turmeric obtained from the rhizomes of the plant *Curcuma longa* (Zingiberaceae) (Figure 1.2). In Ayurvedic medicine, turmeric has been used for centuries against inflammatory disorders and to aid wound healing. Curcumin is reported as exhibiting antioxidant, anticancer and antibacterial activities via numerous mechanisms. The antiinflammatory activities of curcumin are also well documented[55)]. This compound has been reported to inhibit important proinflammatory signalling cascades, such as the NFκB-, MAPK-, COX-, and LOX-pathways.[57, 58)] Curcumin also downregulates the secretion of prominent cytokines, like TNF-α, IL-1 β, and IL-6[59)] and blocks the expression of cell adhesion molecules (e.g., ICAM-1), which are necessary for the interaction of leukocytes with endothelial cells.[60)]

1.3.2.2 Resveratrol

Resveratrol represents a stilbene derivative and phytoalexin. It is present in many different plants and their dietary products, with peanuts, grapevines, and red wine being the most prominent sources (Figure 1.2). Resveratrol has antiinflammatory, antiallergic, antioxidant, proapoptotic, chemopreventive, and antimicrobial properties.[55)] In inflammation, resveratrol inhibits the NFκB-, AP-1-, and COX-2-pathways[61-63] and activates PPAR, eNOS, and SIRT1.[64-67)] Over 40 clinical trials on resveratrol have been reported by various authors in the broad context of inflammation associated disorders, many of them dealing with diabetes, obesity, and coronary artery disease.[56)]

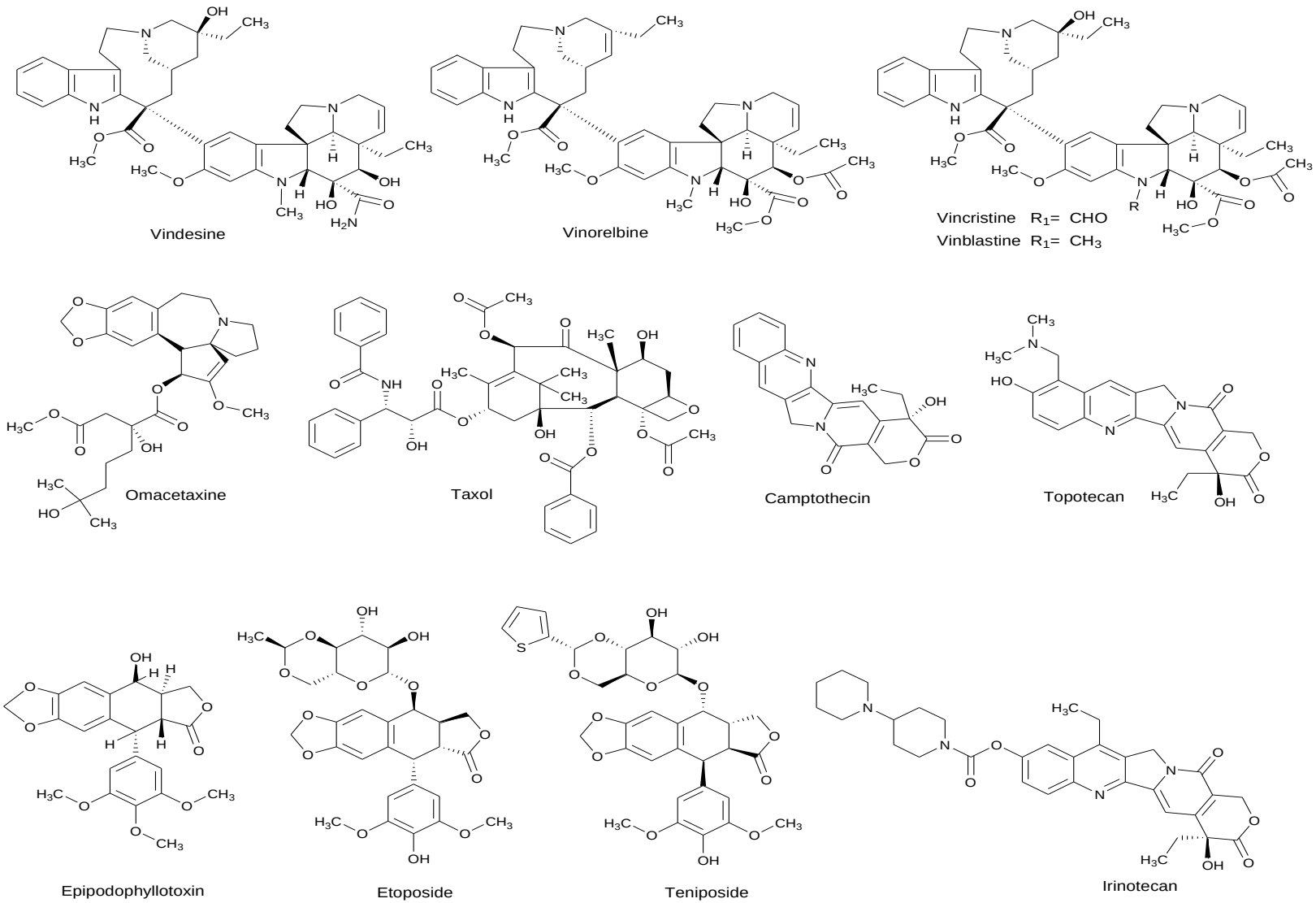

Figure 1.1 Some Anticancer Compounds from Natural Products

1.3.2.3 Capsaicin

Capsaicin is an alkaloid produced from chili peppers (*Capsicum* species; Solanaceae) and is responsible for the typical pungency of the fruits of the genus *Capsicum* (Figure 1.2). In traditional medicine, it is used as a topical rubefacient and counterirritant to relieve pain of muscles and joints. The importance of capsaicin in healthcare dates backs several centuries and even today an 8% capsaicin cutaneous patch has recently been clinically approved by the authorities in the European Union for the use against neuropathic pain in nondiabetic adults and in the US against neuropathic pain associated with post herpetic neuralgia. The transient receptor potential channel vanilloid subfamily member 1 (TRPV1), which is the direct target of capsaicin[68)] is activated by chemical and physical stimuli, such as heat, low pH, capsaicin, and certain inflammatory mediators.[69)] Prolonged activation of TRPV1 by capsaicin is reported to cause desensitization and, thus, reduced pain sensation.[70)] Capsaicin inhibits paw inflammation in arthritic rats[71)] and ethanol-induced inflammation of the gastric mucosa in rats,[72)] inhibit COX-2 activity, iNOS expression, and the NFκB pathway in macrophages in a TRPV1 independent way.[56,73)]

1.3.2.4 Epigallocatechin-3-gallate

Epigallocatechin-3-gallate (EGCG), is an ingredient of green tea, *Camellia sinensis* (Theaceae) (Figure 1.2). It is the most prominent member of the family of green tea catechins (polyphenols) and accounts for 50-80% of all catechins in a cup of green tea.[74)] EGCG was found to exert profound antiinflammatory, antioxidant, antiinfective, anticancer, antiangiogenetic, and chemopreventive effects.[74-78)] EGCG promotes cell growth arrest and induces apoptosis by affecting regulatory proteins of the cell cycle and inhibition of NFκB.[78-80)] It also inhibits growth factor-dependent signalling (e.g., of EGF, VEGF, and IGF-I), the MAPK pathway, proteasome dependent degradation, and expression of COX-2.[81,82)] Even molecular targets of EGCG have been identified. It seems to directly interact with and to modulate the character of membrane lipid rafts, which explains the ability to alter signalling processes of growth factor receptors.[83-85)]

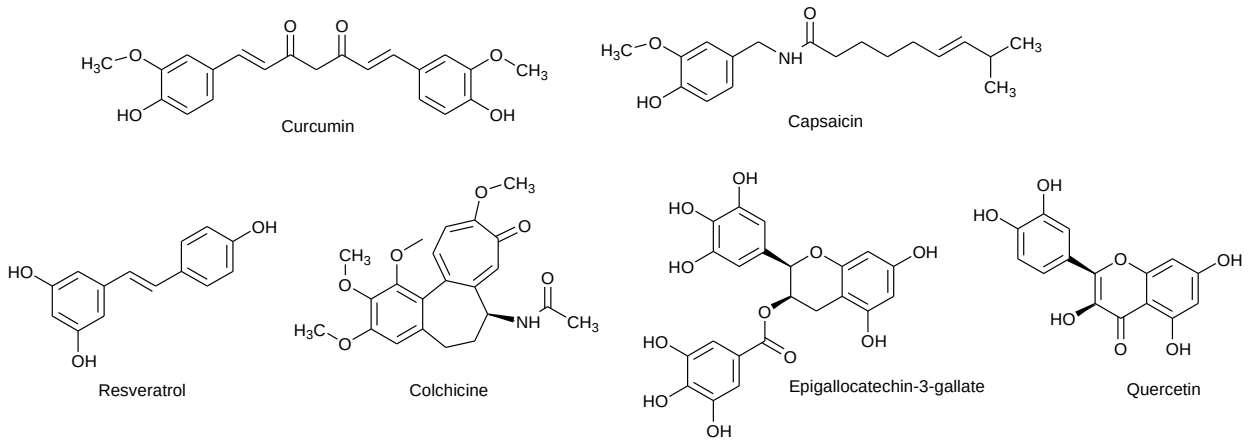

Figure 1.2 Antiinflammatory Compounds from Medicinal Plants

1.3.2.5 Quercetin

Quercetin, a yellow coloured flavonol is potent antioxidant flavonoid in onions, grapes, berries, broccoli, and citrus fruits (Figure 1.2). It is a naturally occurring auxin transport inhibitor known to possess both mast cell stabilizing and gastrointestinal cytoprotective activity. Quercetin also inhibits production of inflammation-producing enzymes COX and LOX.[86,87] and lipopolysaccharide (LPS)-induced TNF-α production in macrophages and LPS-induced IL-8 production in lung A549 cells.[88] In glial cells, quercetin can inhibit LPS-induced mRNA levels of TNF-α and IL-1α, resulting in diminished apoptotic neuronal cell death induced by microglial activation.[89] It limits LPS-induced inflammation via inhibition of Src- and Syk-mediated phosphatidylinositol-3-Kinase (PI3K)-(p85) tyrosine phosphorylation and subsequent Toll Like Receptor 4 (TLR4)/MyD88/PI3K complex formation that limits activation of downstream signalling pathways in RAW 264.7 cells.[90,91]

1.3.2.6 Colchicine

The tropolone derivative colchicine is the major alkaloid of the plant *Colchicum autumnale* (Colchicaceae), commonly known as autumn crocus or meadow saffron (Figure 1.2). In ancient folk medicine, extracts of this plant have been used against gout attacks. Interestingly, the US FDA has only recently approved colchicine for the treatment of familial Mediterranean fever as well as for the treatment and prevention of acute gout flares.

Colchicine is a microtubular inhibitor that is used in hepatobiliary disease primarily for its antifibrotic effects. Colchicine's main mechanism of action is to inhibit collagen secretion, but it can also suppress inflammation by inhibiting neutrophil migration and degranulation and promote collagen degradation by stimulating collagenase activity.[92)]

A significant number of trials have also been undertaken on the antiinflammatory effect of colchicine as an adjunct treatment in acute[93)] and recurrent pericarditis[94,95)] for the prevention of atrial fibrillation after radiofrequency ablation[96)] and for post pericardiotomy syndrome prevention.[97, 56)]

1.4 The Plant *Thonningia sanguinea* Vahl

Thonningia sanguinea Vahl, is a flowering plant in the monotypic genus *Thonningia* of the family Balanophoraceae. Synonyms for the plant include *T. angolensis, T. coccinea Mangenot, T. dubia* Hemsl., *T. elegans* Hemsl., and *T. ugandensis* Hemsl. (Figure 1.3).

1.4.1 Description of *Thonningia sanguinea* Vahl

Thonningia sanguinea Vahl is a fleshy subterranean herb growing from an underground tuber. It is a parasitic plant growing on the terminal roots of host plants such as *Hevea brasiliensis, Phoenix dactylifera* and *Theobroma cacao*.[98)] The flowering stem produces a bright red or pink inflorescence containing male and female flowers. The plant grows in Tropical Africa: from Senegal to Ethiopia, south to Angola, Zambia and Tanzania. It is commonly found in rain-forest, gallery forest and adjacent woodland.[98)] Commonly known in English as "ground pineapple", it is also known as "kwaebedwaa" in the local Akan language of Ghana. *T. sanguinea* is best known for its use in traditional medicine in many African countries.

1.4.2 Medicinal Uses of *Thonningia sanguinea* Vahl

In Ghanaian traditional medicine for instance, this plant is used in treatment of bronchial asthma sometimes for prophylaxis,[99)] sexually transmitted diseases and as an aphrodisiac. It is used to treat diarrhoea and worm infestation in Cote d'Ivoire and Congo. It is also mixed with Capsicum to produce a topical cream for treating haemorrhoids and torticollis. It is also used to treat dysentery, sore throat, skin infections, abscesses, dental caries, gingivitis, fever, malaria, heart disease, rickets, and rheumatism.[98,100,101)]

1.4.3 Chemical Constituents of *Thonningia sanguinea* Vahl

Preliminary phytochemical screening of an aqueous and hydroalcoholic flower extract of *T. sanguinea* revealed the presence of alkaloids, catechin tannins, flavonoids, saponins, quinones and polyphenols.[102)] Brevifolin carboxylic acid (BCA),[103)] gallic acid (GA)[103)] and two ellagitannins: thonningianins A (Th A) and Th B[104)] are the only four compounds reported to have been isolated from the plant (Figure 1.4).

Figure 1.3 The flower heads (a & b) and whole plant (c) of *Thonningia sanguinea*

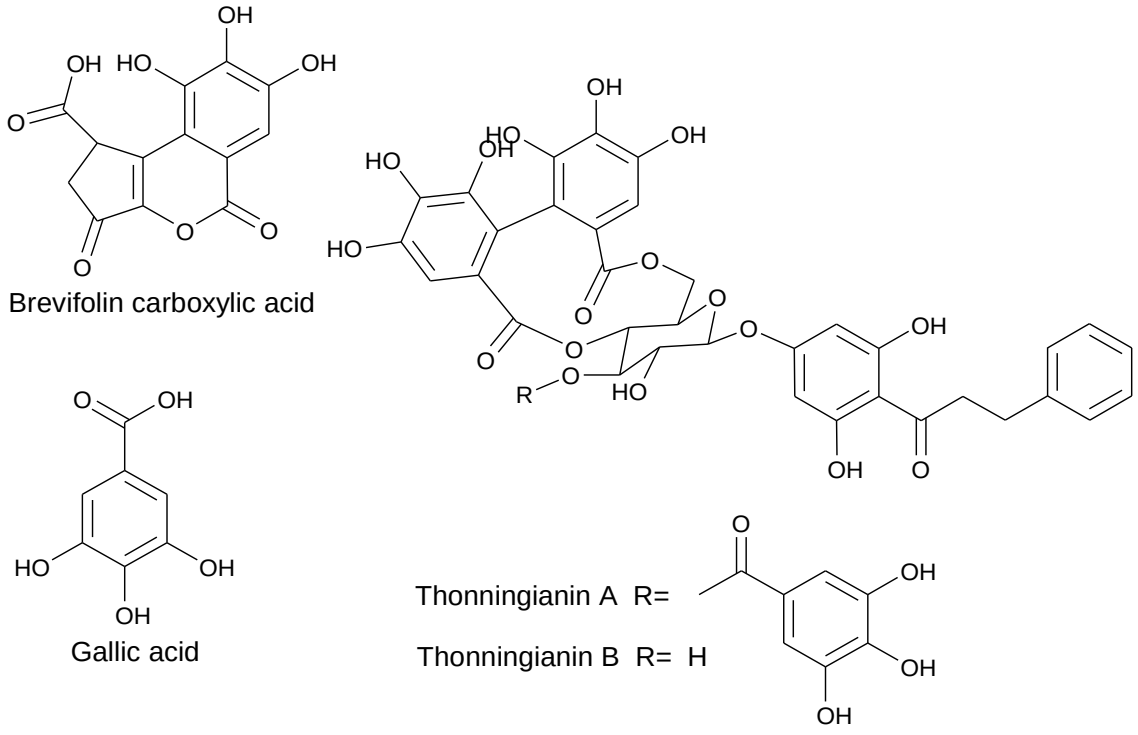

Figure 1.4 Previously isolated compounds from *Thonningia sanguinea*

1.4.4 Pharmacological studies on *Thonningia sanguinea* Vahl

N'guessan *et al*., (2007) reported that both GA and BCA, isolated from *Thonningia sanguinea* demonstrated moderate antibacterial activity against *Salmonella enteritidis, Salmonella typhimurium,* and *Salmonella abony* in the disc diffusion method, with significant antioxidant activity in the DPPH radical scavenging activity assay.[103)] GA is well known as a potent antioxidant phenolic compound, with numerous biological activities including antitumour, antimicrobial and antimelanogenic.[103)] BCA has been shown to inactivate HBsAg and inhibit hepatitis B virus replication and tumour growth.[105)]

The ellagitannins isolated from the plant also possessed hepatoprotective actions, potent antimicrobial effects[101,103,104,106)] and significant free radical scavenging activity against DPPH by ESR analysis.[104)] Th A effectively inhibited of the proliferation of HepG-2 human hepatocellular carcinoma cells by inducing apoptosis. This was observed as an increase in the sub-G1 cell population, DNA fragmentation, and increase in the content of reactive oxygen species.[107)] Th A was also shown to be a potent *in vitro* inhibitor of rat liver crude Glutathione S-transferases (GSTs) and hGSTP1-1 activity.[108)]

Biological study on *T. sanguinea* plant extracts (*in vivo* and *in vitro* assays) indicated the prophylactic potential of the aqueous extract and its *n*-butanolic fraction in bronchial asthma. The active agents extracted into *n*-butanol and may be flavonoids and/or phenolic in nature.[109)] The anticoccidial activity of the extract against *Eimeria sp.* Sporazoites,[110)] antibacterial effects against some multidrug resistant strains of *Salmonella enterica*[113)] and their effects on extended spectrum-β-Lactamases (ESBL) producing *Escherichia coli* and *Klebsiela pneumoniae* strains[100)] have been reported. The significant antimalarial effects of *T. sanguinea* root extracts against *Plasmodium falciparum* (*in vitro*)[111)], *Plasmodium berghei* and *Plasmodium chabaudi* (*in vivo*)[98)] have also been reported. The aqueous extract of *T. sanguinea* exhibited hepatoprotective activity towards a variety of different toxicants including galactosamine, carbon tetrachloride and aflatoxin B1.[99,112)] It also suppressed CYP3A2 and CYP1A2 expression at the level of transcription,[113)] protects against aflatoxin B1 acute hepatotoxicity in Fischer 344 rats[99)] and also inhibits the liver drug metabolising enzymes of rats.[114)]

1.5 Justification for the Study

The aqueous decoction of *T. sanguinea* has been used for more than thirty-five years as a mono-herbal product produced by the Centre for Plant Medicine Research, Akuapem-Mampong, Ghana (CPMR) under the registered names *CAMPA-T*® and *NINGER*®. Due to the reported clinical effectiveness of these herbal formulations at the CPMR clinic, they have been approved for use as standardised herbal medicines by the Food and Drug Authority. *CAMPA-T*® and *NINGER*® are now part of the Essential Herbal Medicines List recommended for use in pilot herbal clinics under the Integrated Herbal Medicine Services Programme in public hospitals. These *T. sanguinea*-based products are prescribed for the management of arthritic pain, sexual weakness, male and female infertility, dysmenorrhoea, amenorrhoea and uterine fibroids. Therefore, *T. sanguinea* is an important medicinal plant that is contributing immensely to public health care in Ghana.

Despite the interesting clinical usage in Ghana, as well as the reported pharmacological activities of the extracts of *T. sanguinea*, there is no detailed study on the chemical composition of the plant.

1.6 Aim of the Study

The study aimed to use a combination of biological and chemical approaches as valuable tools to investigate the chemical profile of the methanolic extract of *T. sanguinea* Vahl whole plant, to better understand these reported pharmacological activities and give credence for its use in Ghanaian traditional medicine.

1.6.1 Specific Objectives

i. Assess the antimicrobial potential of the *n*-hexane, ethyl acetate, *n*-butanol, aqueous fractions and the total crude methanolic extract of *T. sanguinea* Vahl using *Vibrio parahaemolyticus* bacterial strain.

ii. Identify and isolate compounds from the *n*-hexane and ethyl acetate fraction of the crude methanolic extract of the whole plant of *T. sanguinea* Vahl.

iii. To develop chemical standards for *T. sanguinea*-based herbal medicinal products using the chemical isolates identified from this study.

1.7 General Thesis Contents

This study was conducted as the first comprehensive chemical investigation of the parasitic plant *Thonningia sanguinea* Vahl, an important Ghanaian Traditional medicine. The plant is used currently in primary healthcare for the management of pain, infections and inflammatory conditions like bronchial asthma, arthritis, dysmenorrhea, gastroenteritis, male and female infertility.

The whole plant of *T. sanguinea* was collected from the Eastern region of Ghana. The crude methanolic extract (423 g) obtained from the powdered dry plant (3.5 kg) was partitioned between distilled water and serially extracted with *n*-hexane, ethyl acetate (EtOAc) and *n*-butanol (*n*-BuOH) solvents into the *n*-hexane (20 g), ethyl acetate (260 g) and *n*-butanol (88 g) fractions. The resultant aqueous layer was applied on a Diaion HP-20 column and eluted serially with appropriate solvents (20% ~ 100% MeOH, 80% acetone and 100% acetone) to yield the 20% MeOH (7.9 g), 50% MeOH (9.5 g), 80% MeOH (7.6 g), 100% MeOH (1.3 g), 80% acetone (2.3 g) and 100% acetone (1.3 g) fractions.

Chapter 1 therefore gives a background to the importance and relevance of natural products as a source of therapeutic compounds use in various diseases. The description of the plant *Thonningia sanguinea* Vahl, its relevance to traditional medicine, its biological actions reported in literature, the aims and specific objectives for this research work are also discussed.

Chapter 2.1 details the antimicrobial activity of total methanolic crude extract of *T. sanguinea* and its fractions [*n*-hexane, *n*-BuOH, EtOAc and the Diaion HP-20 column-eluted fractions (20% MeOH, 50% MeOH, 80% MeOH, 100% MeOH, 80% acetone and 100% acetone)] against the selected standard bacterial strain *Vibrio parahaemolyticus* in the paper disc method. All fractions except for the 50% MeOH and crude methanolic extract showed moderate to significant antibacterial action against the test microbe.

Chapter 2.2 details the isolation and characterization of compounds from the *n*-hexane fraction of *T. sanguinea*: one sphingosine-type cerebroside (**TSC-1**) and one phytosphingosine-type cerebroside (**TSC-2**), with both containing mainly a 2-hydroxy fatty acid and β-D-glucopyranose moieties, β-sitosteryl-3-*O*-β-D-glucopyranoside-6′-*O*-fatty

acid molecular species (**TSS-1**), six known sterols: β-sitosterol-3-*O*-β-D-(6′-*O*-palmitoyl)-glucopyranoside (**1**), β-sitosterol (**2**), β-sitosterol-3-*O*-β-D-glucopyranoside (**3**), β-stigmasterol (**4**), β-stigmasterol-3-*O*-β-D-glucopyranoside (**5**) and cholesterol (**6**), one pentacyclic triterpenoid betulinic acid (**7**), one saturated fatty acid methyl ester (**14**) and one saturated fatty acid (**15**). Their structures were clarified on the basis of chemical methods, spectroscopic techniques (IR, NMR experiments and mass spectrometry) and comparison with appropriate literature data.

Chapter 2.3 details the isolation and characterization of compounds from the ethyl acetate fraction of *T. sanguinea*: five known lignans: (+)-epipinoresinol (**8**), (+)-pinoresinol (**9**), (+)-cycloolivil (**10**), (+)-secoisolariciresinol (**11**) and (+)-isolariciresinol (**12**), one known flavanone (+)-eriodictyol (**13**), as well as one saturated fatty acid (**16**) and one unsaturated fatty acid (**17**). Their structures were also clarified on the basis of spectroscopic techniques (NMR experiments and mass spectrometry) and comparison with appropriate literature data.

Chapter 3.1 details the HPLC profiles of the crude methanolic extract, its fractions, fifteen (15) of the isolated compounds [(**1** ~ **13**), **TSC-1** and **TSC-2**] and the herbal medicinal product from *Thonningia sanguinea*. The HPLC fingerprints of the herbal medicinal product and the crude methanolic extract of *T. sanguinea* were also compared. All 15 compounds were present and their retention time (min) corresponded exactly with that seen in the crude methanolic extract. Analytical markers and chromatographic fingerprints were therefore provided for *T. sanguinea* and its herbal medicinal product.

Chapter 4 is the Experimental section. It describes all methods and procedures used in this study. Chapter 4.1 details the methods used in the antimicrobial screening of the crude methanolic extract of *T. sanguinea* and its fractions. Chapter 4.2 details the General experimental procedures for the chemical study. Chapter 4.3 details *T. sanguinea* plant collection and identification. Chapter 4.4 details the extract preparation and compound isolation procedures. Chapter 4.5 details the conditions and procedures used to develop HPLC fingerprints for the crude methanolic extract, fractions and an herbal medicinal product from *T. sanguinea.*

Chapter 2

RESULTS AND DISCUSSION

2.1 Antimicrobial screening of the crude methanolic extract of *Thonningia sanguinea* and its fractions.

The crude methanolic extract and fractions of *Thonningia sanguinea* were tested against *Vibrio parahaemolyticus* (NBRC No. 12711) at 5 mg/10 µl per paper disc in the paper disc diffusion method (See Chapter 4.1: Experimental Section for details of methods and procedure).

Table 2.1 Antibacterial screening of *Thonningia sanguinea* methanolic crude extract and fractions against *Vibrio parahaemolyticus*[*]

Fraction	Results against *Vibrio parahaemolyticus*
Crude extract	-
n-Hexane	+
n-BuOH	+
EtOAc	+
80% acetone	+
100% acetone	+
20% MeOH	++
50% MeOH	+
80% MeOH	+
100% MeOH	+

[*]Grading of Zone of Inhibition:(-) if the test organism was not susceptible to the test agent, (+) if the diameter obtained was within 25% – 50%, (++) if between 50% – 75% and (+++) if between 75% – 100% when compared to the positive control ciprofloxacin.

Discussion

In the antimicrobial assay, all tested fractions showed moderate inhibition (+) against the gram-negative *Vibrio parahaemolyticus* except for the crude methanolic extract and 50% MeOH fraction, which showed no inhibition. The 20% MeOH fraction however showed the most significant activity (++) (Table 2.1).

The transmission of virulent *V. parahaemolyticus* strains occurs through the consumption of raw or undercooked seafood (oysters, clams etc.) leading to acute gastroenteritis. It may also cause wound infection, ear infection or septicaemia, which could be life-threatening in individuals with pre-existing medical conditions.[138)] Traditionally, *T. sanguinea* has been used in the treatment of abscesses, wounds and gastroenteritis. Previous antimicrobial assays of the *n*-butanol extract of *T. sanguinea* roots showed moderate activity against some multi drug resistant strains of *Salmonella enterica,*[113)] as well as ESBL-producing *Escherichia coli* and *Klebsiela pneumoniae* strains.[100)]

Conclusion

The *n*-hexane, *n*-butanol and Diaion HP column eluted fractions of *Thonningia sanguinea* have antibacterial action against *Vibrio parahaemolyticus*. The yields of these fractions suggest that the most important fractions are the EtOAc, *n*-BuOH and the 20% MeOH fractions and therefore contain compounds which have potent antibacterial actions. These findings therefore validate the use of *T. sanguinea* in Ghanaian traditional medicine as an anti-infective agent.

2.2 Secondary metabolites isolated from the *n*-hexane fraction of *Thonningia sanguinea*

Chromatographic separation of the *n*-hexane fraction from the crude methanolic extract of *Thonningia sanguinea* led to the isolation of one sphingosine-type (**TSC-1**) and one phytosphingosine-type (**TSC-2**) cerebroside molecular species, one β-sitosterol-3-*O*-β-D-glucopyranoside-6′-*O*-fatty acid molecular species (**TSS-1**), together with six known sterols: β-sitosterol-3-*O*-β-D-(6′-*O*-palmitoyl)-glucopyranoside (**1**), β-sitosterol (**2**), β-sitosterol-3-*O*-β-D-glucopyranoside (**3**), β-stigmasterol (**4**), β-stigmasterol-3-*O*-β-D-glucopyranoside (**5**) and cholesterol (**6**), one known pentacyclic triterpenoid betulinic acid (**7**), one unsaturated fatty acid methyl ester (**14**) and one saturated fatty acid (**15**). Their structures were also clarified on the basis of chemical methods, spectroscopic techniques (IR, NMR experiments and mass spectrometry) and comparison with appropriate literature data. The chemical investigation of the natural products produced from the *n*-hexane fraction are discussed in this section.

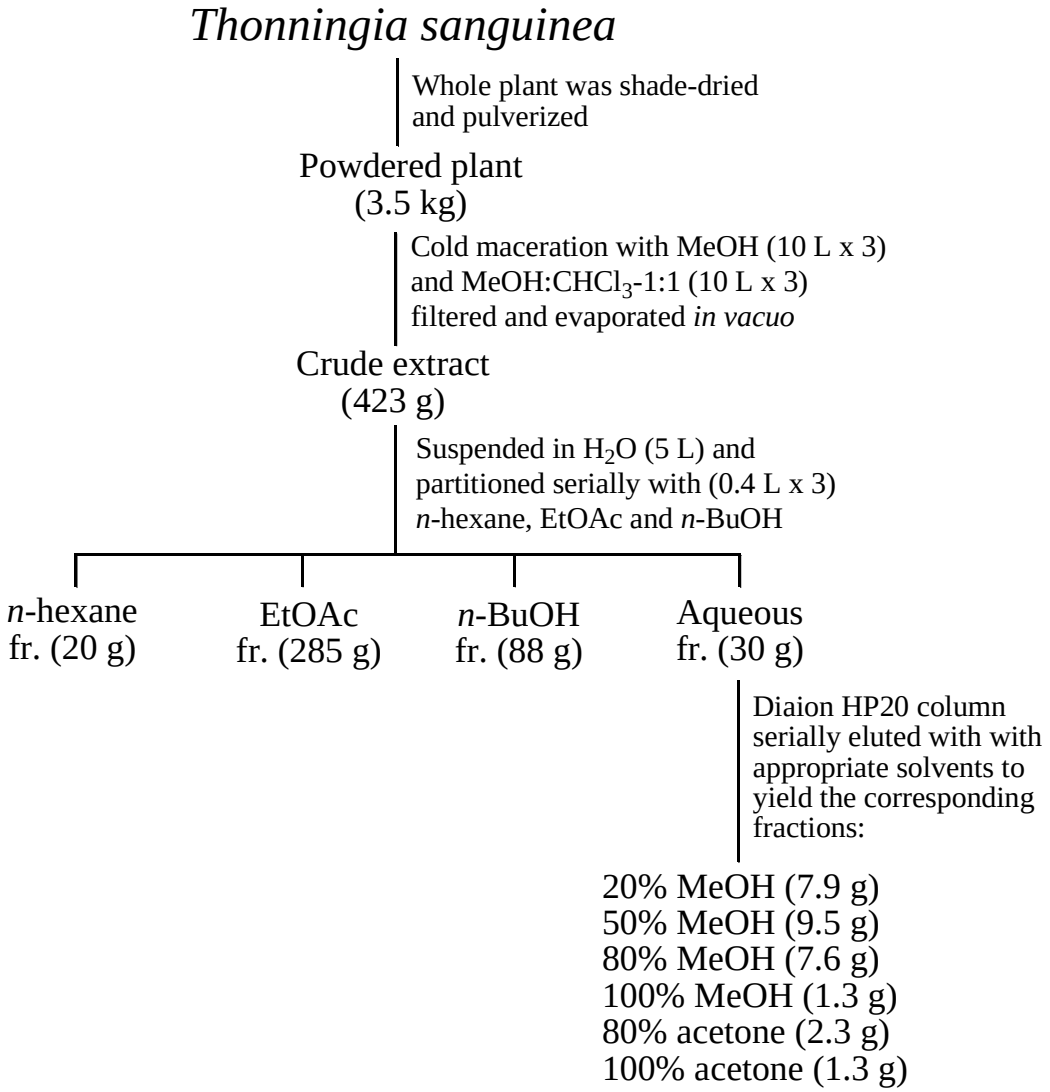

Figure 2.1 Extraction scheme of *Thonningia sanguinea* whole plant

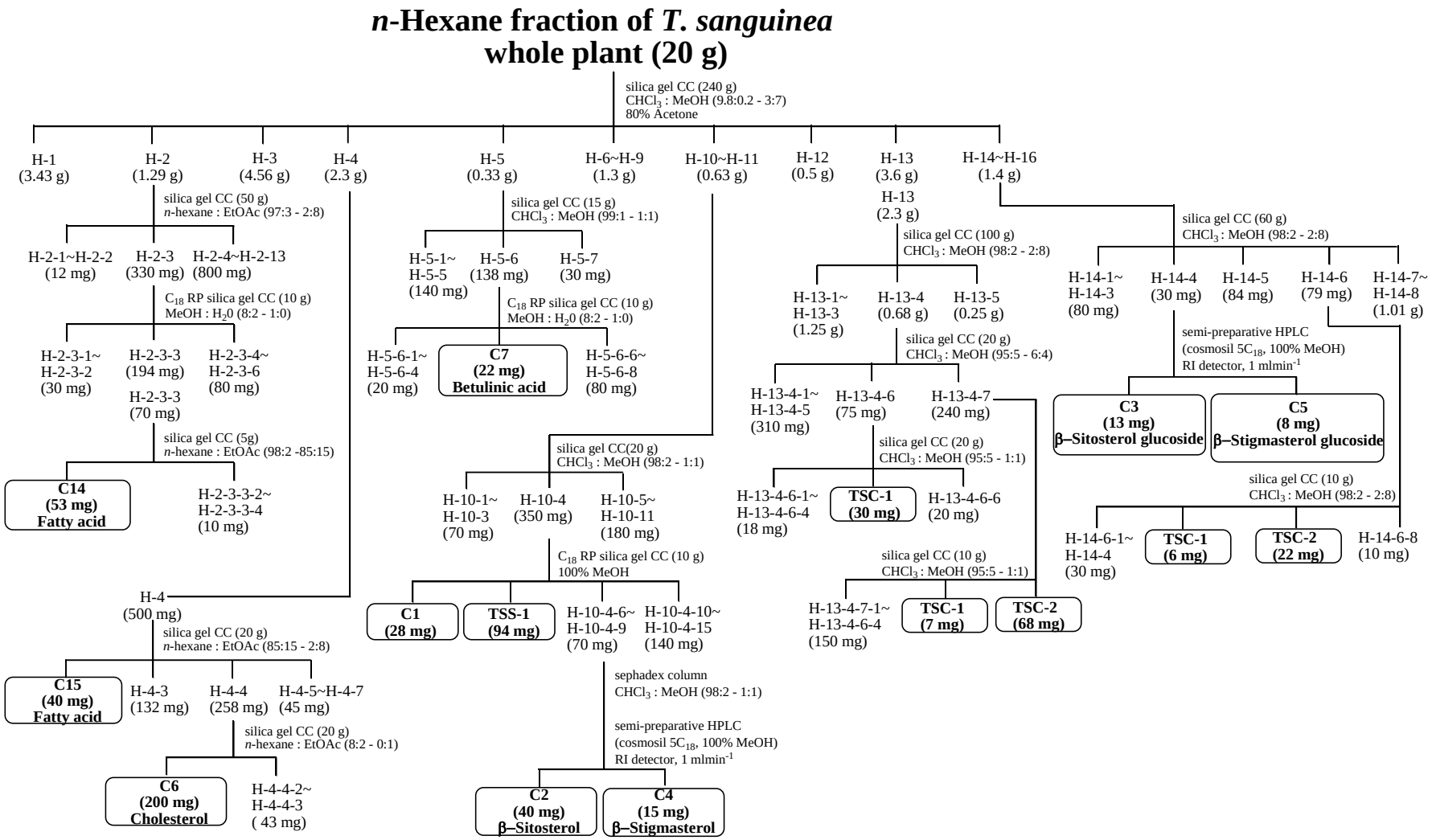

Figure 2.2 Isolation scheme of the *n*-hexane fraction of *Thonningia sanguinea*

TSS-1

TSS-1 (94 mg) was obtained as a white amorphous solid showing as a single spot on silica gel TLC plate.

Spectroscopic analysis:

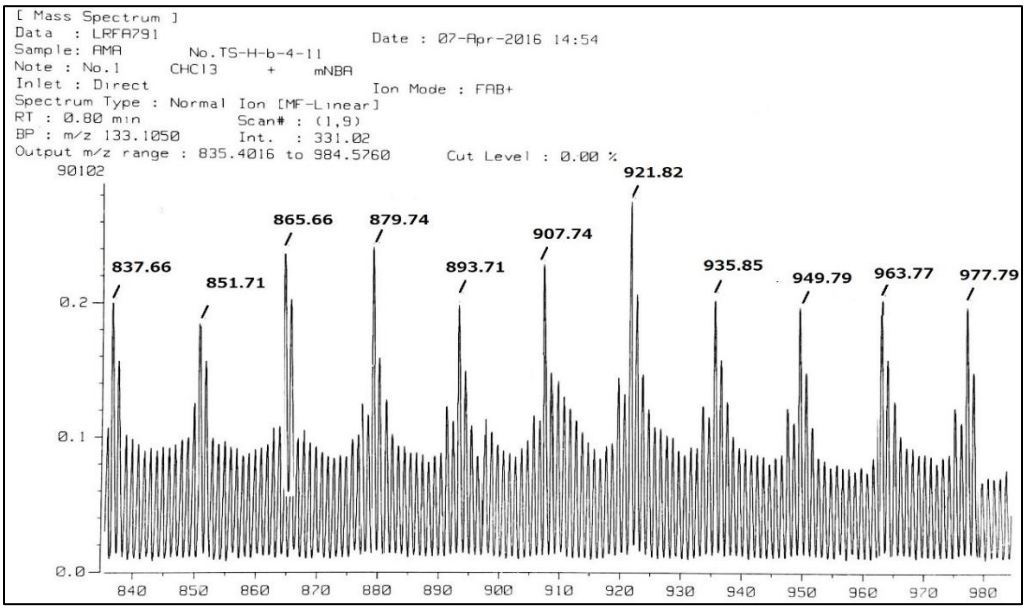

Figure 2.3 FAB-MS (positive ion mode) of TSS-1

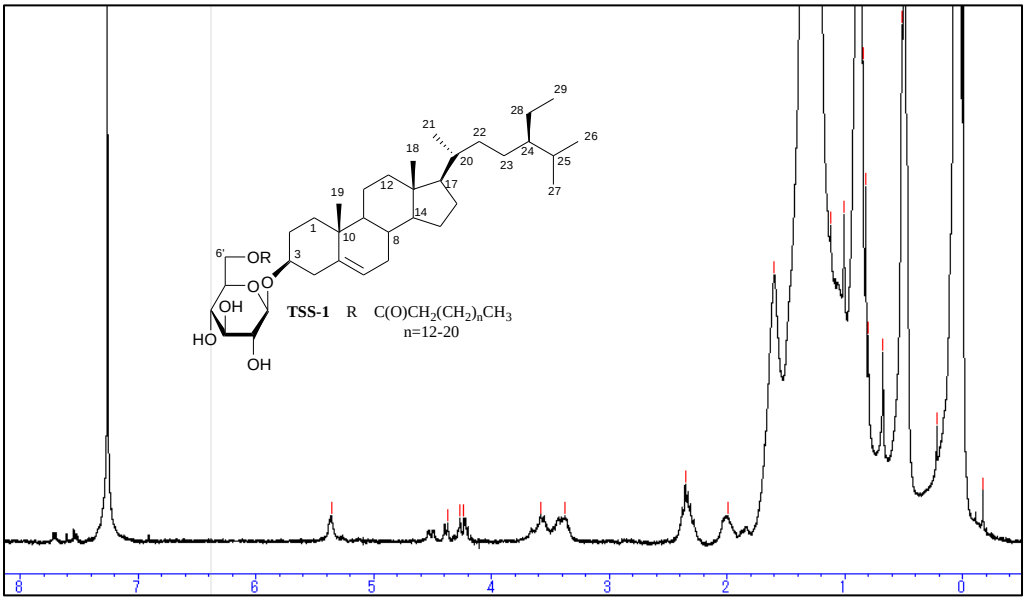

Figure 2.4 ^{1}H NMR spectrum of TSS-1 (chloroform-*d*, 400 MHz)

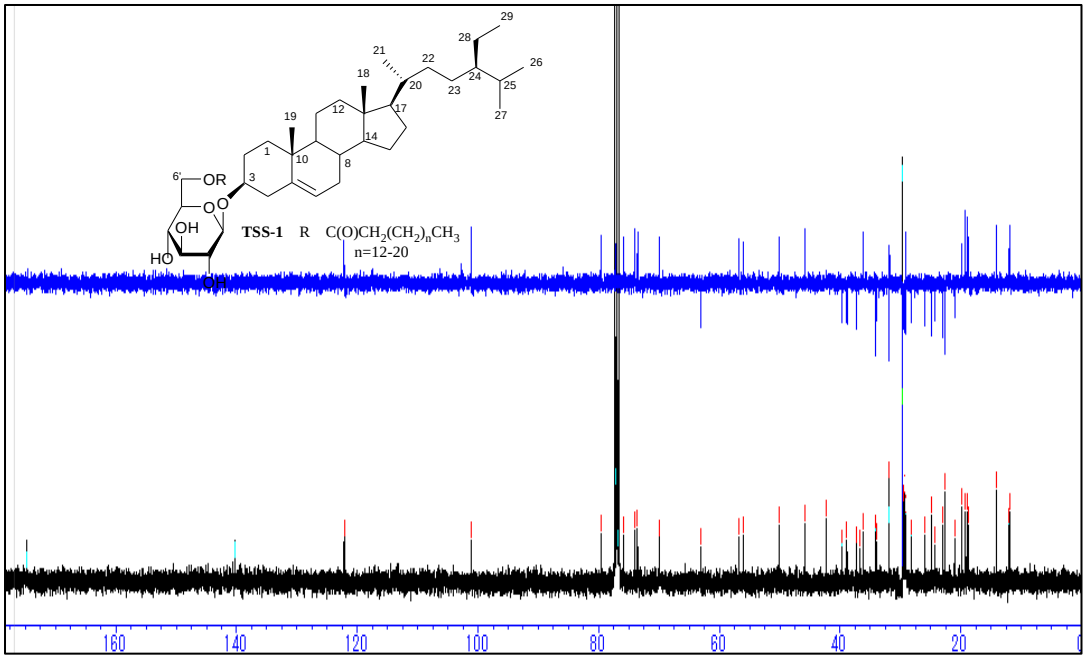

Figure 2.5 ^{13}C NMR spectrum of TSS-1 (chloroform-*d*, 100 MHz)

Table 2.2 ^{1}H (400 MHz) and ^{13}C NMR (100 MHz) spectroscopic data of TSS-1 (chloroform-*d*, δ values in ppm, *J* values in Hz)

Position	***δ_C (ppm)***	***δ_H (No., M, J_{Hz})***	***Position***	***δ_C (ppm)***	***δ_H (No., M, J_{Hz})***
1	37.4(CH_2)		21	18.8(CH_3)	0.95 (3H, d, *J* = 6.5)
2	29.7(CH_2)		22	33.9(CH_2)	
3	79.5(CH)	3.55 (1H, m)	23	26.1(CH_2)	
4	38.9(CH_2)		24	51.3(CH)	
5	140.3(C)		25	29.1(CH)	
6	122.2(CH)	5.36 (1H, m)	26	19.8(CH_3)	0.84 (3H, d, *J* = 6.5)
7	32.9(CH_2)		27	19.0(CH_3)	0.87 (3H, d, *J* = 6.5)
8	32.0(CH)		28	23.0(CH_2)	
9	50.2(CH)		29	12.0(CH_3)	0.88 (3H, t, *J* = 7.5)
10	36.7(C)		1′	101.2(CH)	4.37 (1H, d, *J* = 8)
11	21.0(CH_2)		2′	73.6(CH)	
12	39.7(CH_2)		3′	75.9(CH)	
13	42.3(C)		4′	70 (CH)	
14	56.7(CH)		5′	74 (CH)	
15	24.3(CH_2)		6′	63.1(CH_2)	
16	28.2(CH_2)		1″	174.8(C)	
17	56.1(CH)		2″	34.2(C)	
18	11.8(CH_3)	0.68 (3H, s)	3″	24.9(CH_2)	
19	19.3(CH_3)	1.01 (3H, s)	*n*CH_2	22.6 ~ 29.8	1.25 (br. s)
20	36.1(CH)		CH_3	14.1	0.84 (3H, s)

Discussion

TSS-1 (94 mg) was obtained as a white amorphous solid from fractions H-10+H-11, showing as a single spot on silica gel TLC plate. The IR spectrum of this compound exhibited a strong absorption at 3350 cm^{-1} attributable to the presence of a hydroxy group and a band at 1720 cm^{-1} (carbonyl) assignable to stretching of a normal aliphatic ester.

The ^{1}H and ^{13}C NMR spectral data of **TSS-1** in chloroform-*d* showed resonances of a carboxylic acid group (δ_C 174.8), a long methylene chain centred at δ_H 1.25 as a broad singlet (δ_C 29.1 ~ 29.9) and overlapped methyls at δ_H 0.68 ~ 0.85 (δ_C 14.1), indicating normal type terminal methyls of the fatty acids. The characteristic signals of a β-sitosterol skeleton were determined as follows: a methine proton at δ_H 3.55 (1H, m, H-3, δ_C 79.5) and an olefinic proton signal at δ_H 5.36 (1H, m, H-6, δ_C 122.2) were assigned as H-3 and H-6 respectively. Two angular methyl protons at δ_H 0.68 (3H, s) and 1.01 (3H, s), corresponding to δ_C 11.8 and 19.3 were assigned as H_3-18 and H_3-19 respectively. The proton signals at δ_H 0.84 (3H, d, J = 6.5 Hz, δ_C 19.8, H_3-26) and 0.87 (3H, J = 6.5 Hz, δ_C 19, H_3-27) indicated the presence of an isopropenyl group in the molecular structure. The proton signal at δ_H 0.88 (3H, t, J = 7.8 Hz, δ_C 11.9) was assigned as H_3-29. Characteristic signals indicative of a presence of a monosaccharide moiety at δ_H 3.38 ~ 4.53 (6H) were observed. This included an anomeric proton of the sugar moiety (I'-H) present as a doublet at δ_H 4.37 (1′-H, d, δ_C 101.2) with a coupling constant of 8 Hz due to axial-axial coupling, thus showing that the glucose was β-linked to the aglycone. (Figure 2.4 ~ 5 and Table 2.2).

Several signals (-CH_2-, -CH_3 protons) in the aliphatic area of the ^{1}H NMR spectrum (δ_H 0.75 ~ 1.6 ppm) and a peak at δ_H 2.31 (2H, t), which is characteristic of a methylene attached to carbonyl group, supported the hypothesis of the occurrence of a fatty acid group in the 6'-*O*-position of the sugar moiety. All other NMR assignments agreed with known β-sitosterol-3-*O*-β-D-glucopyranoside-6′-*O*-fatty acid esters.

To identify the sugar moiety, hydrolysis of the glycosidic bond in **TSS-1** was performed by methanolysis using HCl/MeOH, followed extraction with *n*-hexane. The methylated glucoside in the MeOH layer was analyzed by HPLC against standard sugars (glucose and galactose) and identified as glucose (glucose t_R = 14.11 min, galactose t_R = 13.27 min). The

coupling constant of the anomeric proton at δ_H 4.37 (1H, d, J = 8 Hz) and the chemical shift of the anomeric carbon δ_C (101.2, H-1′) confirmed the β-configuration of the glucopyranoside moiety (α-glucopyranoside: J = 3.7 Hz, δ_C 98.5).[115] The absolute configuration of the sugar moiety was determined by the method described by Tanaka *et al*., 2007.[115] Direct HPLC analysis of the reaction mixture of the sugar moiety exhibited a peak at t_R = 18.7 min, which was coincided with the aryl-isothiocyanate derivative of D-glucose, confirming the absolute configuration of the sugar moiety as D-gucose (L-glucose t_R = 19.22 min).

The positive FAB-MS spectral data showed a series of molecular ion peaks at *m/z*: 851, 865, 879, 893, 907, 921, 935, 949, 963 and 977 $[M + Na]^+$ indicating C-17 ~ C-26 long fatty acid chains (Figure 2.3). Therefore, **TSS-1** is presumed to be a molecular species consisting of β-sitosterol-3-*O*-β-D-glucopyranoside-6′-*O*-fatty acid esters possessing mainly a hydroxy fatty acid moiety (normal type terminal methyl groups at δ_C 14.2) and a β-D-glucopyranose moiety.[116].

Conclusion

TSS-1 was determined therefore and assigned as a molecular species of β-sitosterol-3-*O*-β-D-glucopyranoside-6′-*O*-fatty acid esters as shown in Figure 2.6.

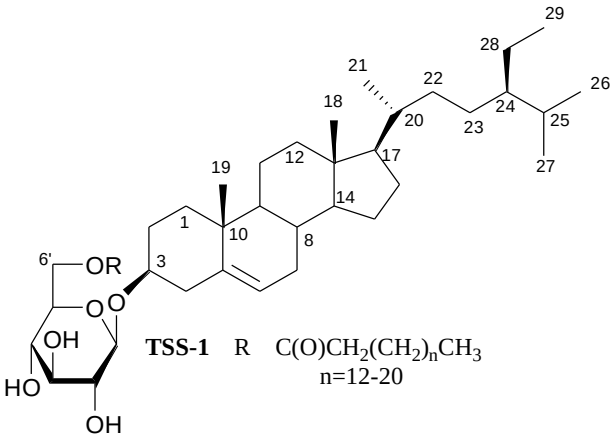

Figure 2.6 Structure of TSS-1

Cerebrosides from *Thonningia sanguinea*

TSC-1 (43 mg) was obtained as a white amorphous solid from fractions H-13 ~ H-16 showing as a single spot on silica gel TLC plate.

Spectroscopic analysis

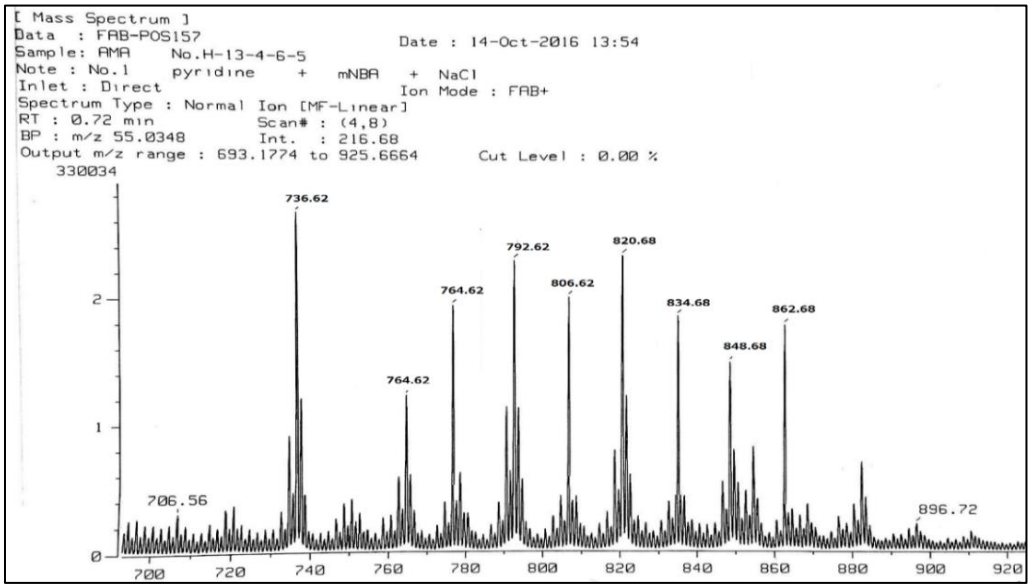

Figure 2.7 FAB-MS (positive ion mode) of TSC-1

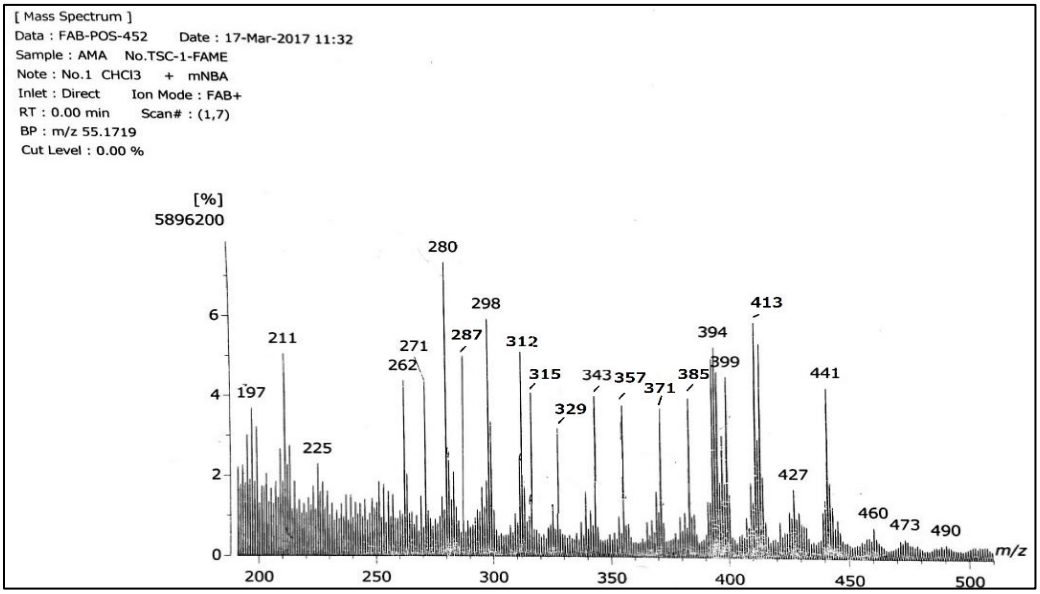

Figure 2.8 FAB-MS data of TSC-1-FAME

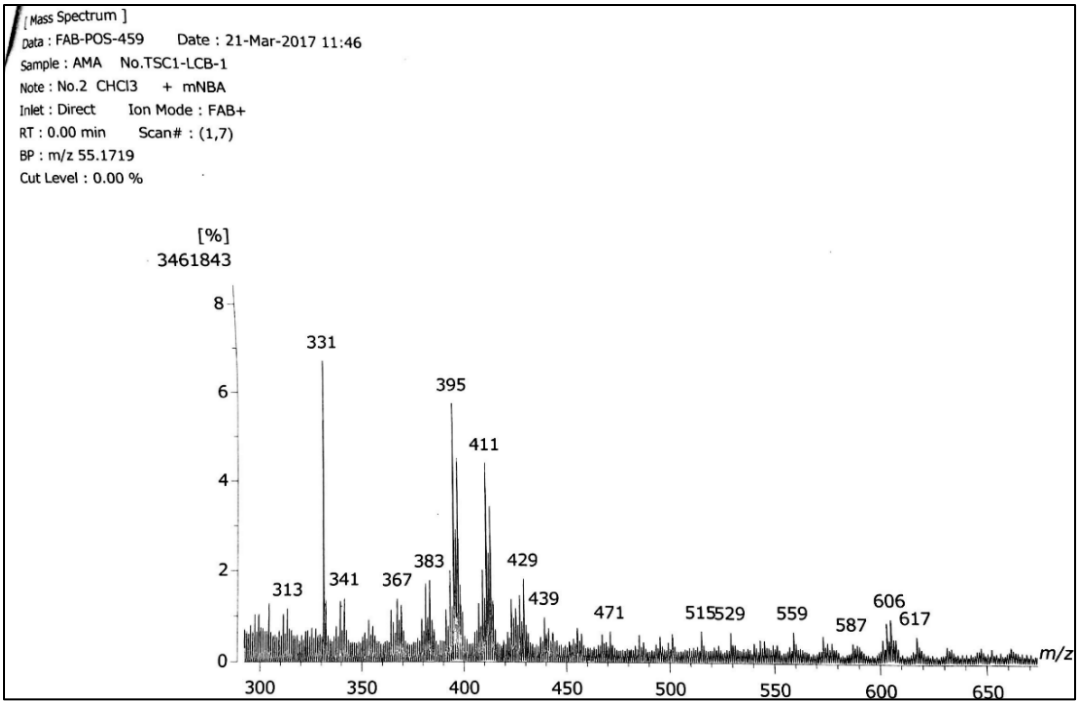

Figure 2.9 FAB-MS (positive ion mode) of TSC-1-LCB-1

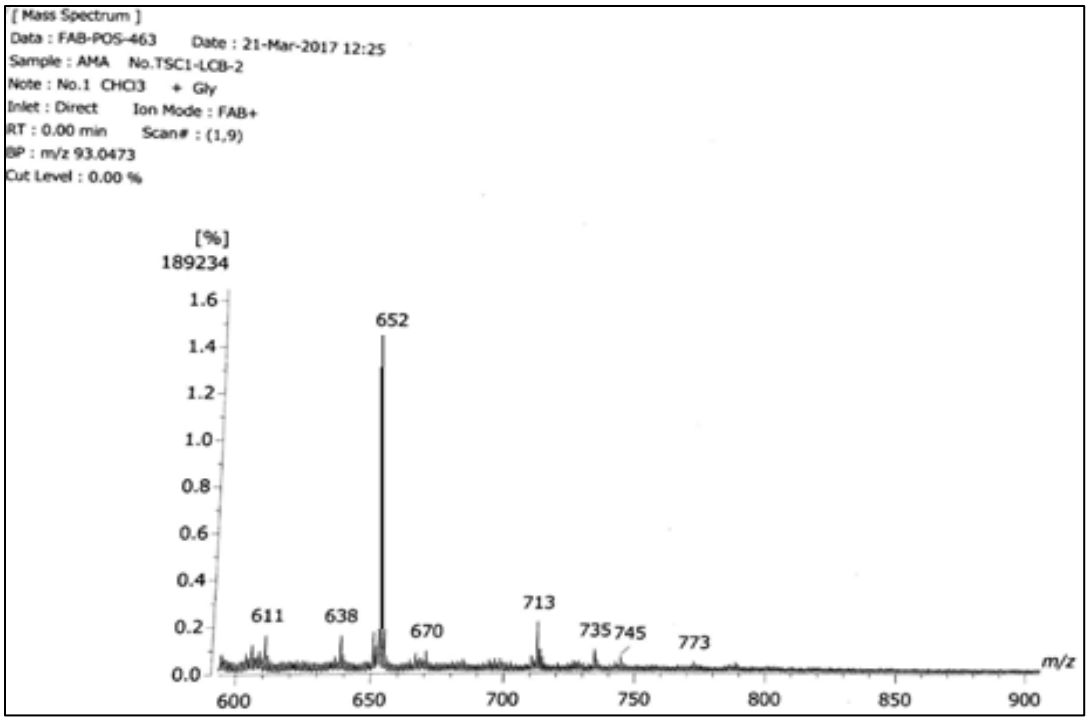

Figure 2.10 FAB-MS (positive ion mode) of TSC-1-LCB-2

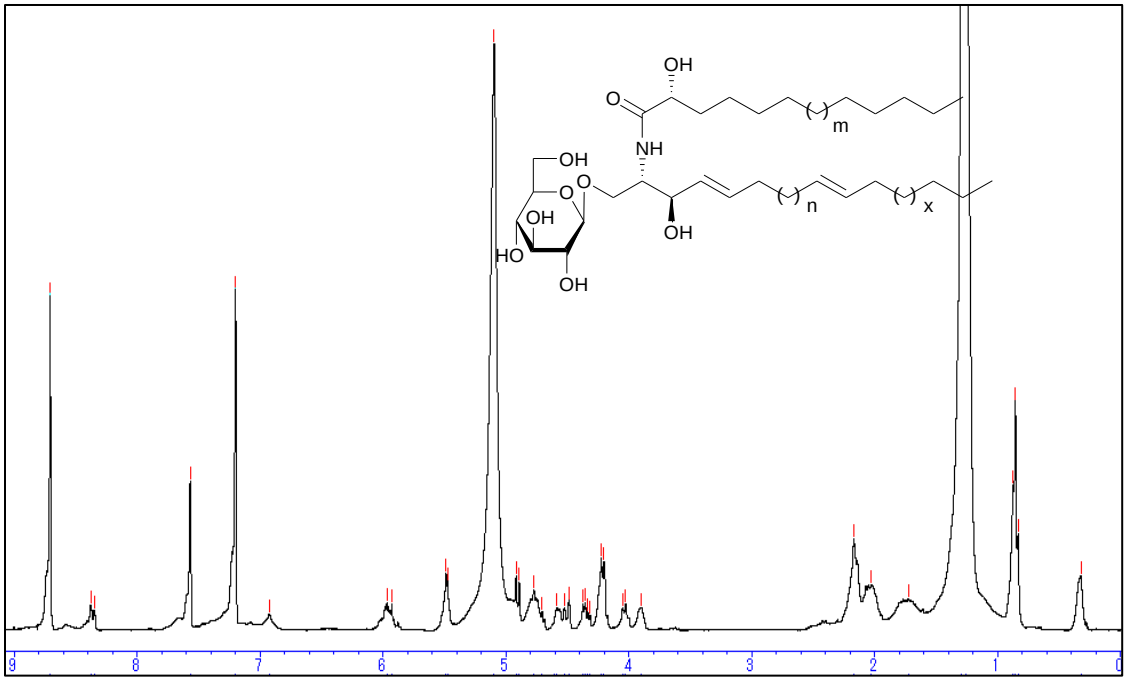

Figure 2.11 ^{1}**H NMR spectrum of TSC-1 (pyridine-d_5, 400 MHz)**

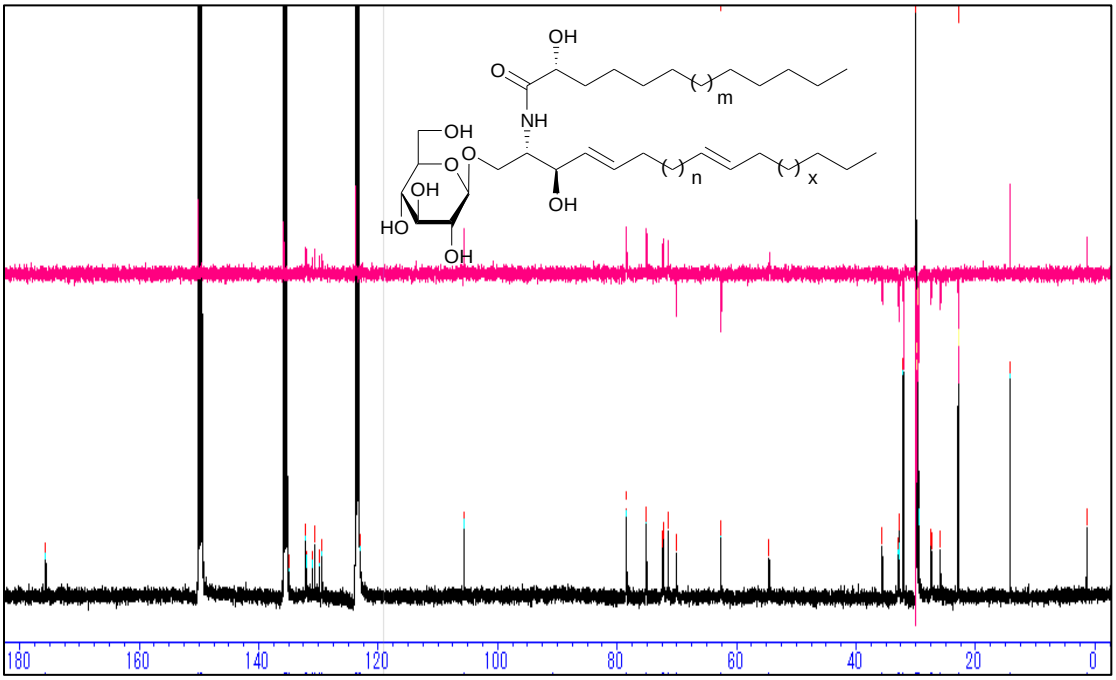

Figure 2.12 ^{13}**C NMR spectrum of TSC-1 (pyridine-d_5, 100 MHz)**

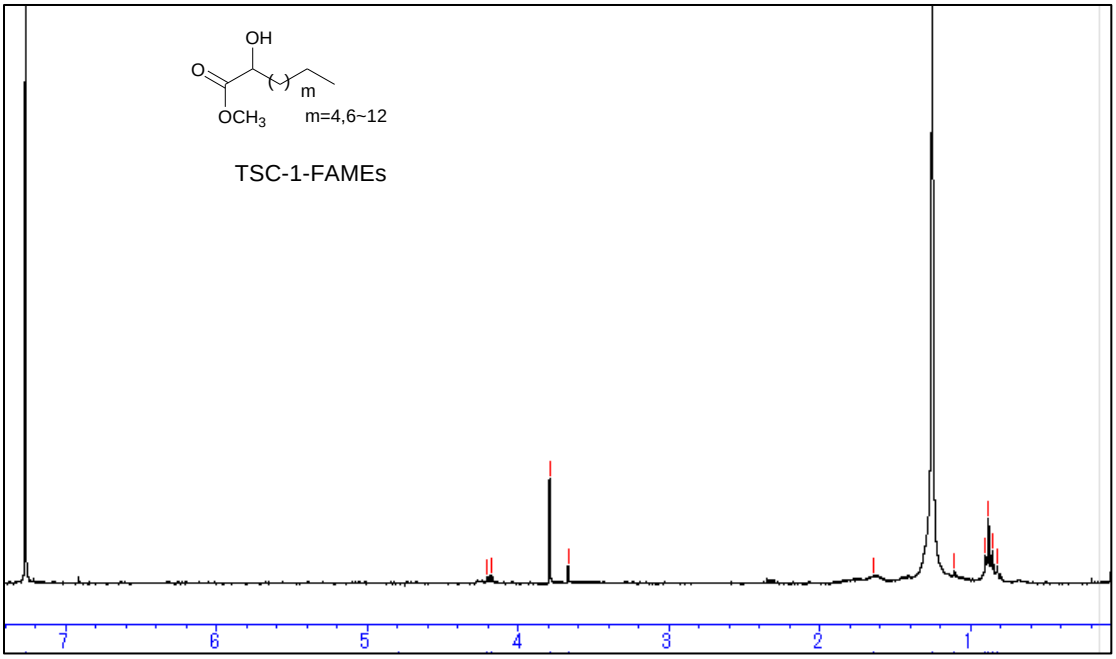

Figure 2.13 ^{1}H NMR spectrum of TSC-1-FAME (chloroform-*d*, 400 MHz)

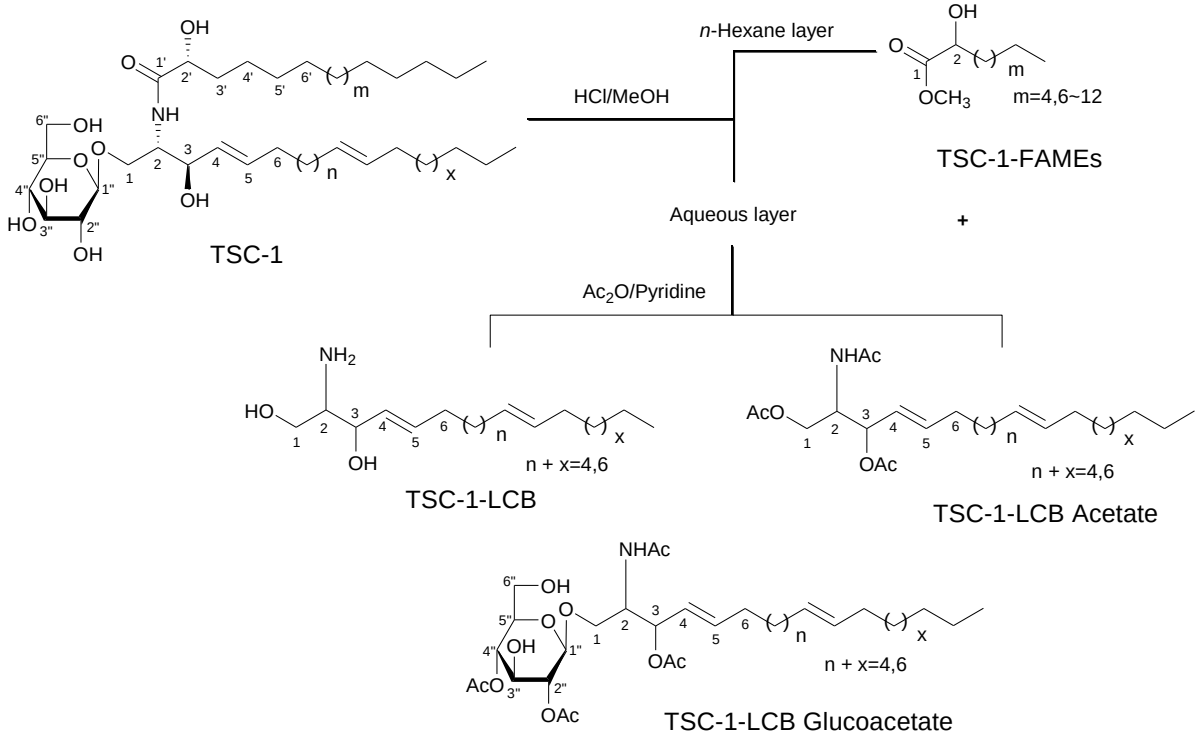

Figure 2.14 Methanolysis and acetylation products of TSC-1

Table 2.3 ^{1}H (300 MHz) and ^{13}C NMR (100 MHz) spectroscopic data of TSC-1 (pyridine-d_5, δ values in ppm, J values in Hz)*

Position	*δ_H (No., M, J_{Hz})*	*δ_C (ppm)*	*Position*	*δ_H (No., M, J_{Hz})*	*δ_C (ppm)*
NH	8.35 (1H, d, J = 8.8)		1′(C)		175.0
1a(CH)	4.21 (1H, dd, J = 10, 5)	70.8	2′(CH)	4.59 (1H, m)	71.8
1b(CH)	4.77 (1H, m)		CH_3	0.86 (3H, t)	13.6
2(CH)	4.77 (1H, m)	54.0	1″(CH)	4.89 (1H, d, J = 8)	105.5
3(CH)	4.71 (1H, m)	71.8	2″(CH)	4.03 (1H, m)	74.5
4(CH)	5.97 (1H, m)	131.4	3″(CH)	4.23 (1H, m)	78.0
5(CH)	5.97 (1H, m)	131.4	4″(CH)	4.21 (1H, m)	71.6
x(CH)	5.48 (1H, m)	129.9	5″(CH)	3.90 (1H, m)	78.0
y(CH)	5.49 (1H, m)	129.9	6a″(CH_2)	4.36 (1H, m)	62.0
			6b″	4.59 (1H, m)	

*Spectra were acquired at 23 °C. Chemical shifts are given in δ (ppm) and are referenced to internal solvent signals for pyridine-d_5 at 7.19 (δ_H) and 123.5 (δ_C) ppm. x and y are olefinic (double bond location)

Discussion

TSC-1 (43 mg) was obtained as a white amorphous solid from fractions H-13 ~ H-16 showing as a single spot on silica gel TLC plate. Strong hydroxy (3422 cm^{-1}) and amide absorptions (1650, 1540 cm^{-1}) were observed in the IR spectrum.

The NMR spectral data of **TSC-1** in pyridine-d_5 showed resonances of a secondary amide proton doublet at δ_H 8.35 (1H, d, J = 8.8 Hz), a long methylene chain, centred at δ_H 1.26, (δ_C 29.1 ~ 29.3) and overlapped methyls at δ_H 0.86 (δ_C 13.6), indicating the presence of a sphingolipid skeleton. Characteristic signals indicative of a monosaccharide moiety at δ_H 3.90 ~ 4.89 (6H), with the anomeric proton signal at δ_H 4.89 (1H, d, J = 8 Hz, δ_C 105.5, H-1″) were observed. The characteristic resonances for the 2-amino-1,3,2′-triol region of the hydrocarbon chain were observed at δ_H 4.77 (1H, m, H-2), 4.59 (1H, m, H-2′), 4.77 (1H, m, H-1b), 4.21 (1H, m, H-1a), and 4.71 (1H, m, H-3) corresponding to the following ^{13}C NMR data: δ_C 54 (C-2), 71.8 (C-2′), 70.8 (C-1), 71.8 (C-3), and an amide carbonyl signal

at δ_C 175 (C-1′) (Figure 2.11 ~ 12 and Table 2.3). The presence of two disubstituted double bonds at δ_C 131.4 (2CH, C-4, C-5) and 129.9 (2CH) were observed. The second double bond was proposed to be at Δ^8 since the double bond in sphingosine cerebrosides isolated from plants are usually located at C-8. The *E* geometry for the double bonds was supported from the characteristic chemical shift of the allylic carbons at δ_C 32.2, 32.3 and 34 (*Z* geometry = δ_C 26 ~ 27).

The positive FAB-MS spectral data showed a series of molecular ion peaks due to $[M + Na]^+$ at *m/z*: 736, 764, 778, 792, 806, 820, 834 and 848 (Figure 2.7). **TSC-1** is hence presumed to be a molecular species consisting of a sphingosine-type cerebroside possessing mainly a 2-hydroxy fatty acid moiety (normal type terminal methyls at δ_C 13.6) and a β-D-glucopyranose moiety. The sphingosine skeleton was characterized by comparison of its ^1H and ^{13}C NMR spectral data with that of known cerebrosides. The relative stereochemistry of the ceramide moiety is presumed to be (2*S*,3*R*,4*E*,2′*R*) since the characteristic ^{13}C NMR signals (C-1, 2, 3, 4, 1′ and 2′) in addition to the optical rotation value of ($[\alpha]^{20}_D$ = +31.3) are in good agreement with those of the sphingosine-type glucocerebroside molecular species possessing a 2*S*,3*R*,4*E*,2′*R* configuration.

In the same way as in **TSS-1**, the methanolysis of **TSC-1** was performed using HCL/MeOH to hydrolysize the glucosidic bond. HPLC analysis of the methylated glucoside against standard sugars indicated it was glucose (glucose t_R = 14.11 min, galactose t_R = 13.27 min). The coupling constant of the anomeric proton (*J* = 8 Hz, δ_C 105.5, C-1″) confirmed the β-configuration of the glucopyranoside moiety (α-glucopyranoside: *J* = 3.7 Hz, δ_C 98.5).

The absolute configuration of the sugar moiety was determined using the method described by Tanaka *et al*., 2007.[115)] HPLC analysis of the reaction mixture exhibited a peak at t_R = 18.68 min, which was coincided with the arylisothiocyanate derivative of D-glucose, confirming the absolute configuration of the sugar moiety (L-glucose t_R = 19.22 min).

To determine the length of the FAMEs and LCB in the glucocerebrosides, the methanolysis and acetylation products of **TSC-1** were subjected to ^1H, ^{13}C NMR, and FAB-MS analyses. Molecular ion peaks at 286, 314, 327, 343, 357, 371, 385, 399 and 413 $[M + H]^+$ indicated the presence of C-16, C-18 ~ C-25 fatty acid methyl esters, possessing normal terminal

methyl groups (δ_C 13.6). The LCB mixture showed molecular ion peaks at 395 $[M]^+$ (LCB) and 424 $[M + H]^+$ (LCB acetate) indicating the presence of a C-16 LCB, while 652 $[M + Na]^+$ (LCB glucoacetate) indicated the presence of a C-18 LCB in **TSC-1** (Figure 2.8 ~ 10, Figure 2.13 ~ 14).

Conclusion

TSC-1 was therefore confirmed as a sphingosine-type glucocerebroside molecular species containing mainly a 2-hydroxy fatty acid and β-D-glucopyranose moieties as shown in Figure 2.15.

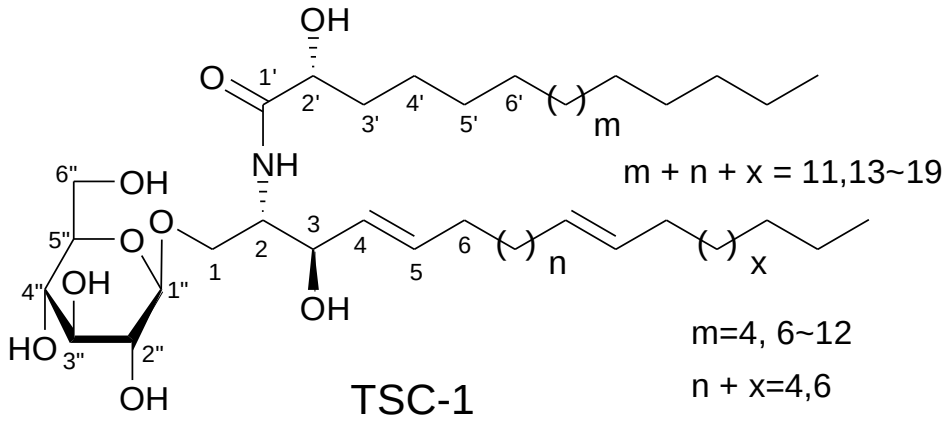

Figure 2.15 Structure of TSC-1

TSC-2

TSC-2 (90 mg) was obtained as a white amorphous solid from fractions H-13 ~ H-16 seen as a single spot on normal phase (silica gel) TLC plate.

Spectroscopic analysis

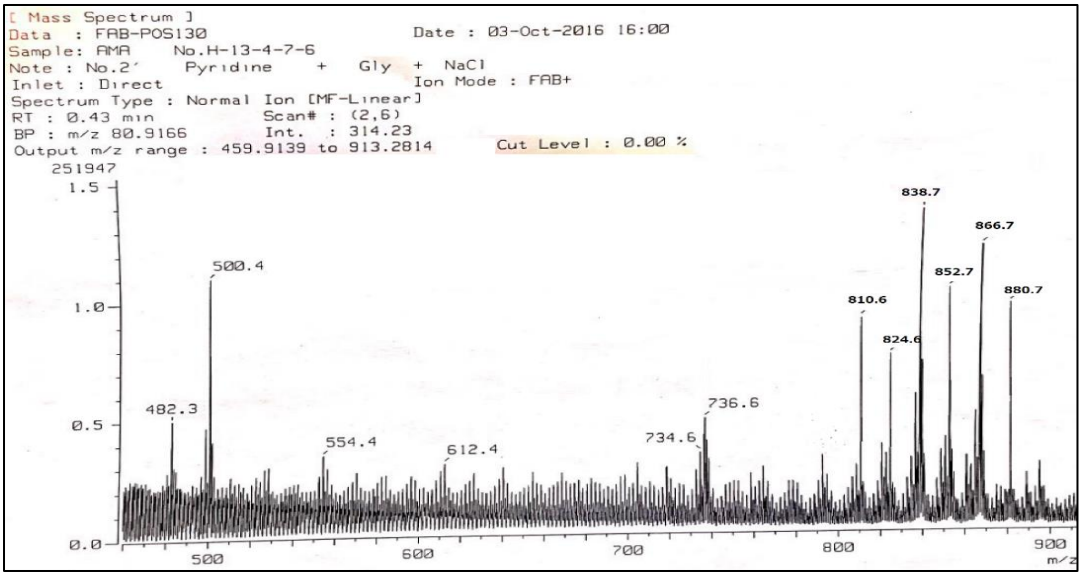

Figure 2.16 FAB-MS (positive ion mode) of TSC-2

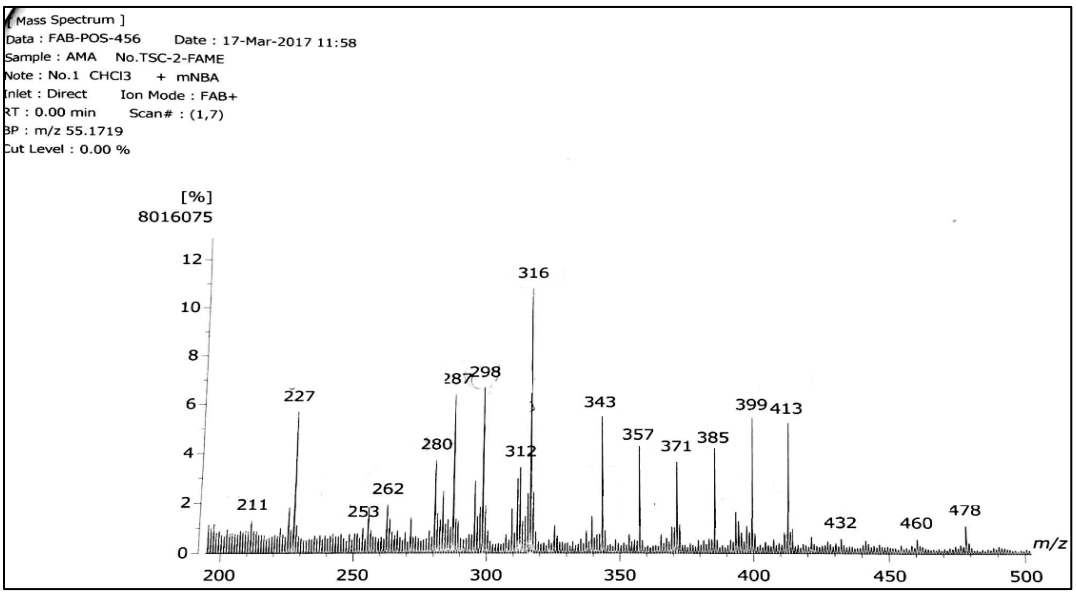

Figure 2.17 FAB-MS (positive ion mode) of TSC-2-FAME

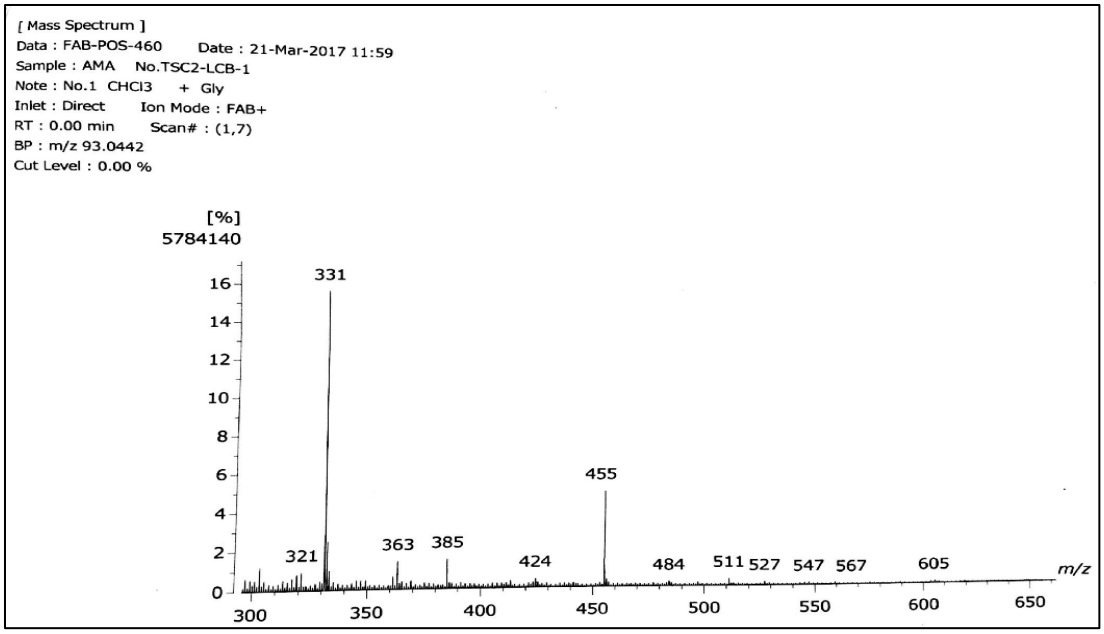

Figure 2.18 FAB-MS (positive ion mode) of TSC-2-LCB-1

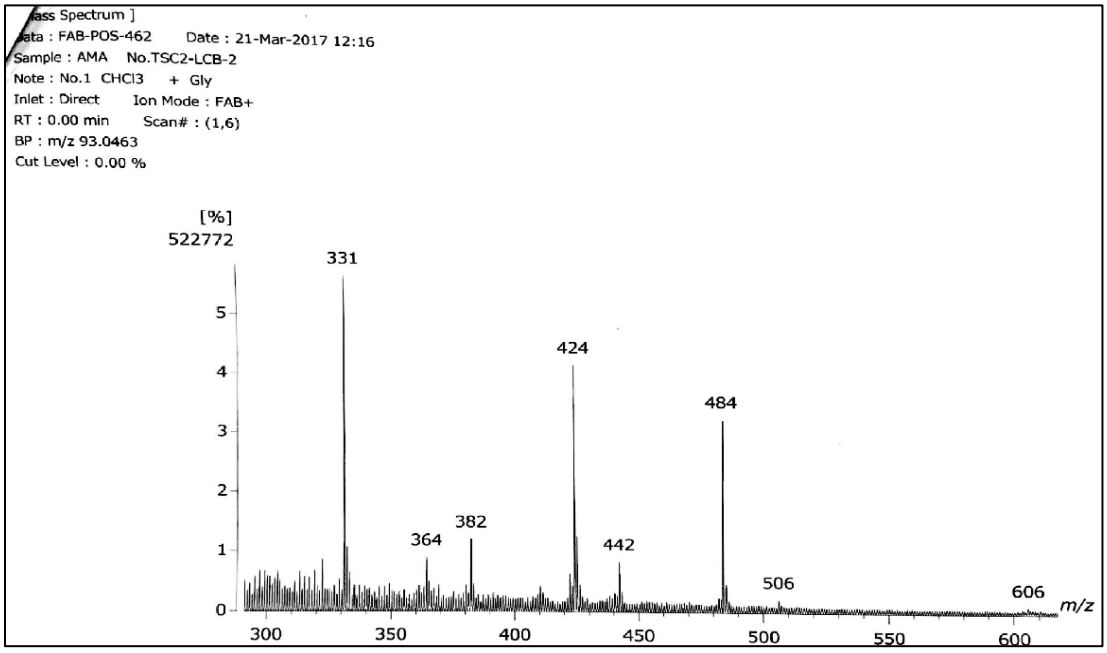

Figure 2.19 FAB-MS (positive ion mode) of TSC-2-LCB-2

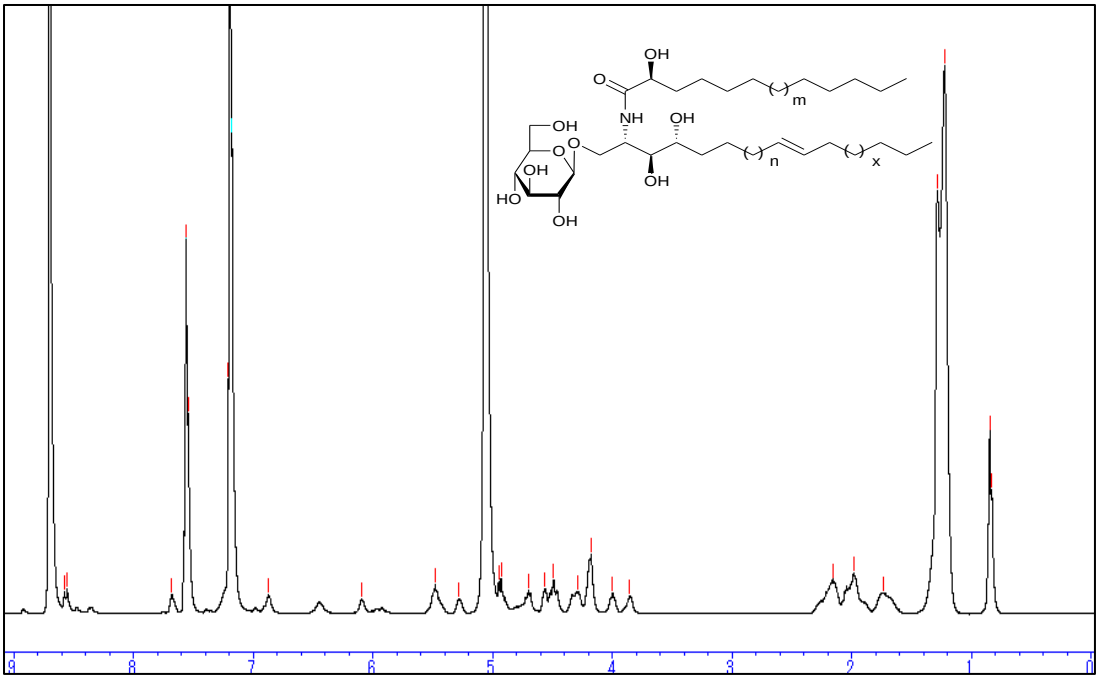

Figure 2.20 ^{1}H NMR spectrum of TSC-2 (pyridine-d_5, 400 MHz)

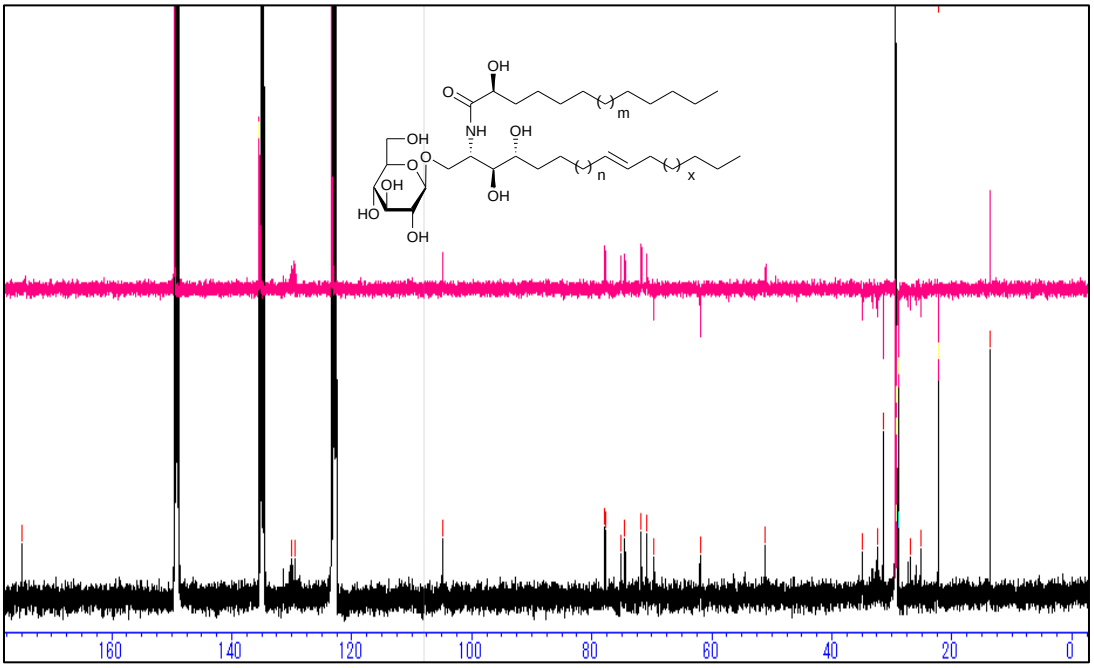

Figure 2.21 ^{13}C NMR spectrum of TSC-2 (pyridine-d_5, 100 MHz)

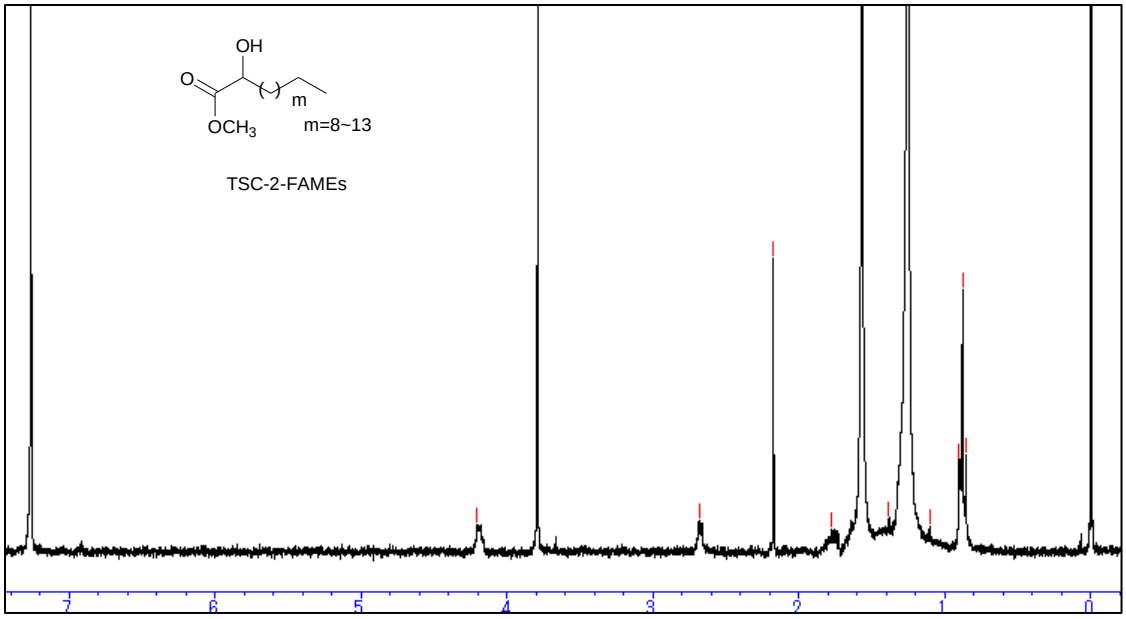

Figure 2.22 ^{1}H NMR spectrum of TSC-2-FAME (chloroform-*d*, 400 MHz)

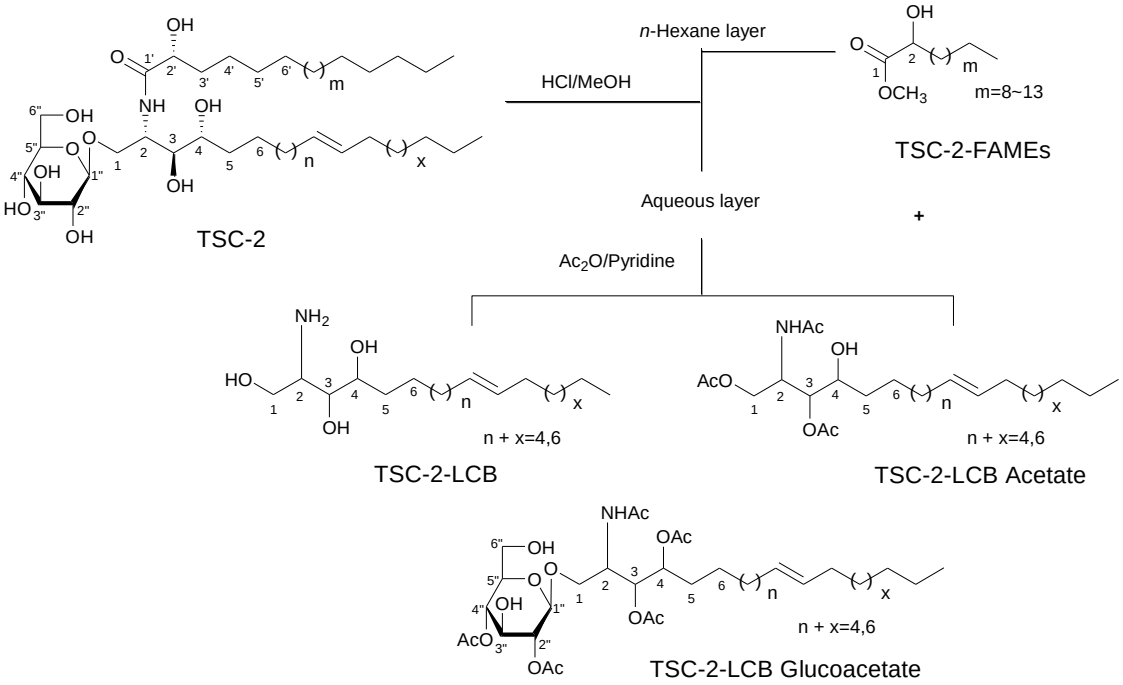

Figure 2.23 Methanolysis and acetylation products of TSC-2

Table 2.4 ^{1}H (300 MHz) and ^{13}C NMR (100 MHz) spectroscopic data of TSC-2 (pyridine-d_5, δ values in ppm, J values in Hz)*

Position	δ_H *(No., M,* J_{Hz}*)*	δ_C *(ppm)*	*Position*	δ_H *(No., M,* J_{Hz}*)*	δ_C *(ppm)*
NH	8.55 (1H, d, J = 8.8)		1′(C)		175
1a(CH)	4.29 (1H, dd, J = 10, 5)	69.8	2′(CH)	4.29 (1H, m)	71.8
1b(CH)	4.70 (d, J = 5, 1)		CH_3	0.83 (3H, t)	13.6
2(CH)	4.70 (1H, m)	51.1	1″(CH)	4.93 (1H, d, J = 8)	104.9
3(CH)	4.70 (1H, m)	71.8	2″(CH)	4.(1H, m)	75.2
4(CH)	4.49 (1H, m)		3″(CH)	4.18 (1H, m)	77.9
5(CH)			4″(CH)	4.18 (1H, m)	70.8
x(CH)	5.48 (1H, m)	129.5	5″(CH)	3.85 (1H, m)	77.9
y(CH)	5.48 (1H, m)	130.0	6a″(CH_2)	4.29 (1H, m)	62.0
			6b″	4.56 (1H, m)	

*Spectra were acquired at 23 °C. Chemical shifts are given in δ (ppm) and are referenced to internal solvent signals for pyridine-d_5 at 7.19 (δ_H) and 123.5 (δ_C) ppm. x and y are olefinic (double bond location)

Discussion

TSC-2 (90 mg) was obtained as a white amorphous solid from fractions H-13 ~ H-16 seen as a single spot on normal phase (silica gel) TLC plate. It exhibited strong hydroxy (3289 cm^{-1}) and amide absorptions (1650, 1540 cm^{-1}) in the IR spectrum.

The NMR spectra of **TSC-2** in pyridine-d_5 showed resonances for a secondary amide proton doublet at δ_H 8.55 (1H, d, J = 8 Hz), protons of a long methylene chain, centred at δ_H 1.25, (δ_C 29.1 ~ 29.8) and overlapped methyls at δ_H 0.83 (δ_C 13.6), indicating the presence of a sphingolipid skeleton. The proton signals at δ_H 3.85 ~ 4.93 (6H) and the anomeric proton signal at δ_H 4.93 (1H, d, J = 8 Hz, δ_C 104.9, C-1′) confirmed the presence of a monosaccharide moiety. **TSC-2** showed characteristic resonances for the 2-amino1,3,4,2′-triol region of hydrocarbon chain with proton signals at δ_H 4.7 (1H, m, H-2), 4.29 (1H, m, H-2′), 4.7 (1H, m, H-1b), 4.29 (1H, m, H-1a), 4.59 (1H, m, H-3), and 4.49

(1H, m, H-4), corresponding to the following ^{13}C NMR data: δ_C 51.1 (C-2), 71.8 (C-2′), 69.8 (C-1), 71.8 (C-3) and an amide carbonyl signal at δ_C 175 (C-1′), (Figure 2.20 ~ 21 and Table 2.4.) A disubstituted double bond in the side chain of the base was observed at δ_C 129.5 and 130 and was proposed to be at Δ^8 since the double bond in phytosphingosine cerebrosides isolated from plants are usually located at C-8. The *E* geometry for the double bond was supported from the chemical shift of the allylic carbons at δ_C 32.3 and 34.9 (*Z* geometry = δ_C 26 ~ 27).

In the same way as in **TSC-1**, methanolysis was performed using HCL/MeOH on **TSC-2** to hydrolysize the glucosidic bond and free the glucose moiety. HPLC analysis of the methylated glucoside indicated the sugar moiety to be glucose (glucose t_R = 14.11 min, galactose t_R = 13.27 min). The coupling constant of the anomeric proton at δ_H 4.93 (1H, d, *J* = 8 Hz) and the ^{13}C chemical shift of the anomeric carbon δ_C (104.9, C-1″) confirmed the β-configuration of the glucopyranoside moiety (α-glucopyranoside: *J* = 3.7 Hz, δ_C 98.5).[115] The absolute configuration of the sugar moiety was determined using the method described by Tanaka *et al*., 2007.[115] HPLC analysis of the reaction mixture exhibited a peak at t_R = 18.5 min, which was coincided with the arylisothiocyanate derivative of D-glucose, confirmed the absolute configuration of the sugar moiety (L-glucose t_R = 19.22 min).

In the positive FAB-MS spectral of **TSC-2**, a series of molecular ion peaks due to 810, 824, 838, 852, 866 and 880 $[M + Na]^+$ were observed. Therefore, **TSC-2** is presumed to be a molecular species consisting of a phytosphingosine-type cerebroside possessing mainly a 2-hydroxy fatty acid moiety (normal methyls at δ_C 13.6) and a β-D-glucopyranose moiety (Figure 2.16).

The core structure of the phytosphingosine skeleton in **TSC-2** was characterized by comparison of its ^1H and ^{13}C NMR spectral data with that of known cerebrosides.[125] The relative stereochemistry of the ceramide moiety is presumed to be (2*S*,3*S*,4*R*,2′*R*) since the characteristic ^{13}C NMR signals (C-1, 2, 3, 4, 1′ and 2′) and the optical rotation value ($[\alpha]^{22}_D$ = +29.4) are in good agreement with those of the phytosphingosines-type glucocerebroside molecular species possessing a 2*S*,3*S*,4*R*,2′*R* configuration.[125]

In the FAB-MS analyses of the methanolysis and acetylation products of **TSC-2**, the FAME mixture showed molecular ion peaks at *m/*: 343, 357, 371, 383 and 413 $[M + H]^+$, indicating the presence of C-20 ~ C-25 fatty acid methyl esters, possessing normal terminal methyl groups (δ_C 13.6). The LCB also indicated the presence of a C-16 and C-18 long chain base identified from the corresponding molecular ion peaks at of the LCB acetates at *m/z* 455 [M + H]+ and 484 $[M + H]^+$ respectively (Figure 2.17 ~ 19, Figure 2.22 ~ 23 and Table 2.4).

Conclusion

TSC-2 was therefore confirmed as a phytosphingosine-type glucocerebroside molecular species containing mainly a 2-hydroxy fatty acid and β-D-glucopyranose moieties as shown in Figure 2.24.

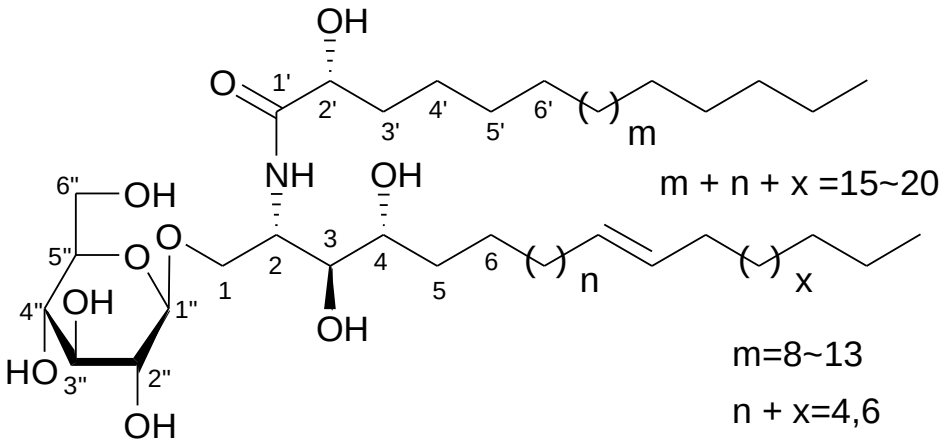

Figure 2.24 Structure of TSC-2

Compound 1:

Compound **1** (28 mg) was obtained as white amorphous solid from fraction H-10 showing as a single spot on normal phase silica gel TLC.

Spectroscopic analysis:

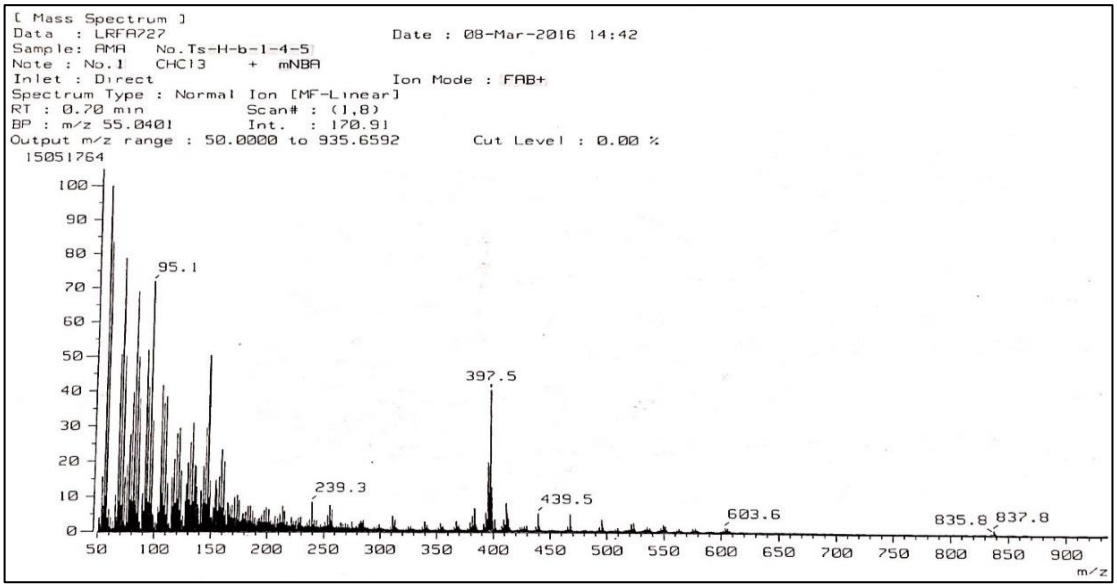

Figure 2.25 FAB-MS (positive ion mode) of compound 1

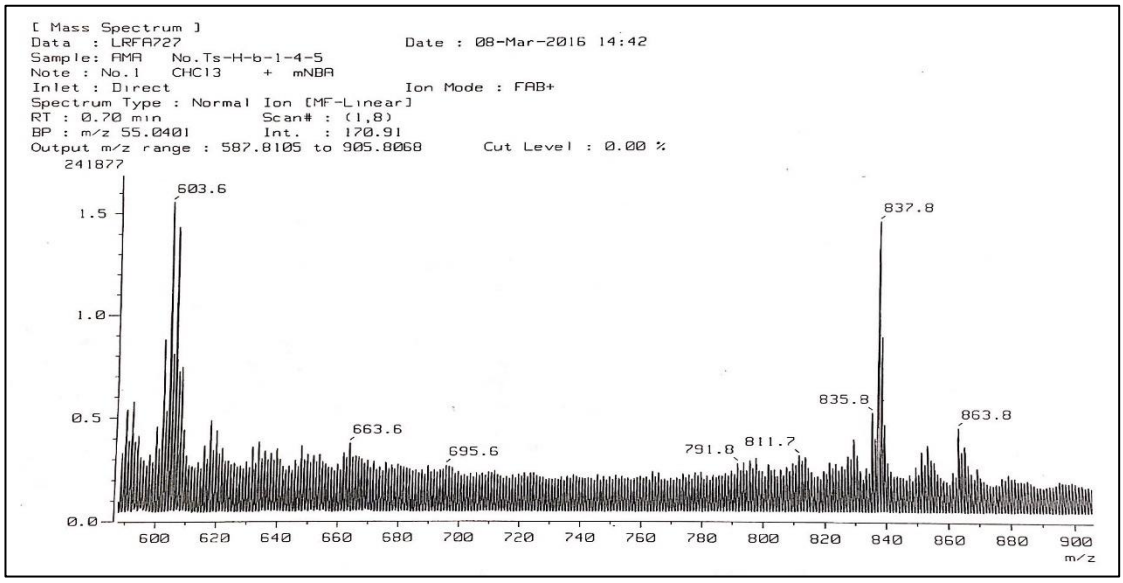

Figure 2.26 FAB-MS (positive ion mode) of compound 1

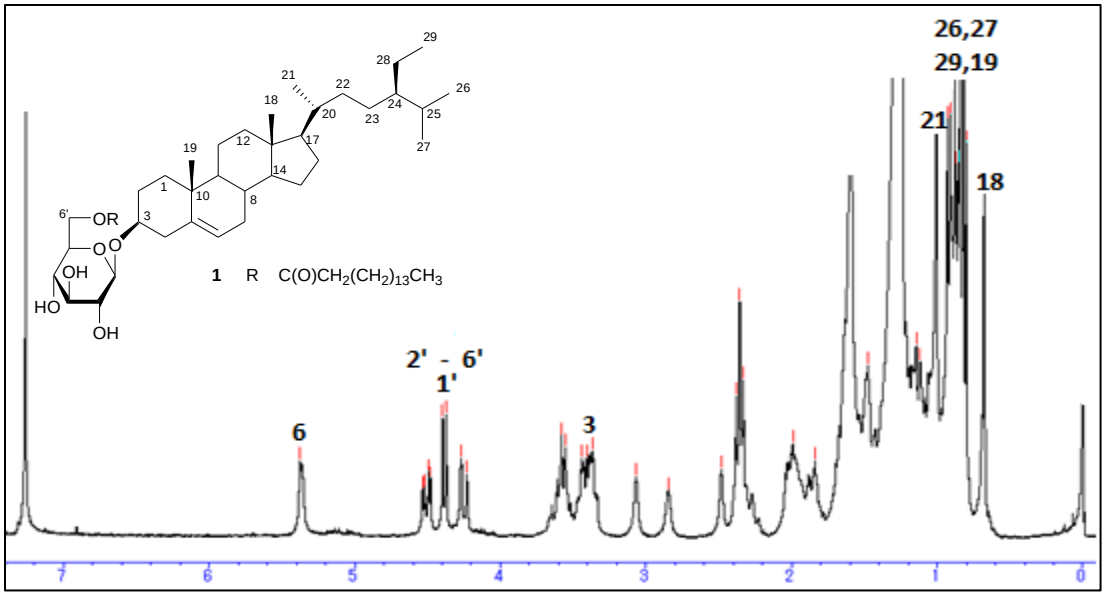

Figure 2.27 ^{1}H NMR spectrum of compound 1 (chloroform-*d*, 400 MHz)

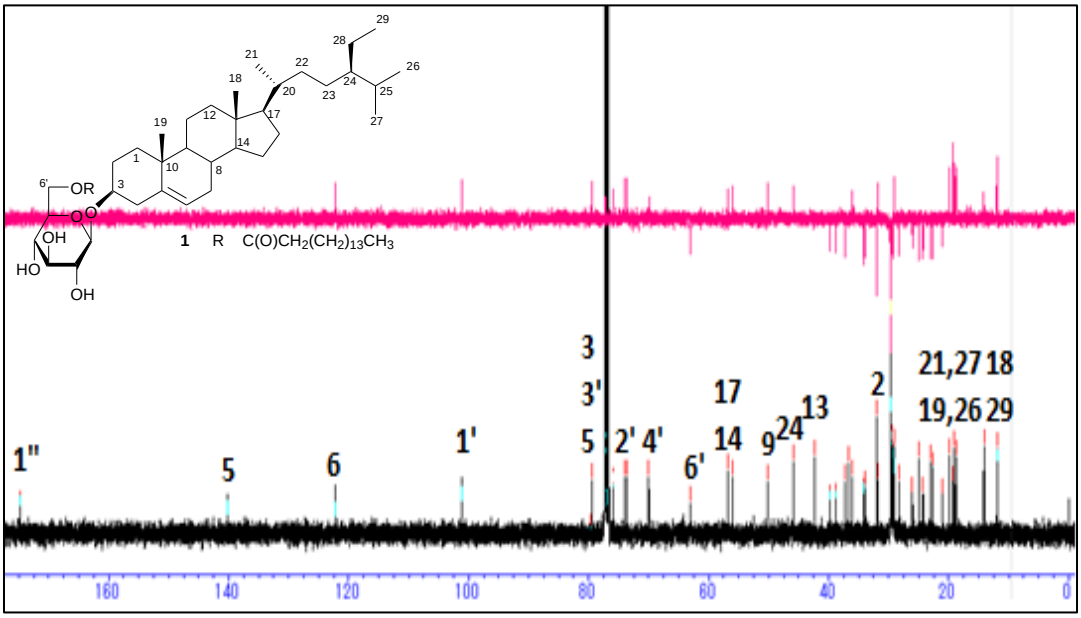

Figure 2.28 ^{13}C NMR spectrum of compound 1 (chloroform-*d*, 100 MHz)

Table 2.5 **^{1}H (300 MHz) and ^{13}C NMR (100 MHz) spectroscopic data of compound 1 (chloroform-*d*, δ values in ppm, *J* values in Hz)**

Position	***δ_C (ppm)***	***δ_H (No., M, J_{Hz})***	***Position***	***δ_C (ppm)***	***δ_H (No., M, J_{Hz})***
1	37.4(CH_2)		24	51.3(CH)	
2	29.7(CH_2)		25	29.1(CH)	
3	79.5(CH)	3.55 (1H, m)	26	19.9(CH_3)	0.89 (3H, d, *J* = 6.4)
4	38.9(CH_2)		27	19.1(CH_3)	0.87 (3H, d, *J* = 6.4)
5	140.3(C)		28	23.0(CH_2)	
6	122.2(CH)	5.38 (1H, m)	29	11.9(CH_3)	0.84 (3H, t, *J* = 7.8)
7	32.9(CH_2)		1′	101.2(CH)	4.37 (1H, d, *J* = 8)
8	32.0(CH)		2′	73.6(CH)	
9	50.2(CH)		3′	75.9(CH)	
10	36.7(C)		4′	70.0(CH)	
11	21.0(CH_2)		5′	74.0(CH)	
12	39.7(CH_2)		6′	63.1(CH_2)	
13	42.3(C)		1″	174.8(C)	
14	56.7(CH)		2″	34.2(C)	
15	24.3(CH_2)		3″	24.9(CH_2)	
16	28.2(CH_2)		4″	29.3(CH_2)	
17	56.1(CH)		5″	29.5(CH_2)	
18	11.8(CH_3)	0.68 (3H, s)	6″	29.7(CH_2)	
19	19.3(CH_3)	1.01 (3H, s)	7″ ~ 12″	29.7(CH_2)	1.25 (12H, br. s)
20	36.1(CH)		13″	29.3(CH_2)	
21	18.8(CH_3)	(0.97, d, *J* = 6.4)	14″	31.8(CH_2)	
22	33.9(CH_2)		15″	22.7(CH_2)	
23	26.1(CH_2)		16″	14.1(CH_3)	0.84 (3H, s)

Discussion

Compound **1** (28 mg) was obtained as a white amorphous solid from fraction H-10 showing as single spot on silica gel TLC plate. In the IR spectrum, compound **1** exhibited a strong absorption at 3350 cm^{-1} indicating the presence of a hydroxy group and a band at 1720 cm^{-1} (carbonyl) indicating a stretching of a normal aliphatic ester.

The ^{1}H, ^{13}C NMR and DEPT spectral data of compound **1** in chloroform-*d* showed resonances of a carboxylic acid group (δ_C 174.8), a long methylene chain centred at δ_H 1.25 as a broad singlet, (δ_C 29.1 ~ 29.9) and overlapped methyls at δ_H 0.68 ~ 0.85 (δ_C 14.1), indicating normal type terminal methyls of the fatty acids. The characteristic signals of a β-sitosterol skeleton were determined as follows: a methine proton at δ_H 3.55 (1H, m, H-3, δ_C 79.5) and an olefinic proton signal at δ_H 5.38 (1H, m, H-6, δ_C 122.2) were assigned as H-3 and H-6 respectively. Two angular methyl protons at δ_H 0.68 (3H, s) and 1.01 (3H, s), corresponding to δ_C 11.8 and 19.3 were assigned as H_3-18 and H_3-19 respectively. The proton signals at δ_H 0.89 (3H, d, J = 6.4, δ_C 19.9, H_3-26) and 0.87 (3H, d, J = 6.4, δ_C 19.1, H_3-27) indicated the presence of an isopropenyl group in the molecular structure. The proton signal at δ_H 0.84 (3H, t, J = 7.8 Hz, δ_C 11.9) was assigned as H_3-29. All other NMR assignments agreed with known β-sitosterol-3-*O*-β-D-glucopyranoside-6′-*O*-fatty acid esters. Characteristic signals indicative of a presence of a monosaccharide moiety at δ_H 3.38 ~ 4.53, 6H with an anomeric proton signal at δ_H 4.37 (1H, d, J = 7.8 Hz, δ_C 101.2) were observed (Figure 2.27 ~ 8 and Table 2.5).

The coupling constant of the anomeric proton at δ_H 4.38 (1H, d, J = 8 Hz) and the chemical shift of the anomeric carbon δ_C (101.2, C-1′) confirmed the β-configuration of the glucopyranoside moiety (α-glucopyranoside: J = 3.7 Hz, δ_C 98.5).

The molecular formula of compound **1** was deduced to be $C_{51}H_{90}O_7$ on the basis of the NMR spectra and further confirmed by the mass spectra. The positive FAB-MS spectral data showed molecular ion peaks at *m/z*: 837.8 $[M + Na]^+$, characteristic fragments at *m/z* 395.5 $[M]^+$ (aglycone), 439.5 $[M + Na]^+$ (glycone + palmitate). These spectral analyses were compared with a reference data from literature and found to be matched (Figure 2.25 ~ 6).[126)]

Conclusion

Therefore, compound **1** was determined and assigned as β-sitosterol-3-*O*-β-D-(6'-*O*-palmitoyl)-glucopyranoside as shown in Figure 2.29.

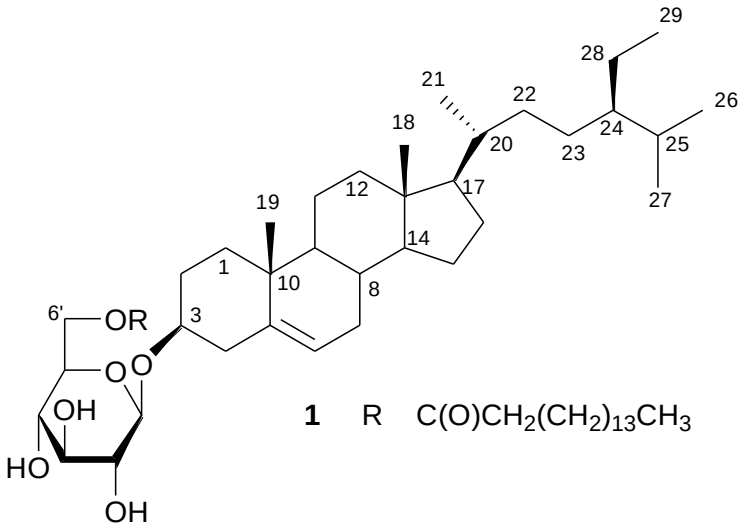

Figure 2.29 Structure of β-sitosterol-3-*O*-β-D-(6'-*O*-palmitoyl)-glucopyranoside (1)

Compound 2:

Compound **2** (40 mg) was obtained as white amorphous solid from fraction H-10 showing as a single spot on normal phase silica gel TLC.

Spectroscopic analysis:

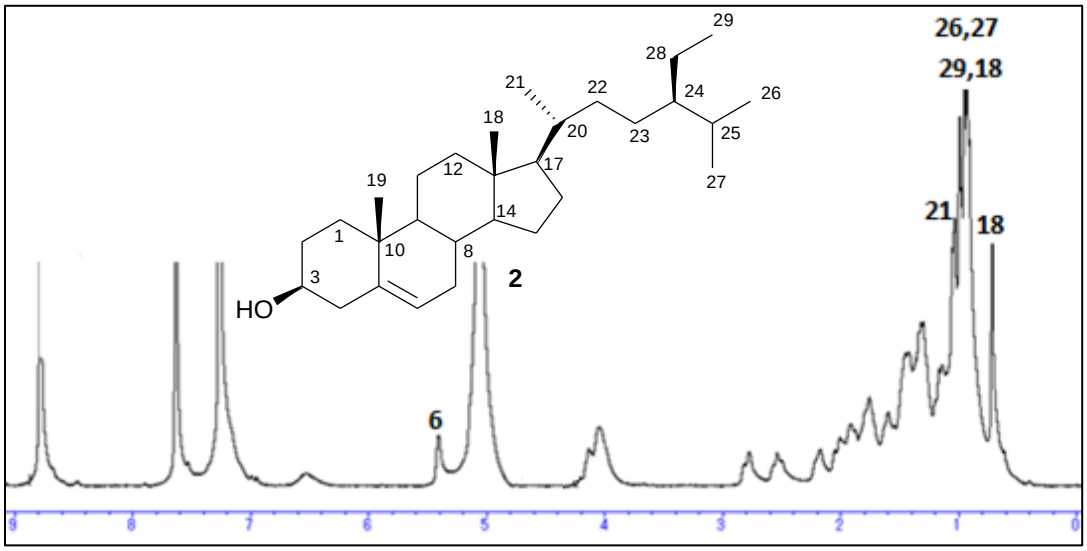

Figure 2.30 ^{1}**H NMR spectrum of compound 2 (pyridine-*d*$_5$, 300 MHz)**

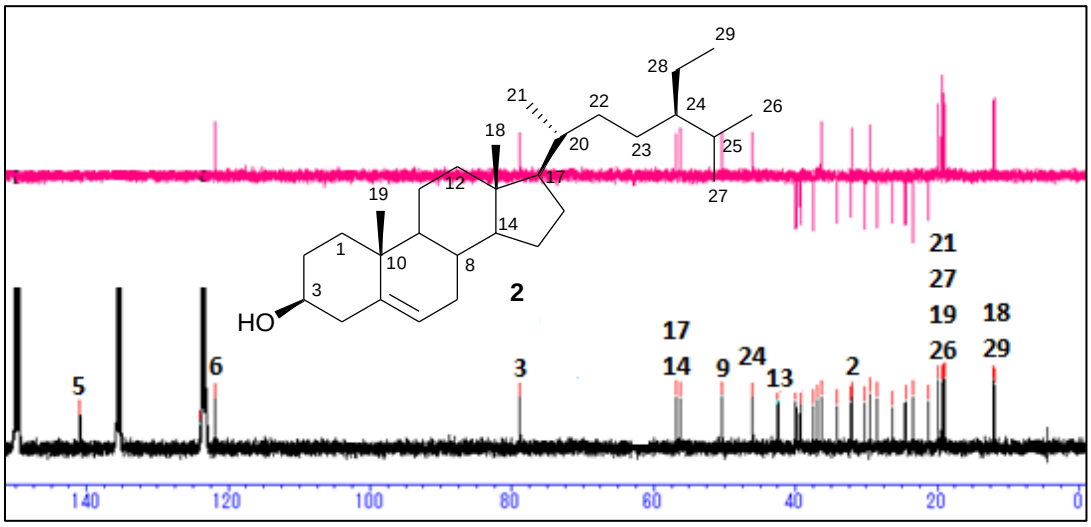

Figure 2.31 ^{13}**C NMR spectrum of compound 2 (pyridine-*d*$_5$, 100 MHz)**

Table 2.6 **^{1}H (300 MHz) and ^{13}C NMR (100 MHz) spectroscopic data of compound 2 (chloroform-*d*, δ values in ppm, *J* values in Hz)**

Position	***δ_C (ppm)***	***δ_H (No., M, J_{Hz})***	***Position***	***δ_C (ppm)***	***δ_H (No., M, J_{Hz})***
1	37.4(CH_2)		16	28.5(CH_2)	
2	30.2(CH_2)		17	56.2(CH)	
3	78.4(CH)	3.51 (1H, m)	18	11.9(CH_3)	1.03 (3H, s)
4	39.3(CH_2)		19	19.4(CH_3)	0.71 (3H, s)
5	140.9(C)		20	36.3(CH)	
6	121.9(CH)	5.31 (1H, m)	21	21.2(CH_3)	1.09 (3H, d, *J* = 6.4)
7	32.1(CH_2)		22	34.2(CH_2)	
8	32.0(CH)		23	26.4(CH_2)	
9	50.3(CH)		24	51.3(CH)	
10	36.9(C)		25	29.4(CH)	
11	21.2(CH_2)		26	19.9(CH_3)	0.80 (3H, d, *J* = 6.4)
12	39.9(CH_2)		27	21.2(CH_3)	0.82 (3H, d, *J* = 6.4)
13	42.5(C)		28	25.4(CH_2)	
14	56.8(CH)		29	12.1(CH_3)	0.83 (3H, t, *J* = 7.5)
15	24.5(CH_2)				

Discussion

Compound **2** (40 mg) was obtained as a white amorphous solid from fraction H-10 and showed as a dark purple single spot on silica gel TLC plate.

The ^{1}H, ^{13}C NMR and DEPT spectral data of compound **2** in pyridine-d_5 showed 29 resonances: six methyls, eleven methylenes, nine methines and three quaternary carbons. One methine proton at δ_H 3.51 (1H, m, H-3, δ_C 78.4) and an olefinic proton signal at δ_H 5.31 (1H, m, H-5, δ_C 121.9) were assigned as H-3 and H-6 respectively. Two angular methyl protons at δ_H 1.03 (3H, s) and 0.71 (3H, s), corresponding to δ_C 11.9 and 19.4 were assigned as H_3-18 and H_3-19 respectively. The proton signals at δ_H 0.8 (3H, d, J = 6.5 Hz, δ_C 19.9, C-26) and 0.82 (3H, d, J = 6.5 Hz, δ_C 21.2, C-27) indicated the presence of an isopropenyl group in the molecular structure. The proton signal at δ_H 0.83 (3H, d, J = 7.5 Hz, δ_C 12.1) was assigned as H_3-29 (Figure 2.30 ~ 1 and Table 2.6).

The molecular formula of compound **2** was deduced to be $C_{29}H_{50}O$ on the basis of the NMR spectra. The data were compared with reference data from literature and found to be matched.[117)]

Conclusion

Compound **2** was therefore assigned to be of β-sitosterol as shown in Figure 2.32.

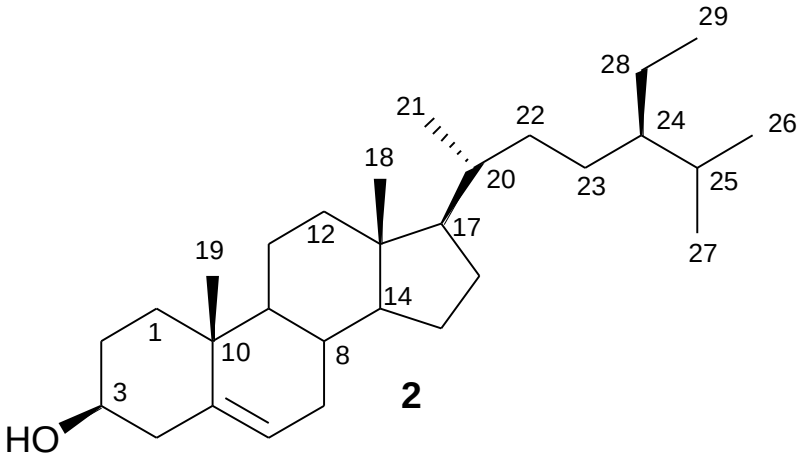

Figure 2.32 Structure of β-sitosterol (2)

Compound 3:

Compound **3** (13 mg) was obtained as white amorphous solid from fraction H-14 showing as a single spot on normal phase silica gel TLC.

Spectroscopic analysis:

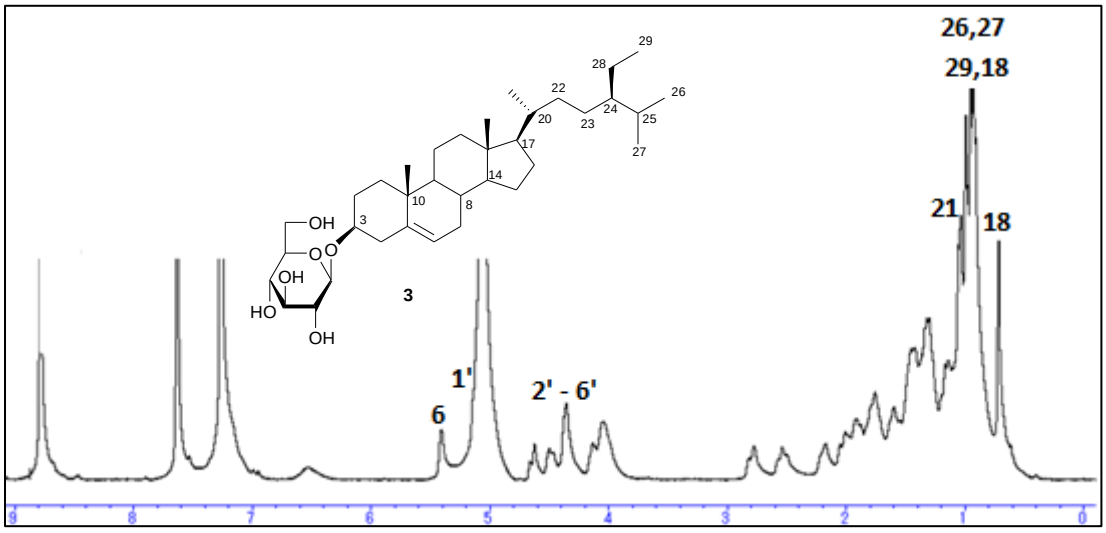

Figure 2.33 ^{1}H NMR spectrum of compound 3 (pyridine-d_5, 300 MHz)

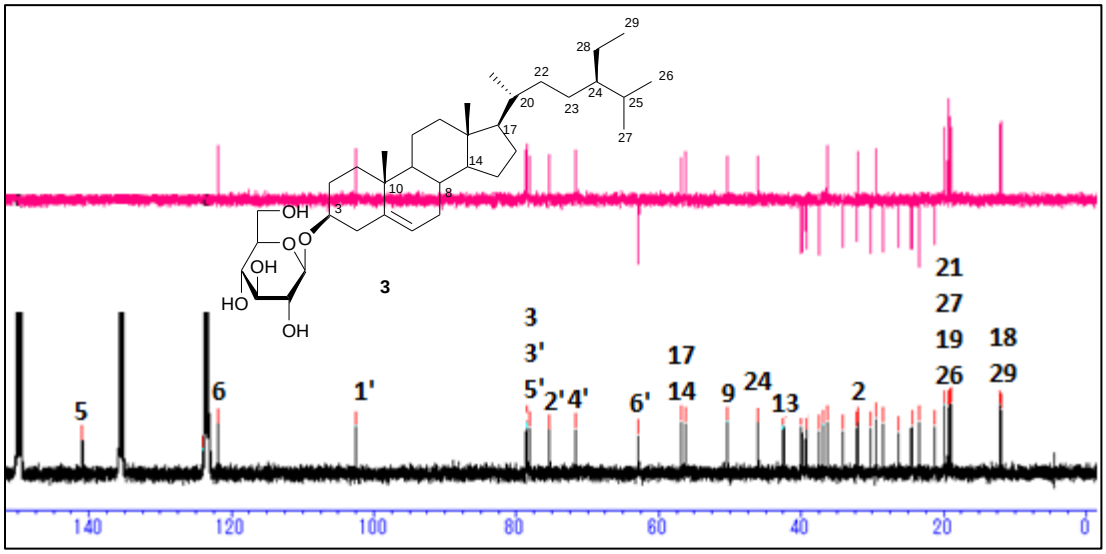

Figure 2.34 ^{13}C NMR spectrum of compound 3 (pyridine-d_5, 100 MHz)

Table 2.7 **^{1}H (300 MHz) and ^{13}C NMR (100 MHz) spectroscopic data of compound 3 (pyridine-d_5, δ values in ppm, J values in Hz)**

Position	***δ_C (ppm)***	***δ_H (No., M, J_{Hz})***	***Position***	***δ_C (ppm)***	***δ_H (No., M, J_{Hz})***
1	37.4(CH_2)		21	19.0(CH_3)	1.09 (3H, d, J = 6.4)
2	30.2(CH_2)		22	34.2(CH_2)	
3	78.4(CH)	4.06 (1H, m)	23	26.4(CH_2)	
4	39.3(CH_2)		24	46.0(CH)	
5	140.9(C)		25	29.4(CH)	
6	121.9(CH)	5.33 (1H, br. s)	26	19.9(CH_3)	0.85 (3H, d, J = 6.5)
7	32.1(CH_2)		27	19.2(CH_3)	0.87 (3H, d, J = 6.5)
8	32.0(CH)		28	23.4(CH_2)	
9	50.3(CH)		29	12.1(CH_3)	0.88 (3H, t, J = 7.5)
10	36.9(C)		1’	102.6(CH)	5.06 (1H, br. m)
11	21.2(CH_2)		2’	75.3(CH)	
12	39.9(CH_2)		3’	78.1(CH)	
13	42.5(C)		4’	71.7(CH)	
14	56.8(CH)		5’	78.4(CH)	
15	24.5(CH_2)		6’	62.8(CH_2)	
16	28.5(CH_2)				
17	56.2(CH)				
18	11.9(CH_3)	0.65 (3H, s)			
19	19.4(CH_3)	0.92 (3H, s)			
20	40.7(CH)				

Discussion

Compound **3** (13 mg) was obtained as a white amorphous solid from fraction H-14 and showed as a single spot on silica gel TLC plate.

The ^{1}H, ^{13}C NMR and DEPT spectral data of compound **3** in pyridine-d_5 showed 35 resonances: six methyls, ten methylenes, sixteen methines and three quaternary carbons. One methine proton signals at δ_H 4.06 (1H, m, H-3, δ_C 78.4) and an olefinic proton signal at δ_H 5.33 (1H, m, H-6, δ_C 121.9) were assigned as αH-3 and H-6 respectively.

Two angular methyl protons at δ_H 0.65 (3H, s) and 0.92 (3H, d, J = 6.4 Hz), corresponding to δ_C 11.9 and 19.4 were assigned as H_3-18 and H_3-19 respectively. The proton signals at δ_H 0.85 (3H, d, J = 6.5 Hz, δ_C 19.9, H_3-26) and 0.87 (3H, d, J = 6.5 Hz, δ_C 21.2, H_3-27) indicated the presence of an isopropenyl group in the molecular structure. The proton signal at δ_H 0.88 (3H, t, J = 7.5 Hz, δ_C 12.1) was assigned for H_3-29.

Characteristic signals indicative of a presence of a monosaccharide moiety at δ_H 3.38 ~ 5.06 (6H). The chemical shift of the anomeric carbon (δ_C 102.6) confirmed the β-configuration of the glucopyranoside moiety (α-glucopyranoside: J = 3.7 Hz, δ_C 98.5), (Figure 2.33 ~ 4 and Table 2.7). The signal due to αH-3 proton shifted downfield at δ_H 4.06 (1H, m, αH-3) which was expected at δ_H 3.505 for the Δ^5 –sterols also indicated that the glucose moiety was attached at C-3 of the aglycone in the β position

The molecular formula of compound **3** was deduced to be $C_{35}H_{60}O_6$ on the basis of the NMR spectra. The data were compared with reference data from literature and found to be matched.[117)]

Conclusion

Compound **3** was therefore assigned as β-sitosterol-3-*O*-β-D-glucopyranoside as shown in Figure 2.35.

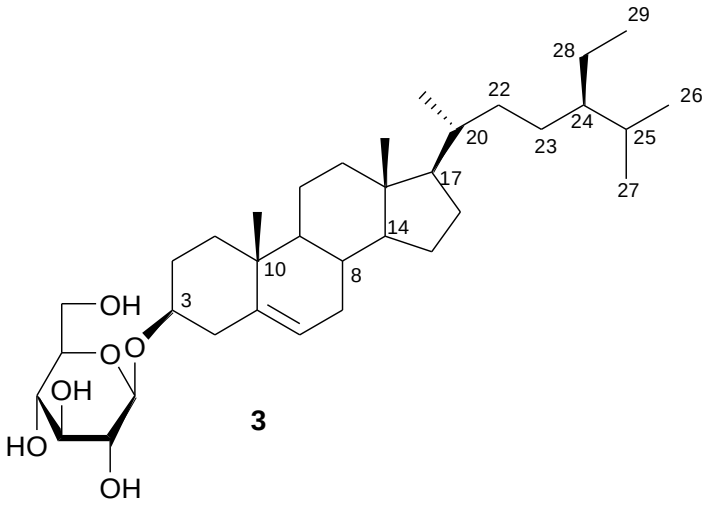

3

Figure 2.35 Structure of β-sitosterol-3-*O*-β-D-glucopyranoside (3)

Compound 4:

Compound **4** (15 mg) was obtained as white amorphous solid from fraction H-10 showing as a single spot on normal phase silica gel TLC.

Spectroscopic analysis:

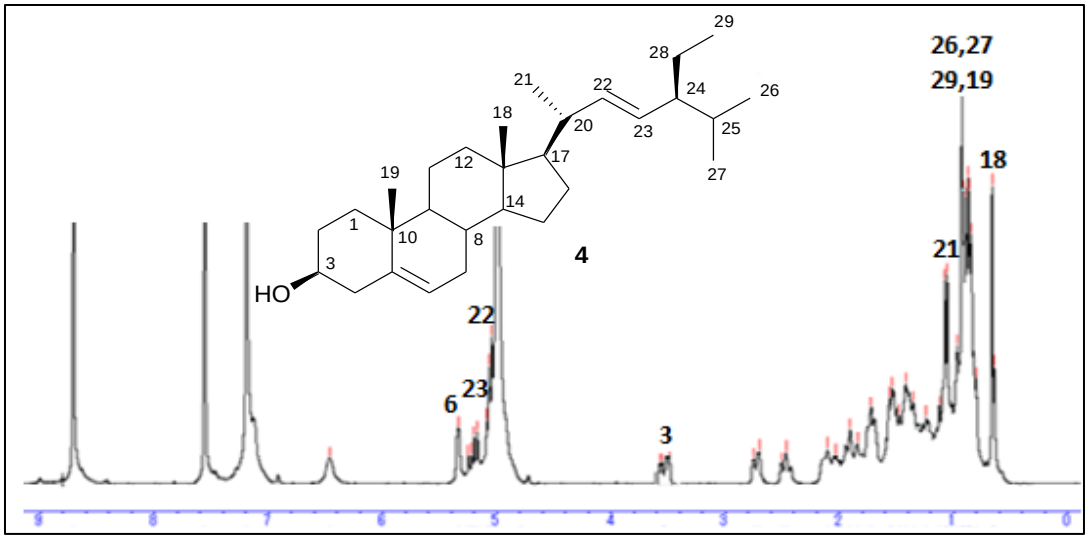

Figure 2.36 **^{1}H NMR spectrum of compound 4 (pyridine-d_5, 400 MHz)**

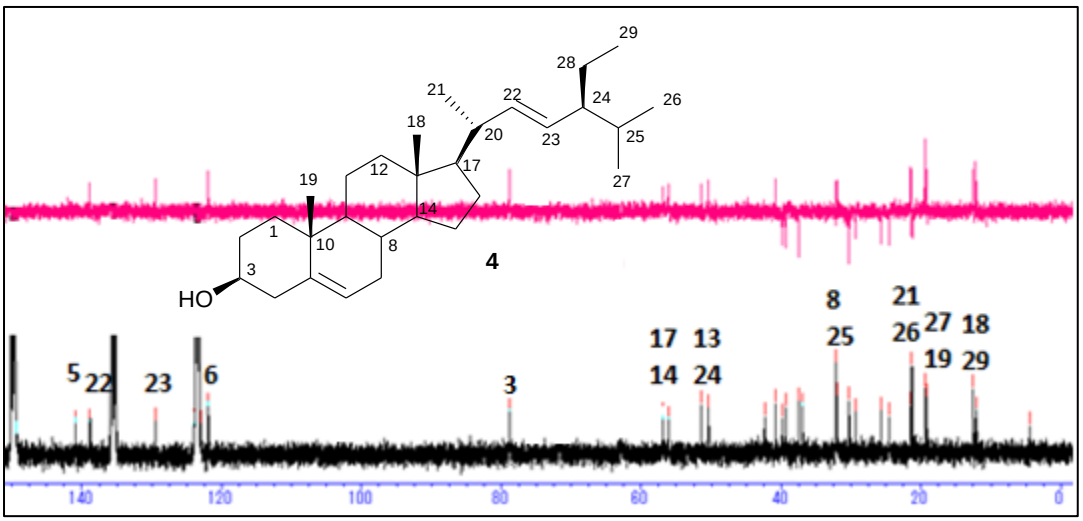

Figure 2.37 **^{13}C NMR spectrum of compound 4 (pyridine-d_5, 100 MHz)**

Table 2.8 **^{1}H (300 MHz) and ^{13}C NMR (100 MHz) spectroscopic data of compound 4 (pyridine-d_5, δ values in ppm, J values in Hz)**

Position	***δ_C (ppm)***	***δ_H (No., M, J_{Hz})***	***Position***	***δ_C (ppm)***	***δ_H (No., M, J_{Hz})***
1	37.4(CH_2)		16	28.3(CH_2)	
2	30.2(CH_2)		17	56.9(CH)	
3	78.6(CH)	3.53 (1H, m)	18	12.1(CH_3)	0.66 (3H, s)
4	39.3(CH_2)		19	19.4(CH_3)	1.01 (3H, s)
5	140.9(C)		20	40.7(CH)	
6	121.9(CH)	5.33 (1H, m)	21	21.4(CH_3)	1.05 (3H, d, J = 6.5)
7	32.1(CH_2)		22	138.8(CH)	5.15 (1H, dd, J = 8.4, 15.1)
8	32.0(CH)		23	129.4(CH)	5.02 (1H, dd, J = 8.4, 15.1)
9	50.3(CH)		24	51.4(CH)	
10	36.9(C)		25	32.1(CH)	
11	21.2(CH_2)		26	21.2(CH_3)	0.86 (3H, d, J = 7.7)
12	39.8(CH_2)		27	19.1(CH_3)	0.84 (3H, d, J = 6.1)
13	42.3(C)		28	25.7(CH_2)	
14	56.9(CH)		29	12.5(CH_3)	0.88 (3H, t, J = 7.5)
15	24.5(CH_2)				

Discussion

Compound **4** (15 mg) was obtained as a white amorphous solid from fraction H-10 and showed as a single spot on silica gel TLC plate.

The ^{1}H, ^{13}C NMR and DEPT spectral data of compound **4** in pyridine-d_5 were similar to those of compound **2**. They showed 29 resonances: six methyls, eleven methylenes, nine methines and three quaternary carbons. One methine proton at δ_H 3.53 (1H, m, H-3, δ_C 78.6) and an olefinic proton signal at δ_H 5.33 (1H, m, H-5, δ_C 121.9) were assigned as H-3 and H-6 respectively. Two angular methyl protons at δ_H 1.01 (3H, s) and 0.66 (3H, s), corresponding to δ_C 12.1 and 19.4 were assigned as H_3-18 and H_3-19 respectively.

Olefinic proton signals at δ_H 5.15 (1H, dd, J = 8.4, 15.1 Hz) and δ_H 5.02 (1H, dd, J = 8.4, 15.1 Hz) corresponding to δ_C 138.8 and δ_H 129.4 were assigned to H-22 and H-23. The proton signals at δ_H 0.86 (3H, J = 7.7, δ_C 21.2, H_3-26) and 0.84 (3H, J = 6.1, δ_C 19.1, H_3-27) indicated the presence of an isopropenyl group in the molecular structure. The proton signal at δ_H 0.88 (3H, t, J = 7.5, δ_C 12.5) was assigned as H_3-29. (Figure 2.36 ~ 7 and Table 2.8).

The molecular formula of compound **4** was deduced to be $C_{29}H_{58}O$ on the basis of the NMR spectra. The data were compared with reference data from literature and found to be matched.[117)]

Conclusion

Compound **4** was therefore assigned as β-stigmasterol as shown in Figure 2.38.

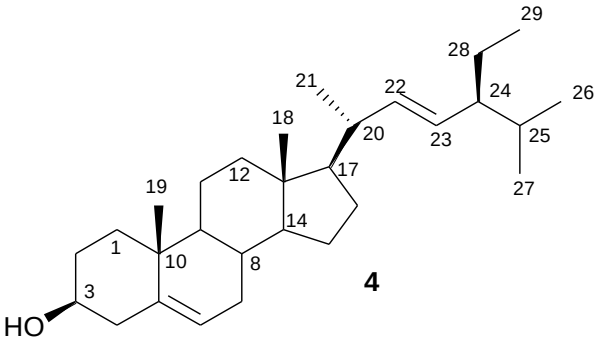

Figure 2.38 Structure of β-stigmasterol (4)

Compound 5:

Compound **5** (8 mg) was obtained as white amorphous solid from fraction H-14 showing as a single spot on normal phase silica gel TLC.

Spectroscopic analysis:

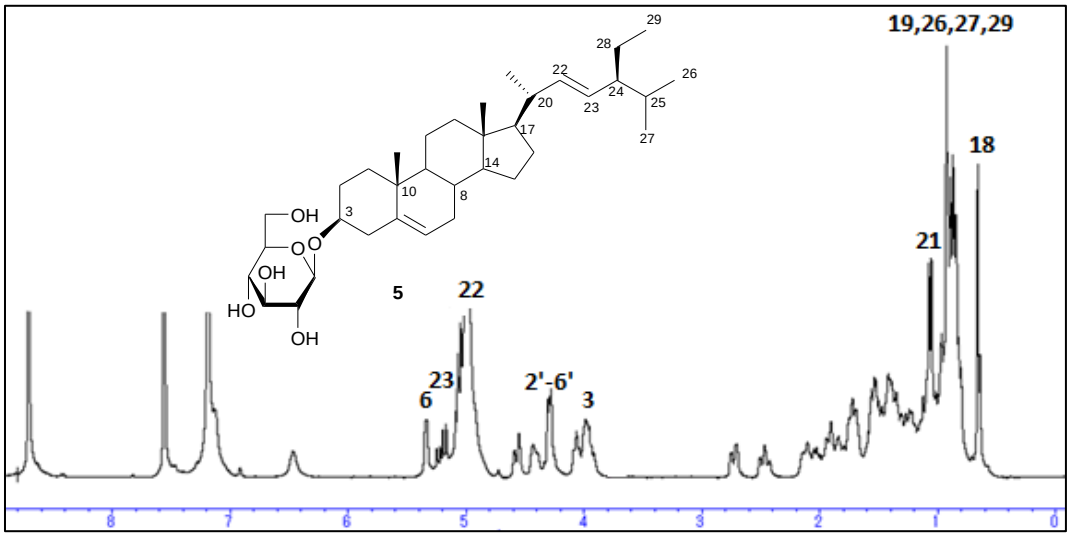

Figure 2.39 ^{1}H NMR spectrum of compound 5 (pyridine-d_5, 400 MHz)

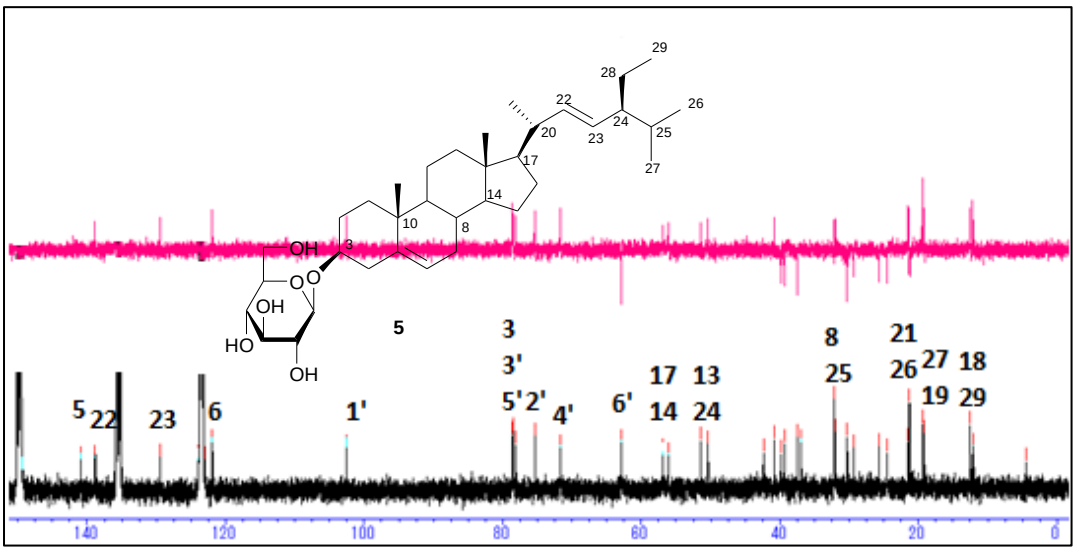

Figure 2.40 ^{13}C NMR spectrum of compound 5 (pyridine-d_5, 100 MHz)

Table 2.9 ^{1}H (300 MHz) and ^{13}C NMR (100 MHz) spectroscopic data of compound 5 (pyridine-d_5, δ values in ppm, J values in Hz)

Position	δ_C *(ppm)*	δ_H *(No., M,* J_{Hz}*)*	*Position*	δ_C *(ppm)*	δ_H *(No., M,* J_{Hz}*)*
1	37.4 (CH_2)		21	21.4 (CH_3)	1.09 (3H, d, J = 6.4 Hz)
2	30.2 (CH_2)		22	138.8 (CH)	5.07 (1H, dd, J = 8.7, 15.1)
3	78.6 (CH)	4.06 (1H, m)	23	129.4 (CH)	5.23 (1H, dd, J = 8.7, 15.1)
4	39.3 (CH_2)		24	51.4 (CH)	
5	140.9 (C)		25	32.1 (CH)	
6	121.9 (CH)	5.33 (1H, br. s)	26	21.2 (CH_3)	0.92 (3H, d, J = 6.4)
7	32.1 (CH_2)		27	19.1 (CH_3)	0.88 (3H, d, J = 6.5)
8	32.0 (CH)		28	25.7 (CH_2)	
9	50.3 (CH)		29	12.5 (CH_3)	0.89 (3H, t, J = 7.2)
10	36.9 (C)		1′	102.5 (CH)	5.07 (1H, d, J = 7.5)
11	21.2 (CH_2)		2′	75.3 (CH)	
12	39.8 (CH_2)		3′	78.1 (CH)	
13	42.3 (C)		4′	71.7 (CH)	
14	56.9 (CH)		5′	78.4 (CH)	
15	24.5 (CH_2)		6′	62.8 (CH_2)	
16	29.3 (CH_2)				
17	56.0 (CH)				
18	12.1 (CH_3)	0.68 (3H, s)			
19	19.4 (CH_3)	0.95 (3H, s)			
20	40.7 (CH)				

Discussion

Compound **5** (8 mg) was obtained as a white amorphous solid from fraction H-14 and showed as a single spot on silica gel TLC.

The NMR data of compound **5** was similar to those of compound **4** with additional signals, suggesting the same β-stigmasterol skeleton. In the ^{1}H NMR spectrum of **5** (Table 2.9), two methyl protons were connected to quaternary carbon atom at δ_H 0.65 (s) and 0.95 (s) and were assigned to H_3-18 and H_3-19 respectively. Three methyl protons were connected to methine carbons δ_H 0.85, 0.87, and 1.09 assigned for H_3-26, H_3-27, and H_3-21 respectively. One methyl (δ_H 0.88) was attached to a methylene carbon at assigned for H_3-29. In addition, a downfield resonance at δ_H 5.33 (1H, br. s) was assigned as a methine for H-6 which indicated it was attached to an olefinic carbon. The chemical shift at δ_H 4.06 indicated the presence of one carbinol proton at position 3 of the proposed skeleton. Characteristic proton signals at δ_H 4.32 ~ 4.88 (5H) and an anomeric proton signal at δ_H 5.07 (1H) indicated the presence of a monosaccharide moiety (Figure 2.39).

The ^{13}C NMR spectra of compound **5** (Table 2.9) showed 35 carbon atoms in the molecule: six methyls, ten methylenes, sixteen methines and three quaternary carbons. The olefinic resonances at δ_C 121.9, 138.8, and 129.4 corresponded to C-6, C-22 and C-23 methine carbons respectively and a signal at δ_C 140.9 corresponded to the C-5 quaternary carbon of the sterol moiety. An anomeric carbon signal at δ_C 102.5 indicated the presence of a monosaccharide moiety. Four methine resonances at δ 75.3, 78.1, 71.7, and 78.4, and a methylene resonance at δ_C 62.8 were due to C-2′, C-3′, C-4′, C-5′ and C-6′, respectively of the β-glucopyranoside. The coupling constant of the anomeric proton signal at δ_H 5.07 (1H, J = 7.5 Hz) indicated that the H-1′ proton is in the axial-axial position to H-2′ proton confirming the glucopyranoside moiety binds to the sterol moiety in the β orientation[117)] (Figure 2.40).

The molecular formula of compound **5** was deduced to be $C_{35}H_{58}O_6$ on the basis of the NMR spectra and further confirmed by comparison with a reference data.[117]

Conclusion

Compound **5** was therefore assigned as β-stigmasterol-3-*O*-β-D-glucopyranoside as shown in Figure 2.41.

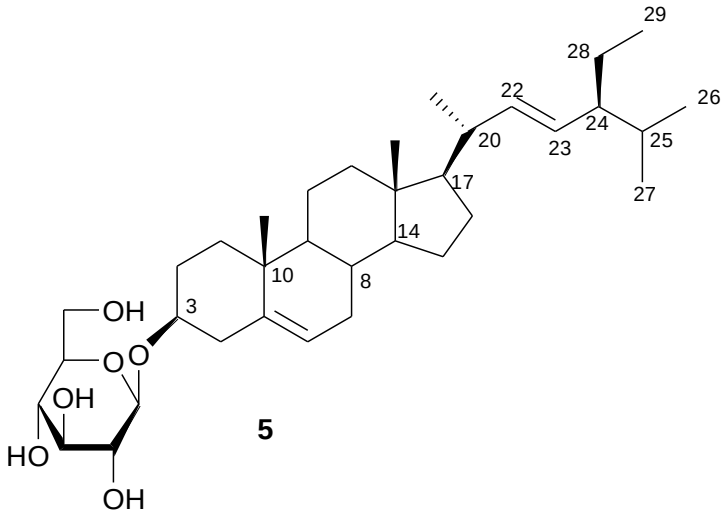

5

Figure 2.41 Structure of β-stigmasterol-3-*O*-β-D-glucopyranoside (5)

Compound 6:

Compound **6** (200 mg) was obtained as white amorphous solid from fraction H-4 showing as a single spot on normal phase silica gel TLC.

Spectroscopic analysis:

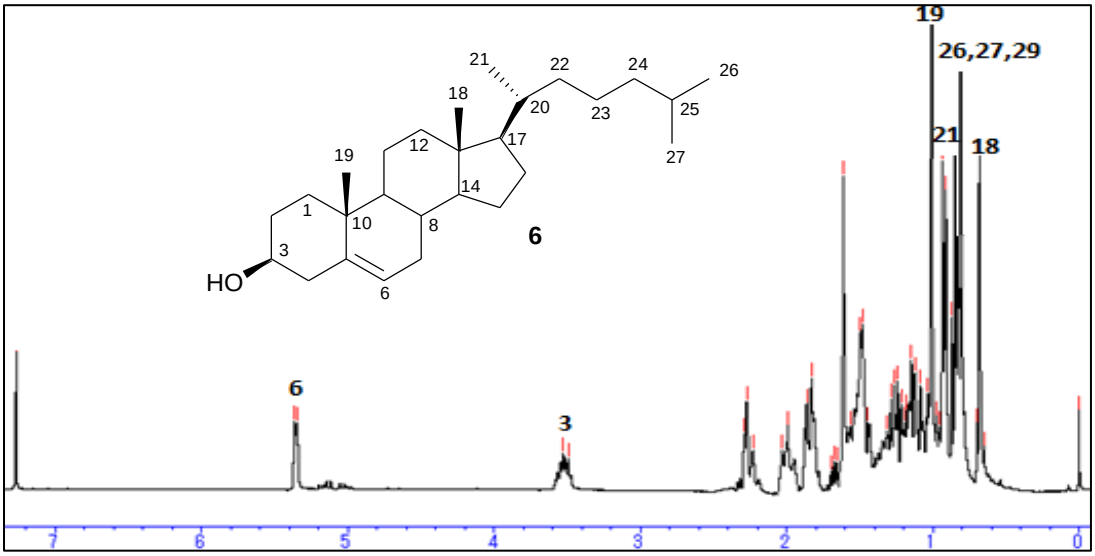

Figure 2.42 ^{1}**H NMR spectrum of compound 6 (chloroform-*d*, 400 MHz)**

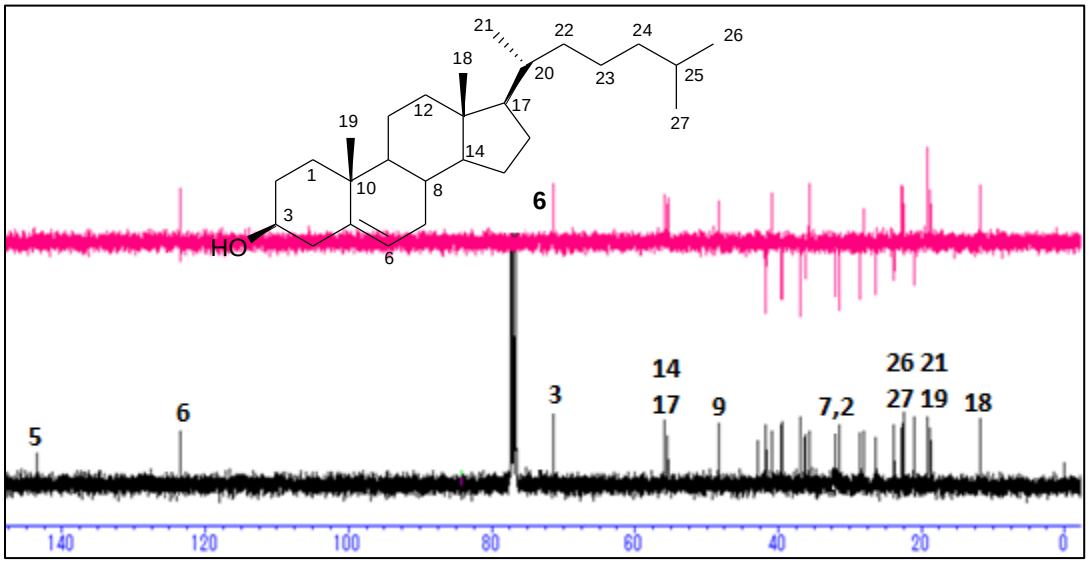

Figure 2.43 ^{13}**C NMR spectrum of compound 6 (chloroform-*d*, 100 MHz)**

Table 2.10 ^{1}H (300 MHz) and ^{13}C NMR (100 MHz) spectroscopic data of compound 6 (pyridine-d_5, δ values in ppm, J values in Hz)

Position	δ_C *(ppm)*	δ_H *(No., M, J_{Hz})*	*Position*	δ_C *(ppm)*	δ_H *(No., M, J_{Hz})*
1	37.4(CH_2)		14	56.8(CH)	
2	31.7(CH_2)		15	24.5(CH_2)	
3	71.8(CH)	3.55 (1H, m)	16	28.5(CH_2)	
4	43.3(CH_2)		17	56.2(CH)	
5	140.9(C)		18	11.9(CH_3)	0.69 (3H, s)
6	121.7(CH)	5.38 (1H, br. s)	19	19.4(CH_3)	1.02 (3H, s)
7	32.0(CH_2)		20	35.8(CH)	
8	31.7(CH_2)		21	18.7(CH_3)	0.93 (3H, d, J = 6.5)
9	50.3(CH)		22	36.2(CH_2)	
10	36.9(C)		23	23.9(CH_2)	
11	12.1(CH_2)		24	39.6(CH_2)	
12	39.8(CH_2)		25	22.6(CH)	
13	42.3(C)		26	22.6(CH_3)	0.87 (3H, d, J = 6.5)
			27	22.8(CH_3)	0.83 (3H, d, J = 6.5)

Discussion

Compound **6** (200 mg) was obtained as white amorphous solid from fraction H-4 showing as a single spot on normal phase silica gel TLC.

The ^{1}H NMR spectrum showed the chemical shift at δ_H 0.69 and 1.02 indicated the presence of two angular methyl signals at position H_3-18 and H_3-19 of the structure. One olefinic proton at δ_H 5.38 (1H, br. s) at position H-6, the signals at δ_H 0.87 (3H, d, J = 6.5 Hz) and δ_H 0.83 (3H, d, J = 6.5 Hz) due to the presence of two secondary methyl groups were assigned for position H_3-26 and H_3-27 of the skeleton respectively. The up field chemical shift at δ_H 0.93 (3H, d, J = 6.5 Hz) was assigned for the terminal methyl group at H_3-21 of the compound. The down field chemical shift at δ_H 3.55 (1H, m) indicated the presence of a carbinol proton at position H-3**.** These resonances were therefore suggestive of a steroidal skeleton (Figure 2.42 and Table 2.10).

The ^{13}C NMR spectra of compound **6** showed the presence of 27 carbons: six methyls, twelve methylenes, six methines and three quaternary carbons. Five characteristic methyl signals at δ_C 11.9, 19.4, 18.7, 22.6, 22.8, were assigned for two angular methyl groups and three terminal methyl groups at position C-18, C-19, C-21, C-26 and C-27 respectively. The downfield signals at δ_C 140.9, 129.7 were assigned for the olefinic carbons at C-5 and C-6 respectively. Similarly, the relative down field chemical shift of δ_C 71.8 was assigned for the oxymethine at position C-3. The relative stereochemistry of the hydroxy group at H-3 was proposed to be β-oriented, since the chemical shifts of the H-3 attached to β-oriented hydroxy group appears in the reference compound[118)] (Figure 2.43 and Table 2.10).

The molecular formula of compound **6** was deduced to be $C_{27}H_{46}O$ on the basis of the NMR spectra and comparison with a reference data and found to be matched.[118)]

Conclusion

Compound **6** was therefore assigned as cholesterol as shown in Figure 2.44.

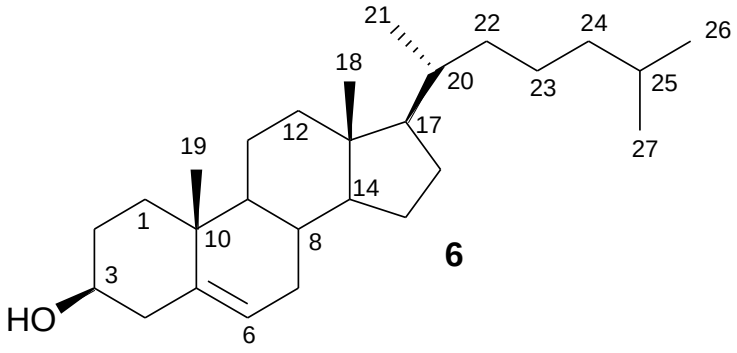

Figure 2.44 Structure of cholesterol (6)

Compound 7:

Compound **7** (22 mg) was obtained as white amorphous solid from fraction H-5 showing as a single spot on normal phase silica gel TLC.

Spectroscopic analysis:

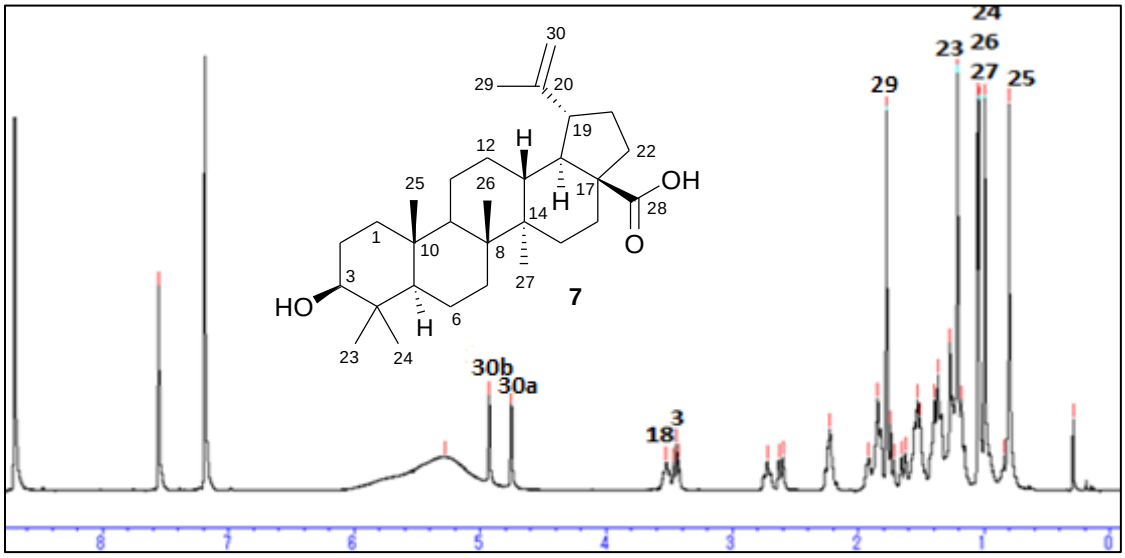

Figure 2.45 ^{1}H NMR spectrum of compound 7 (pyridine-d_5, 400 MHz)

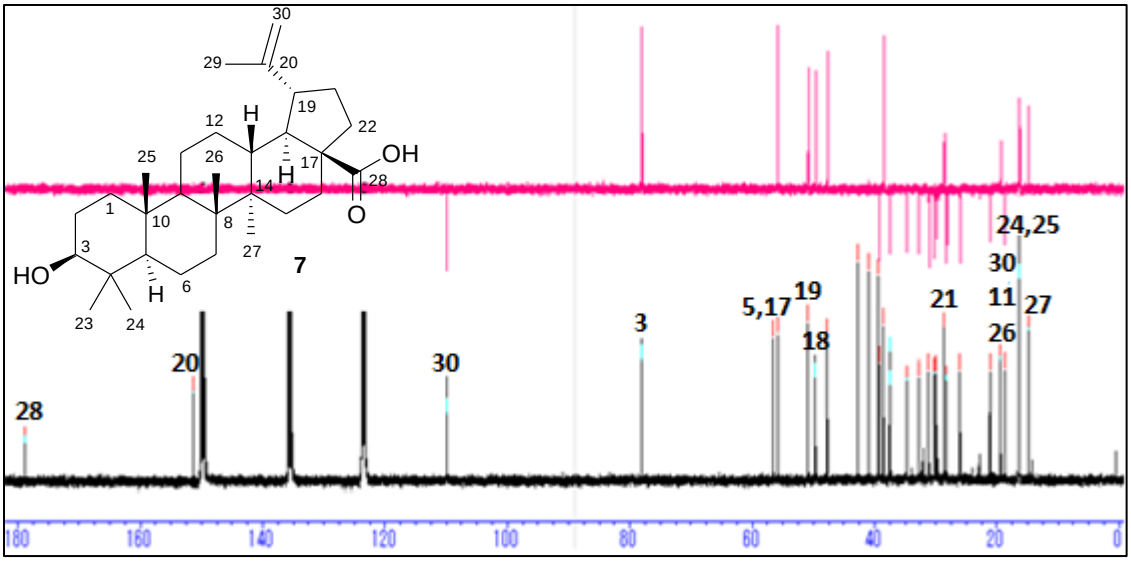

Figure 2.46 ^{13}C NMR spectrum of compound 7 (pyridine-d_5, 100 MHz)

Table 2.11 ^{1}H (300 MHz) and ^{13}C NMR (100 MHz) spectroscopic data of compound 7 (pyridine-d_5, δ values in ppm, J values in Hz)

Position	δ_C *(ppm)*	δ_H *(No., M,* J_{Hz}*)*	*Position*	δ_C *(ppm)*	δ_H *(No., M,* J_{Hz}*)*
1	39.2(CH_2)		16	32.8(CH_2)	
2	28.2(CH_2)		17	56.6(C)	
3	78.1(CH)	3.46 (1H, br. t, J = 7.7)	18	47.7(CH)	3.52 (1H, m)
4	39.5(C)		19	49.7(CH)	
5	55.9(CH)		20	151.3(C)	
6	18.7(CH_2)		21	29.96(CH_2)	
7	34.8(CH_2)		22	37.5(CH_2)	
8	41.1(C)		23	28.6(CH_3)	1.21 (3H, s)
9	50.9(CH)		24	16.3(CH_3)	1.0 (3H, s)
10	37.6(C)		25	16.3(CH_3)	0.84 (3H, s)
11	21.1CH_2)		26	16.4(CH_3)	1.04 (3H, s)
12	26.1(CH_2)		27	14.9(CH_3)	1.05 (3H, s)
13	38.6(CH)		28	178.9(C)	
14	42.8(C)		29	19.4(CH_3)	1.78 (3H, s)
15	30.2(CH_2)		30a	109.9(CH_2)	4. 76 (1H, br. s)
			30b		4. 93 (1H, br. s)

Discussion

Compound **7** (22mg) was obtained as white amorphous solid from fraction H-5 showing as a single spot on normal phase silica gel TLC.

The ^{1}H NMR spectrum showed five tertiary methyl groups at δ_H 0.84 ~ 1.21 and one isopropenyl moiety with signals at δ_H 1.78, 4.55 and 4.67, indicating a lupane-type skeleton. The chemical shift of five tertiary methyls as singlets at δ_H 1.21, 1.0, 0.84, 1.04 and 1.05 and were assigned H_3-23 ~ H_3-27 respectively of the structure. A vicinal methyl at δ_H 1.78 was assigned for H_3-29. Characteristic exomethylene proton signals at δ_H 4.76 (1H, br. s) and 4.93 (1H, br. s) were assigned as H_3-29. The downfield chemical shift at δ_H 3.46 (1H, br. t, J = 7.7 Hz) was assigned as a

secondary carbinol proton at position H-3 of the structure. These resonances were therefore suggestive of lupane-type pentacyclic triterpenoid structure (Figure 2.45 and Table 2.11).

The ^{13}C NMR spectra of compound **7** revealed the presence of 30 carbons which were shown by DEPT experiments to be five methyls, five quaternary carbons, one carboxylic acid, and two olefinic carbons suggesting that compound **7** is a triterpenic acid having five rings. Five characteristic methyl signals at δ_C 28.6, 16.3, 16.3, 16.4 and 14.9 were assigned for five angular methyl groups at position C-23 ~ C-27 respectively. The vicinal methyl group at δ_C 19.4 was assigned for C-30. The downfield signal at δ_C 109.9 was assigned for the exomethylene group as C-29. The relative down field chemical shift of δ_C 78.1 was assigned for the oxymethine at position C-3. The downfield resonance at δ_C 178.9 was assigned as the carboxylic acid group (Figure 2.46 and Table 2.11).

The molecular formula of compound **7** was deduced to be $C_{30}H_{48}O_3$ on the basis of the NMR spectra and comparison with a reference data and found to be matched.[119)]

Conclusion

Compound **7** was therefore assigned as betulinic acid as shown in Figure 2.47.

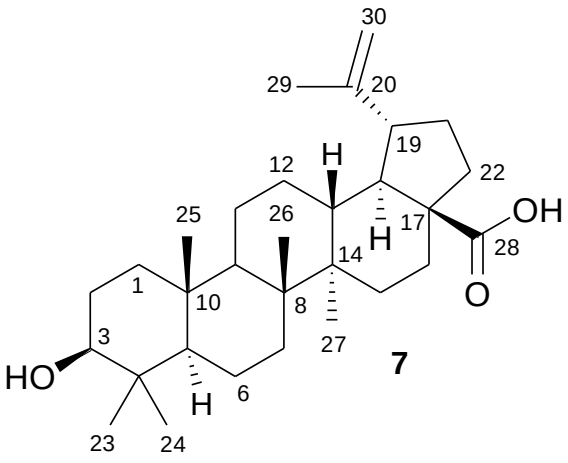

Figure 2.47 Structure of betulinic acid (7)

2.3 Secondary metabolites isolated from the ethyl acetate fraction of *Thonningia sanguinea*

Chromatographic separation of the ethyl acetate fraction, from the methanolic crude extract of *Thonningia sanguinea* led to the isolation of five known lignans: (+)-epipinoresinol (**8**), (+)-pinoresinol (**9**), (+)-cycloolivil (**10**), (+)-secoisolariciresinol (**11**) and (+)-isolariciresinol (**12**) and one known flavanone (+)-eriodictyol (**13**), as well as one saturated fatty acid (**16**) and one unsaturated fatty acid (**17**). Their structures were clarified based on chemical methods, spectroscopic techniques (NMR experiments and mass spectrometry), in addition to, the comparison with appropriate literature data. The chemical investigation of the natural products produced from the ethyl acetate fraction are discussed in this section.

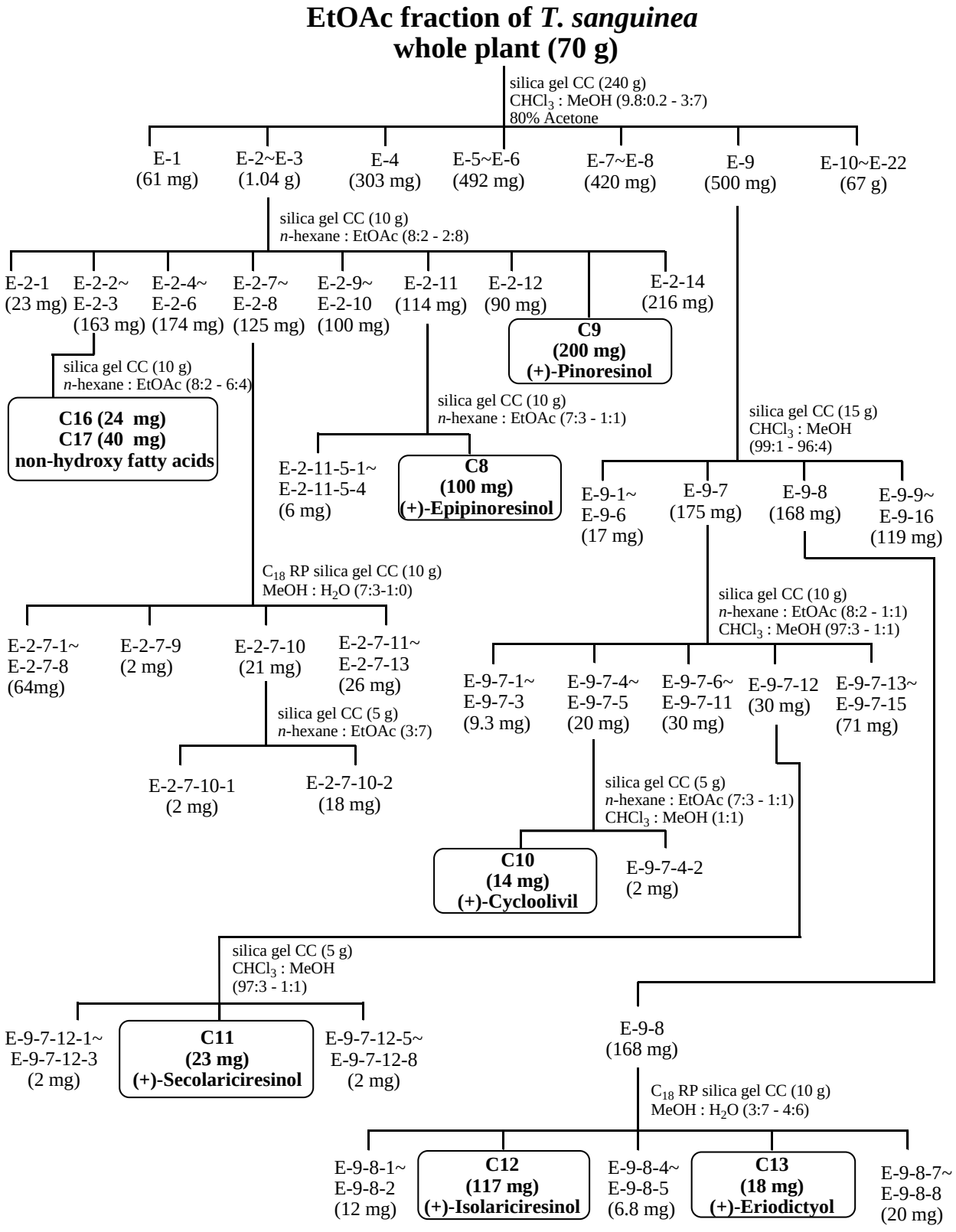

Figure 2.48 Isolation Scheme of the ethyl acetate fraction of *Thonningia sanguinea*

Compound 8:

Compound **8** (100 mg) was obtained as white amorphous solid from fraction E-2 showing as a single spot on normal phase silica gel TLC.

Spectroscopic analysis:

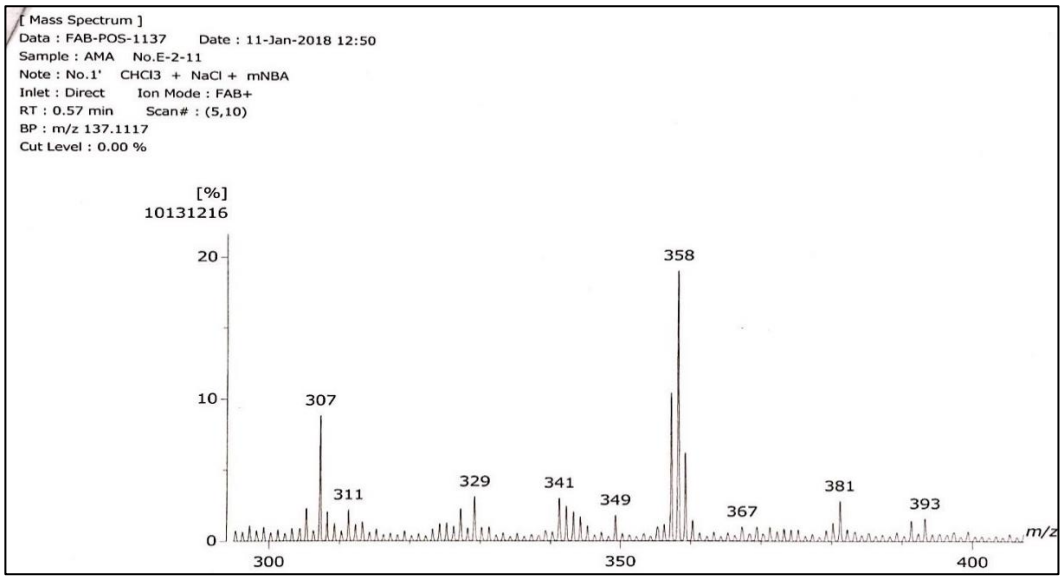

Figure 2.49 FAB-MS (positive ion mode) of compound 8

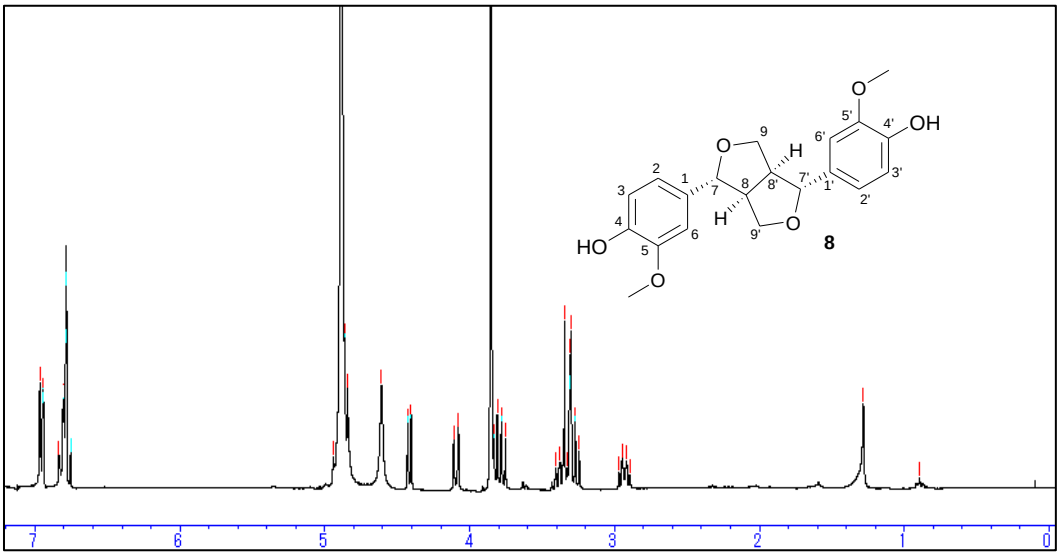

Figure 2.50 ^{1}H NMR spectrum of compound 8 (chloroform-*d*, 400 MHz)

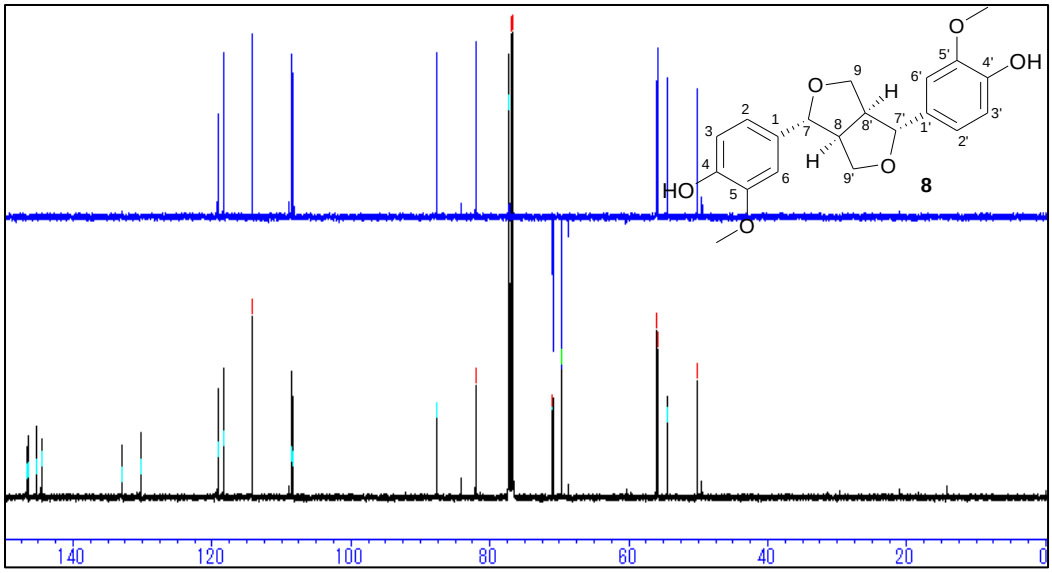

Figure 2.51 ^{13}**C NMR spectrum of compound 8 (chloroform-*d*, 100 MHz)**

Table 2.12 ^{1}H (400 MHz) and ^{13}C NMR (100 MHz) spectroscopic data of compound 8 (chloroform-*d*, δ values in ppm, *J* values in Hz)

Position	***δ_C (ppm)***	***δ_H (No., M, J_{Hz})***	***Position***	***δ_C (ppm)***	***δ_H (No., M, J_{Hz})***
1	133.0(C)		1′	130.3(C)	
2	108.5(CH)	6.95 (1H, d, *J* = 1.7)	2′	108.3(CH)	6.91 (1H, d, *J* = 1.9)
3	114.2(CH)	6.88 (1H, d, *J* = 8.1)	3′	114.9(CH)	6.88 (1H, d, *J* = 8.1)
4	145.3(C)		4′	144.6(C)	
5	146.7 (C)		5′	146.4(C)	
6	119.2(CH)	6.84 (1H, dd, *J* = 8.1, 1.9)	6′	116.4(CH)	6.79 (1H, ddd, *J* = 8.1, 1.7, 0.7)
7	87.1(CH)	4.86 (1H, d, *J* = 5.4)	7′	82.1(CH)	4.42 (1H, d, *J* = 7)
8	54.5(CH)	3.28 ~ 3.37 (1H, m)	8′	50.1(CH)	2.88 ~ 2.93 (1H, m)
9a	71.0(CH_2)	4.11 (1H, dd, *J* = 9.6, 6.3)	9′a	69.7(CH_2)	3.31 (1H, dd, *J* = 8.6, 8.3)
9b		3.85 (1H, dd, *J* = 9.6, 6.3)	9′b		3.84 (1H, dd, *J* = 9.6, 6.3)
OMe	55.9(CH_3)	3.92 (3H, s)	OMe	56.0(CH_3)	3.90 (3H, s)

Discussion

Compound **8** (100 mg) was obtained as white amorphous solid from fraction E-2 showing as a single spot on normal phase silica gel TLC.

The NMR spectra of compound **8** showed characteristic signals suggestive of a 2,6-diaryl-3,7-dioxabicyclo[3.3.0]octane skeleton. The ^{1}H NMR spectrum showed three peaks of the aromatic protons at δ_H 6.95 (1H, d, *J* = 1.7 Hz, H-2), 6.88 (2H, d, *J* = 8.1 Hz, H-3 and H-3′), 6.84 (2H, dd, *J* = 8.1, 1.9 Hz, H-6) and 6.79 (1H, ddd, *J* = 8.1, 1.7, 0.7 Hz, H-6′) suggesting that the aromatic ring has three substituted positions. The presence of oxymethine protons were evident as downfield signals at δ_H 4.86 (1H) and 4.42 (1H) as two doublet of doublets and were assigned for H-7 and H-7′ respectively. Signals of methylene protons bearing an oxygen atom were observed at δ_H 4.11 (1H), 3.89 (1H), 3.31 (1H) and 3.84 (1H), as two doublet of doublets and were assigned for H-9a (axial), H-9b (equatorial), H-9′a (axial) and H-9′b (equatorial) respectively. Two methine proton signals observed at δ_H 3.28 ~ 3.37 (1H, m) and 2.88 ~ 2.93 (1H, m), were assigned for H-8 and H-8' respectively. Two methoxy groups were confirmed at δ_H 3.92 and 3.9 as singlets (6H) and assigned for position 5-OMe and 5′-OMe respectively. The NMR assignments were done based on the proposed to symmetrical lignan structure (Figure 2.50 and Table 2.12).

The ^{13}C NMR spectrum of compound **8** exhibited signals of 20 carbons. The DEPT measurements indicated the presence of two methoxy groups, two methylene groups, ten methine groups, and six quaternary carbon. Two methoxy groups were seen at δ_C 56 and 55.9 and were assigned for C-5-OMe and C-5′-OMe respectively. The characteristic resonances of the aromatic ring were observed at δ_C 133 (C), 108.5 (CH), 114.2 (CH), 146.7 (C), 145.3 (C) and 119.2 (CH), were assigned for C-1 ~ C-6 respectively, while δ_C 130.3 (C), 108.3 (CH), 114.9 (CH), 146.4 (C), 144.6 (C) and 116.4 (CH), were assigned for C-1′ ~ C-6′ respectively. Two downfield signals δ_C 71.0 and 69.7 were determined to be methylene groups bearing an oxygen atom and were assigned C-9 and C-9′ respectively (Figure 2.51 and Table 2.12). All the signals were assigned in accordance with the proposed symmetrical lignan structure.

The molecular formula of compound **8** was deduced to be $C_{20}H_{22}O_6$ on the basis of the NMR spectra. The positive FAB-MS data showed a molecular ion peak at *m/z* 358 $[M]^+$ confirmed the

proposed molecular formula (Figure 2.49). All spectral data were compared with a reference data and found to be matched.[120)]

Conclusion

Compound **8** was therefore assigned as (+)-epipinoresinol as shown in Figure 2.52.

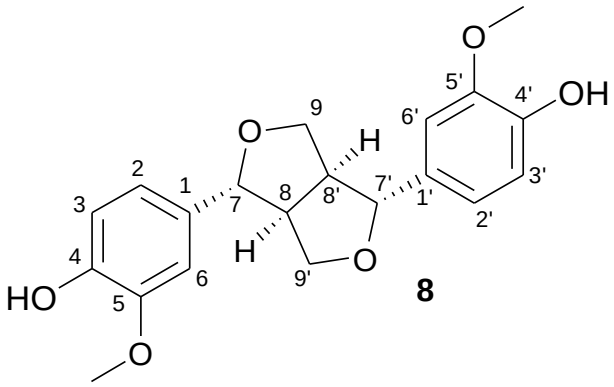

Figure 2.52 Structure of (+)-epipinoresinol (8)

Compound 9:

Compound **9** (200 mg) was obtained as white amorphous solid from fraction E-2 showing as a single spot on normal phase silica gel TLC.

Spectroscopic analysis:

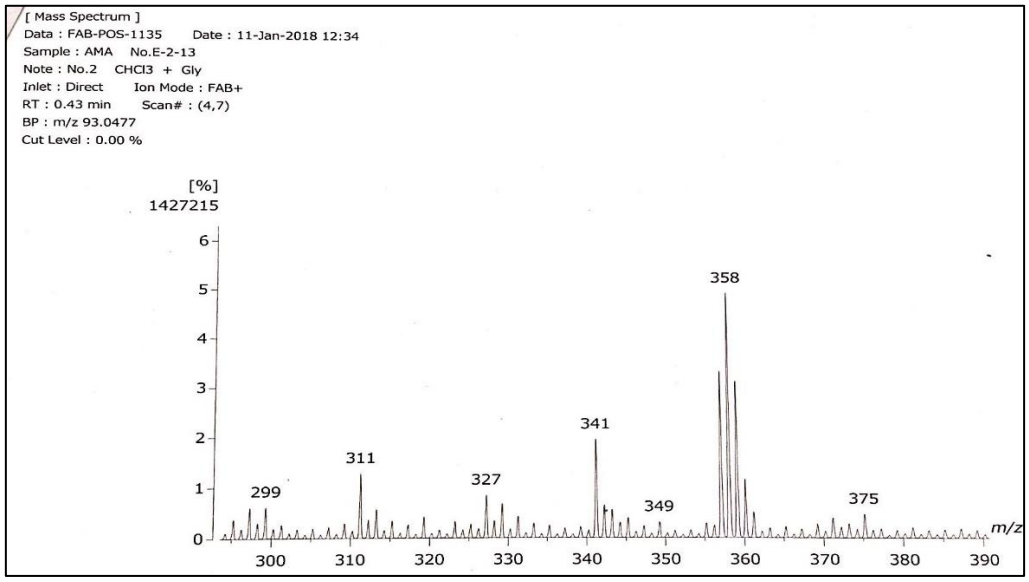

Figure 2.53 FAB-MS (positive ion mode) of compound 9

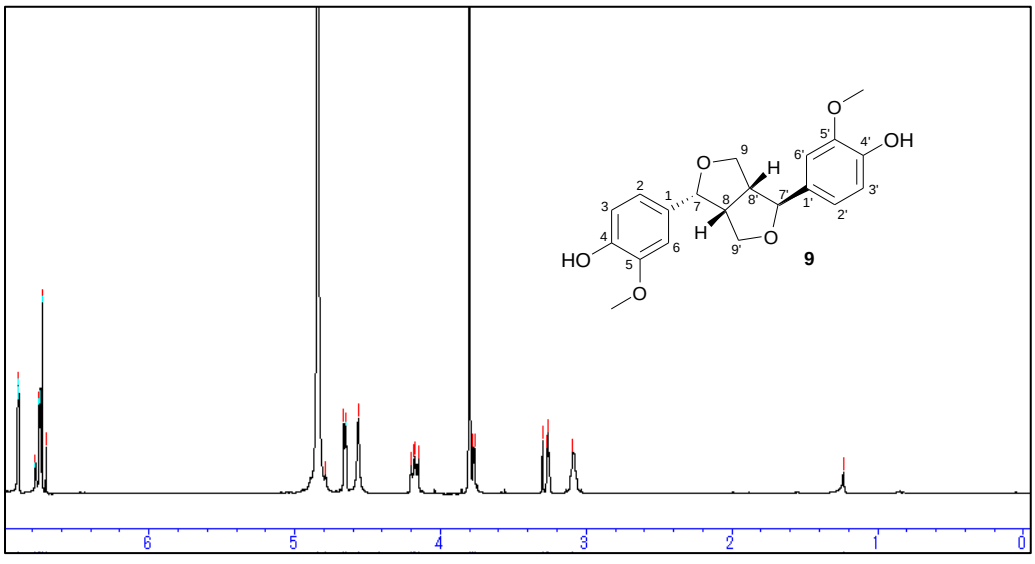

Figure 2.54 ^{1}H NMR spectrum of compound 9 (chloroform-*d*, 400 MHz)

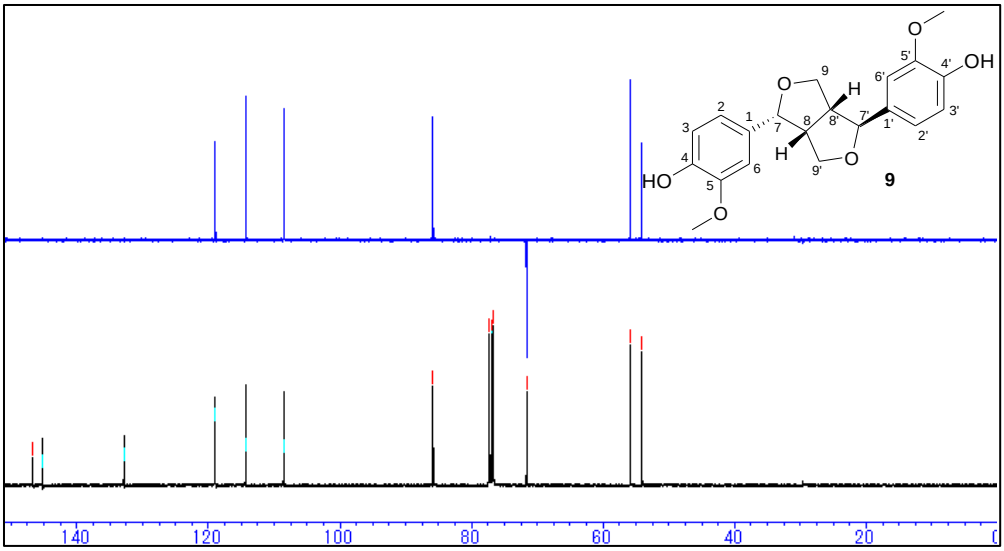

Figure 2.55 ^{13}**C NMR spectrum of compound 9 (chloroform-*d*, 100 MHz)**

Table 2.13 ^{1}H (400 MHz) and ^{13}C NMR (100 MHz) spectroscopic data of compound 9 (chloroform-*d*, δ values in ppm, *J* values in Hz)

Position	***δ_C (ppm)***	***δ_H (No., M, J_{Hz})***	***Position***	***δ_C (ppm)***	***δ_H (No., M, J_{Hz})***
1	132.9(C)		1′	132.9(C)	
2	108.6(CH)	6.9 (2H, d, *J* = 1.5)	2′	108.6(CH)	6.9 (2H, d, *J* = 1.5)
3	114.2(CH)	6.88 (1H, s)	3′	114.2(CH)	6.88 (1H, s)
4	145.2(C)		4′	145.2(C)	
5	146.4(C)		5′	146.4(C)	
6	118.9(CH)	6.81 (1H, dd, *J* = 8, 1.5)	6′	118.9(CH)	6.81 (1H, dd, *J* = 8, 1.5)
7	85.9(CH)	4.73 (1H, d, *J* = 5)	7′	85.9(CH)	4.73 (1H, d, *J* = 5)
8	54.1(CH)	3.1 (1H, m)	8′	54.1(CH)	3.1 (1H, m)
9a	71.6(CH_2)	4.24 (1H, dd, *J* = 9.5, 7)	9′a	71.6(CH_2)	4.24 (1H, dd, *J* = 9.5, 7)
9b		3.88 (1H, dd, *J* = 9.5, 4)	9′b		3.88 (1H, dd, *J* = 9.5, 4)
OMe	55.9	3.9 (3H, s)	OMe	55.9	3.9 (3H, s)

Discussion

Compound **9** (200 mg) was obtained as white amorphous solid from fraction E-2 showing as a single spot on normal phase silica gel TLC.

The NMR spectra of compound **9** showed significant similarities with that of compound **9** and was proposed to be a symmetrical lignan with the same 2,6-diaryl-3,7-dioxabicyclo[3.3.0]octane skeleton and stereochemistry.

In compound **9**, three peaks of the aromatic protons were observed at δ_H 6.9 (2H, d, *J* = 1.5 Hz, H-2, H-2′), 6.88 (2H, s, H-3, H-3′) and 6.81 (2H, dd, *J* = 8, 1.5 Hz, H-6, H-6′), suggesting that the aromatic ring has three substituted positions. The presence of two oxymethine protons were evident as downfield signals at δ_H 4.73 as a doublet and were assigned for H-7 and H-7′ respectively. Signals of methylene protons bearing an oxygen atom observed as doublets of doublets at δ_H 4.24 (2H) were assigned for H-9a (axial) and H-9′a (axial), and δ_H 3.88 (2H) were assigned for H-9b (equatorial) and H-9′b (equatorial) respectively. A methine proton was observed at δ_H 3.1 (2H, m) and was assigned for H-8 and H-8′ respectively. Two methoxy groups were confirmed at δ_H 3.9 (6H, s) and assigned for position 5-OMe and 5′-OMe respectively of the structure (Figure 2.54 and Table 2.13).

The ^{13}C NMR spectrum of compound **9** exhibited resonances for 10 carbons. The DEPT measurements indicated the presence of one methoxy group, one methylene group, five methine groups and three quaternary carbon. However, the integration values of the ^{1}H NMR and the increased intensity of the peaks in the ^{13}C NMR suggested that the structure of compound **9** has plane of symmetry, thus superimposing the identical signals of the other half of the plane of symmetry. This confirmed the proposed structure as a symmetrical lignan structure.

The two methoxy groups were confirmed at δ_C 55.9 and assigned as C-5-OMe and C-5'-OMe. The characteristic resonances of the aromatic ring at δ_C 132.9 (C), 108.6 (CH), 114.2 (CH), 145.2 (C), 146.4 (C) and 118.9 (CH) were assigned for C-1 ~ C-6 and C-1′ ~ C-6′ respectively. The downfield signal at δ_C 71.6 was assigned to two methylene groups bearing oxygen atom as C-9 and C-9′ respectively (Figure 2.55 and Table 2.13). All other signals were assigned in accordance with the proposed symmetrical lignan proposed structure.

The molecular formula of compound **9** was deduced to be $C_{20}H_{22}O_6$ on the basis of the NMR spectra. The positive FAB-MS data showed a molecular ion peak at *m/z* 358 $[M]^+$ confirmed the proposed molecular formula (Figure 2.53). The significant similarities in the NMR data as well as the both compounds **8** and **9** having the same molecular mass and formula suggests that they are epimers. All spectral data of compound **9** were compared with a reference data and found to be matched.[120)]

Conclusion

Compound **9** was therefore assigned as (+)-pinoresinol as shown in Figure 2.56.

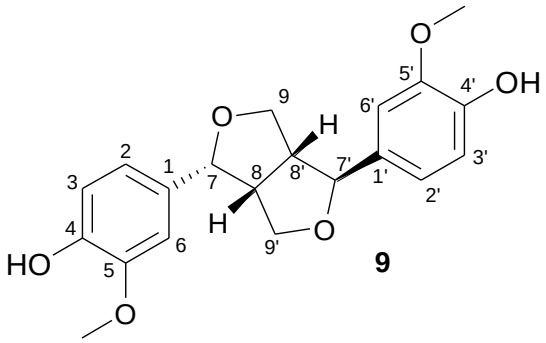

9

Figure 2.56 Structure of (+)-pinoresinol (9)

Compound 10:

Compound **10** (14 mg) was obtained as white amorphous solid from fraction E-9 showing as a single spot on normal phase silica gel TLC.

Spectroscopic analysis:

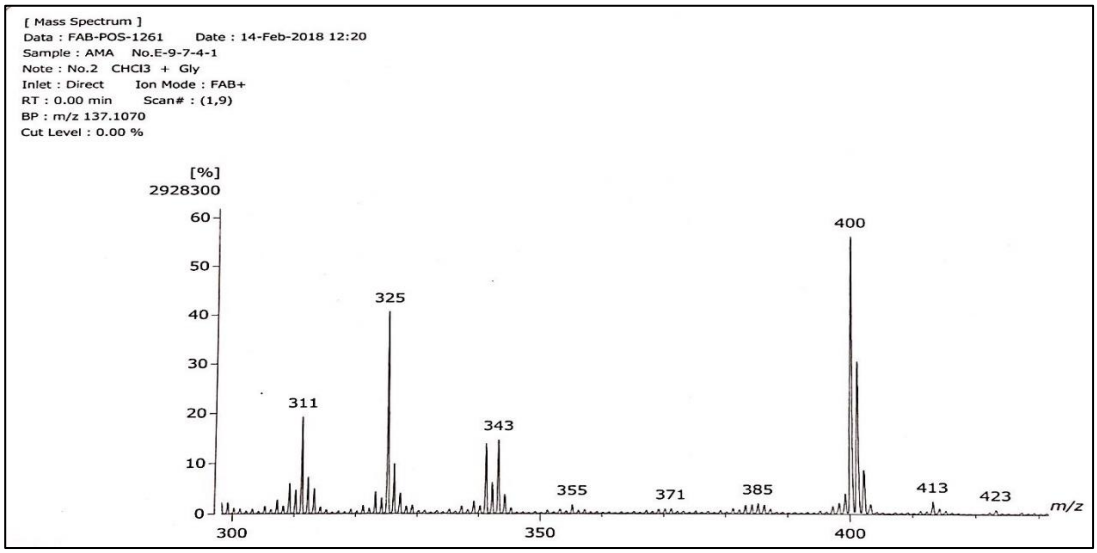

Figure 2.57 FAB-MS (positive ion mode) of compound 10

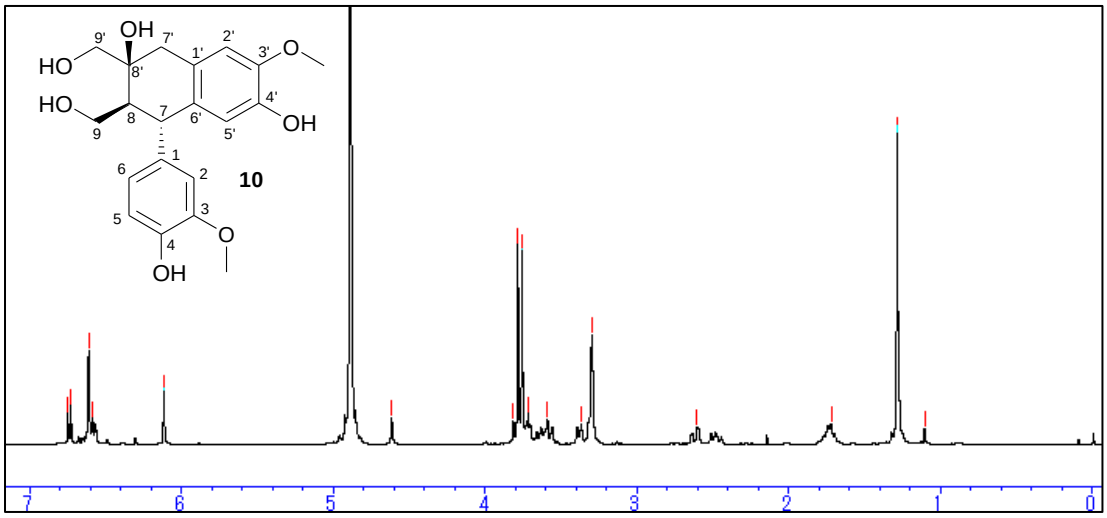

Figure 2.58 ^{1}H NMR spectrum of compound 10 (methanol-d_4, 400 MHz)

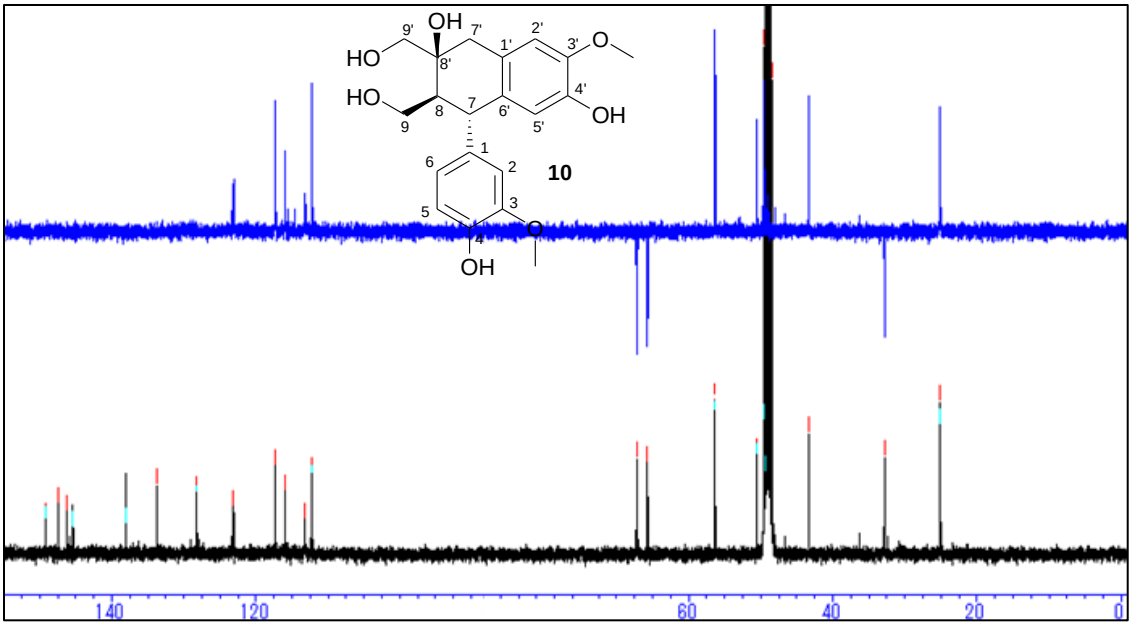

Figure 2.59 ^{13}C NMR spectrum of compound 10 (methanol-d_4, 100 MHz)

Table 2.14 ^{1}H (400 MHz) and ^{13}C NMR (100 MHz) spectroscopic data of compound 10 (methanol-d_4,, δ values in ppm, J values in Hz)

Position	δ_C *(ppm)*	δ_H *(No., M,* J_{Hz}*)*	*Position*	δ_C *(ppm)*	δ_H *(No., M,* J_{Hz}*)*
1	138.0(C)		1′	133.8(C)	
2	113.2(CH)	6.75 (1H, d, J = 8)	2′	112.4(CH)	6.61 (1H, br. s)
3	149.2(C)		3′	147.4(C)	
4	145.4(C)		4′	145.4(C)	
5	117.4(CH)	6.59 (1H, d, J = 8)	5′	116.0(CH)	6.12 (1H, s)
6	123.1(CH)	6.61 (1H, br. s)	6′	126.6(C)	
7	45.0(CH)	4.64 (1H, s)	7′a	40.1(CH_2)	2.6 (1H, m)
			7′b		3.37 (1H, m)
8	47.9(CH)	2.45 (1H, m)	8′	74.9(C)	
9a	69.5(CH_2)	3.37 (1H, m)	9′a	61 (CH_2)	3.59 (1H, m)
9b		3.72 (1H, m)	9′b		3.82 (1H, s)
OMe	56.4	3.79 (3H, s)	OMe	56.3	3.76 (3H, s)

Discussion

Compound **10** (14 mg) was obtained as white amorphous solid from fraction E-9 showing as a single spot on normal phase silica gel TLC.

The ^{1}H NMR spectrum of compound **10** revealed the presence of two methoxy groups at δ_H 3.76 and δ 3.79 and were assigned for position 3-OMe and 3′-OMe respectively. Two –CH_2OH group signals observed at δ_H 3.56 (1H, m, H-9'a -axial), 3.82 (1H, s, H-9'b -equatorial), and 3.59 (1H, m, H-9a) and 3.72 (1H, m, H-9b) were assigned. Signals characteristic of one naphthalene ring were observed at δ_H 2.6 (1H, m, H-7′a), 3.37 (1H, m, H-7′b), 2.45 (1H, m, H-8), 6.12 (1H, s, H-5′) and 6.61 (1H, br. s, H-2′) and, 4.64 (1H, s, H-7). One benzene ring with signals at δ_H 6.75 (1H, d, *J* = 8 Hz), 6.59 (1H, d, *J* = 8 Hz) and 6.61 (1H, br. s) were observed and assigned for H-2, H-5 and H-6 respectively (Figure 2.58 and Table 2.14).

The ^{13}C NMR spectra revealed 20 carbon resonances. The signals at δ_C 56.3 and 56.4 which corresponded to two methoxy groups were confirmed for C-3-OMe and C-3′-OMe. The signals at δ_C 69.5 and 61 confirmed the two –CH_2OH groups and were assigned for C-9 and C-9'. The signals at δ_C 133.8 (C), 112.4 (CH), 147.4 (C), 145.4 (C), 117.4 (CH), 126.6 (C), 40.1 (CH_2), 74.9 (C), 45 (CH) and 47.9 (CH) confirmed the presence of one naphthalene ring and were assigned as C-1' ~ C-8′, C-7 and C-8 respectively. The signals at δ_C 138 (C), 113.2 (CH), 149.2 (C), 145.4 (C), 117.4 (CH) and 123.1 (CH) confirmed the presence of one benzene ring and were assigned for C-1 ~ C-6 respectively (Figure 2.59 and Table 2.14).

The molecular formula of compound **10** was deduced to be $C_{20}H_{24}O_7$ on the basis of the NMR spectra and confirmed from its positive FAB-MS molecular ion peak at *m/z* 400 $[M + Na]^+$ (Figure 2.57). Based on these spectroscopic data and comparison with previously reported literature values, the structure of compound **10** determined.[121)]

Conclusion

Compound **10** was therefore assigned as (+)-cycloolovil as shown in Figure 2.60.

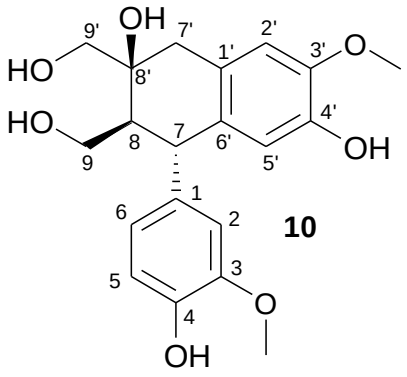

Figure 2.60 Structure of (+)-cycloolivil (10)

Compound 11:

Compound **11** (23 mg) was obtained as a yellow amorphous solid from fraction E-9 showing as a single spot on normal phase silica gel TLC.

Spectroscopic analysis:

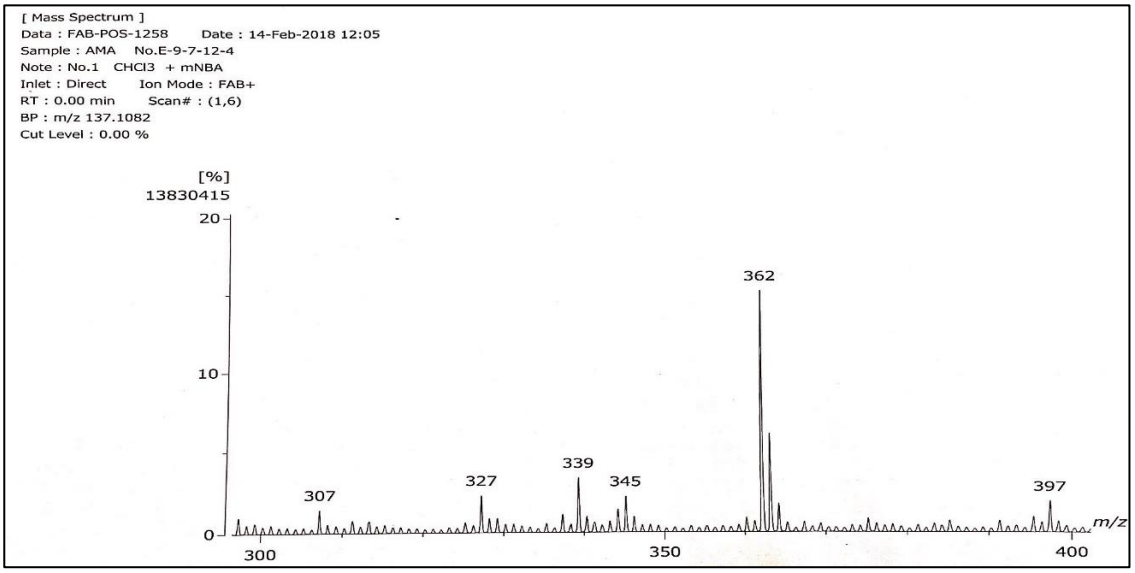

Figure 2.61 FAB-MS (positive ion mode) of compound 11

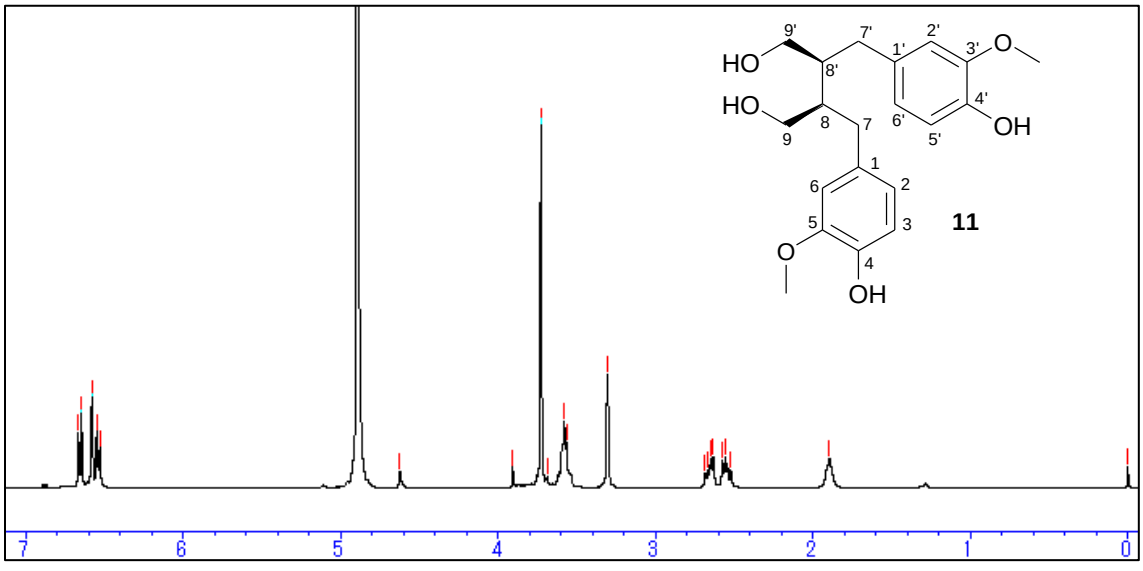

Figure 2.62 ^{1}H NMR spectrum of compound 11 (methanol-d_4, 400 MHz)

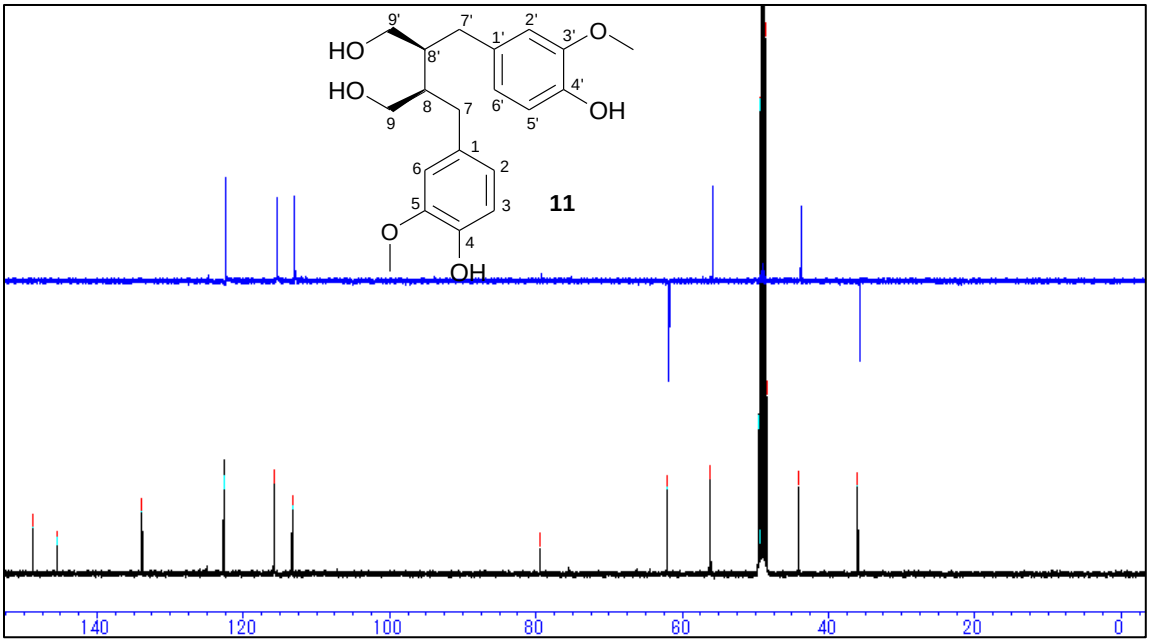

Figure 2.63 ^{13}**C NMR spectrum of 11 (methanol-*d*$_4$, 100 MHz)**

Table 2.15 ^{1}H (400 MHz) and ^{13}C NMR (100 MHz) spectroscopic data of compound 11 (methanol-d_4, δ values in ppm, J values in Hz)

Position	***δ_C (ppm)***	***δ_H (No., M, J_{Hz})***	***Position***	***δ_C (ppm)***	***δ_H (No., M, J_{Hz})***
1	133.7(C)		1′	133.7(C)	
2	122.7(CH)	6.58 (1H, d, J = 2)	2′	113.3(CH)	6.55 (1H, dd, J = 8, 2)
3	115.8(CH)	6.66 (1H, d, J = 8)	3′	148.8(C)	
4	145.5(C)		4′	145.5(C)	
5	148.8(C)		5′	115.8(CH)	6.66 (1H, d, J = 8)
6	113.3(CH)	6.55 (1H, dd, J = 8, 2)	6′	122.7(CH)	6.58 (1H, d, J = 2)
7	36 (CH_2)	2.57 (1H, dd, J = 14, 8)	7′	36.0 (CH_2)	2.57 (1H, dd, J = 14, 8)
		2.68 (1H, dd, J = 14, 7)			2.68 (1H, dd, J = 14, 7)
8	44 (CH)	1.9 (1H, br. m)	8′	44.0 (CH)	1.9 (1H, br. m)
9	62.1(CH_2)	3.58 ~ 3.69 (2H, m)	9′	62.1(CH_2)	3.58 ~ 3.69 (2H, m)
OMe	56.2	3.73 (3H, s)	OMe	56.2	3.73 (3H, s)

Discussion

Compound **11** (23 mg) was obtained as a yellow amorphous solid from fraction E-9 showing as a single spot on normal phase silica gel TLC.

The ^{1}H NMR spectrum of compound **11** showed characteristic signals suggestive of a 2,3-dibenzylbutane-1,4-diol moiety. The signals of a benzene ring at δ_H 6.66 (2H, d, *J* = 8 Hz, H-3, H-5′), 6.58 (2H, d, *J* = 2 Hz, H-2, H-6′) and 6.55 (2H, dd, *J* = 8, 2 Hz, H-6, H-2′). Signals of a two methoxy protons at δ_H 3.73 (6H, s) were assigned as two methoxy protons attached at positions 3 and 5′. A multiplet at δ_H 3.58 (4H) was assigned as two methylene protons for H_2-9 and H_2-9′. The relatively downfield signals at δ_H 2.68 (2H, dd, *J* = 14, 7 Hz) and δ_H 2.57 (2H, dd, *J* = 14, 8 Hz) were suggestive of methylene protons attached to an oxygen atom and were assigned to H-7'a, H-7a (axial), and H-7b, H-7′b (equatorial) respectively. The methine signal at δ_H 1.9 (2H, br. m) was assigned for H-8 and H-8′ respectively (Figure 2.62 and Table 2.15).

The ^{13}C NMR spectra of compound **11** exhibited signals for 10 carbons. The DEPT measurements indicated the presence of two methoxy groups, two methylene groups, two methine groups, and six quaternary carbon. However, from the proposed structure, this meant that compound **11** is a dimer and had a plane of symmetry. A methoxy group signal was seen at δ_C 56.2 and was assigned for C-3-OMe and C-5′-OMe respectively. The characteristic resonances of the benzene ring were observed at δ_C 133.7 (C), 122.7 (CH), 115.8 (CH), 145.5 (C), 148.8 (C), 113.3 (CH), and were assigned for C-1 ~ C-6 and C-1′ ~ C-6′ respectively. A downfield signal δ_C 62.1 was determined to be a methylene group bearing an oxygen atom and was assigned for C-9 and C-9′ respectively. A methylene carbon signal at δ_C 36 was assigned for C-7 and C-7′. A methine carbon signal at δ_C 44.0 was assigned for C-8 and C-8′ respectively (Figure 2.63 and Table 2.15).

The molecular formula of compound **11** was deduced to be $C_{20}H_{26}O_6$ on the basis of the NMR spectra. The positive FAB-MS data showed a molecular ion peak at *m/z* 362 $[M]^+$ confirmed the proposed molecular formula (Figure 2.61). All spectral data were compared with a reference data and found to be matched.[122)]

Conclusion

Compound **11** was therefore assigned as (+)-secoisolariciresinol as shown in Figure 2.64.

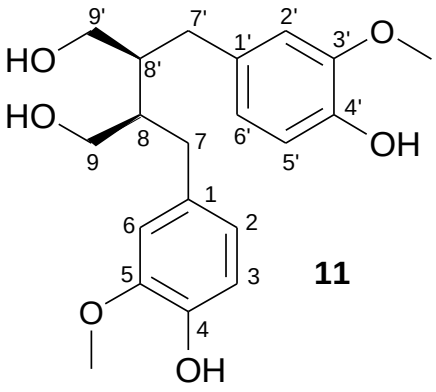

Figure 2.64 Structure of (+)-secoisolariciresinol (11)

Compound 12:

Compound **12** (117 mg) was obtained as a yellow amorphous solid from fraction E-9 showing as a single spot on normal phase silica gel TLC.

Spectroscopic analysis:

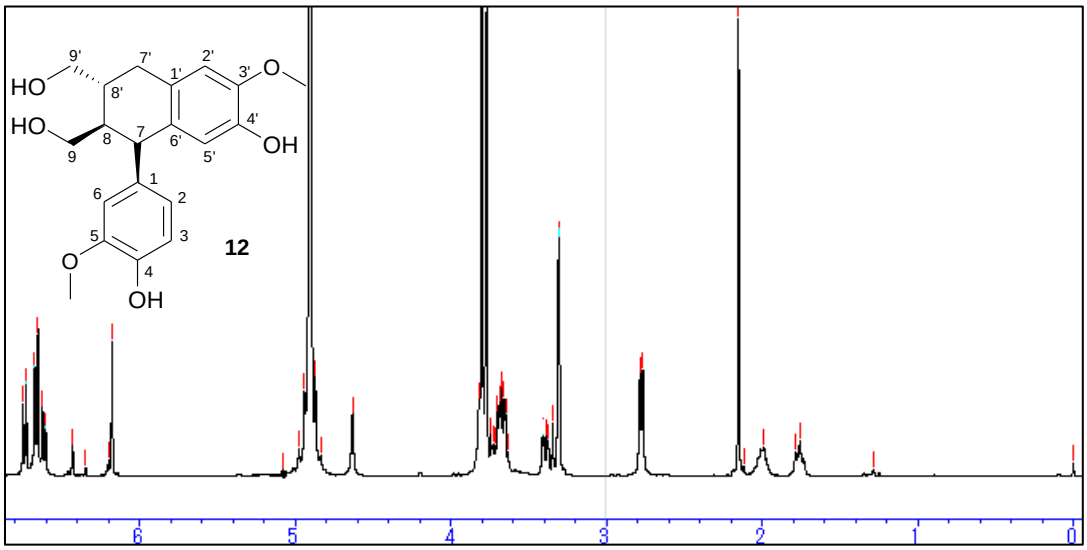

Figure 2.65 ^{1}H NMR spectrum of compound 12 (methanol-d_4, 400 MHz)

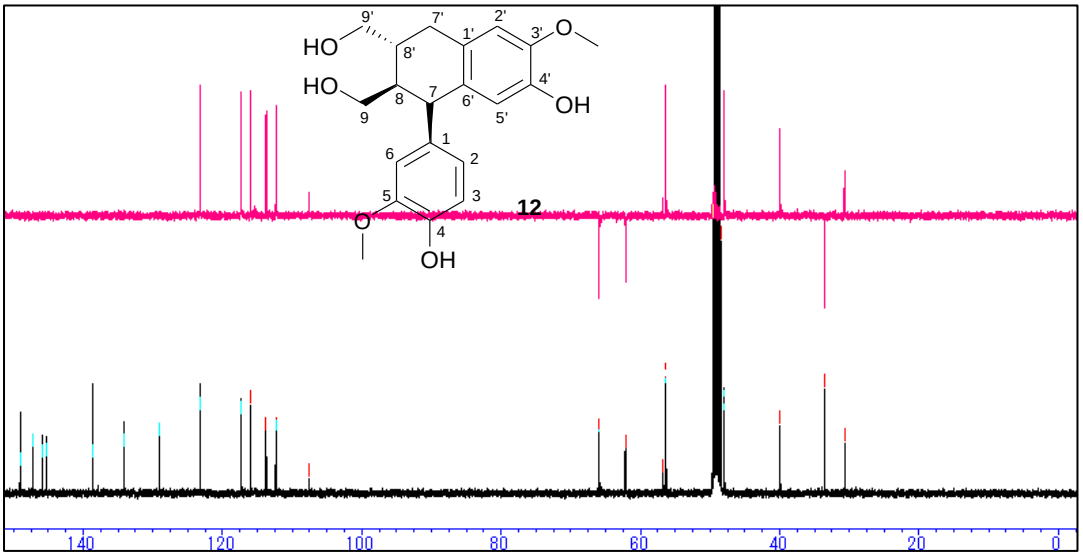

Figure 2.66 ^{13}C NMR spectrum of compound 12 (methanol-d_4, 100 MHz)

Table 2.16 ^{1}H (400 MHz) and ^{13}C NMR (100 MHz) spectroscopic data of compound 12 (methanol-d_4, δ values in ppm, J values in Hz)

Position	δ_C *(ppm)*	δ_H *(No., M,* J_{Hz}*)*	*Position*	δ_C *(ppm)*	δ_H *(No., M,* J_{Hz}*)*
1	138.6(C)		1′	129 (C)	
2	123.2(CH)	6.6 (1H, d, J = 8)	2′	112.4(CH)	6.65 (1H, d, J = 8)
3	116.0(CH)	6.73 (1H, d, J = 8)	3′	147.2(C)	
4	146.0(C)		4′	145.3(C)	
5	149.0(C)		5′	117.4(CH)	6.18 (1H, s)
6	113.8(CH)	6.18 (1H, s)	6′	134.2(C)	
7	48.0(CH)	3.74 (1H, m)	7′	33.6(CH_2)	2.77 (2H, d, J = 8)
8	47.9(CH)	1.76 (1H, br. m)	8′	39.9(CH)	1.99 (1H, br. m)
9a	65.9(CH_2)	3.63 (1H, m)	9′a	62.2(CH_2)	3.37 (1H, m)
9b		3.67 (1H, m)	9′b		3.40 (1H, m)
OMe	56.4	3.8 (3H, s)	OMe	56.3	3.77 (3H, s)

Discussion

Compound **12** (117 mg) was obtained as a yellow amorphous solid from fraction E-9 showing as a single spot on normal phase silica gel TLC.

The NMR spectra of compound **12** suggested that it was a tetrahydronaphthalene lignan hence the structure was assigned based on this proposed structure. In the ^{1}H NMR spectrum, signals of a disubstituted benzene ring at δ_H 6.6 (1H, d, J = 8 Hz, H-2), 6.73 (1H, d, J = 8 Hz, H-3) and 6.18 (1H, s, H-6) were observed. Signals of a two methoxy protons at δ_H 3.77 (3H, s) and 3.8 (3H, s) were assigned as two methoxy protons attached at positions 3 and 5′ of the structure. The relatively downfield methylene signal at δ_H 2.77 (2H, d, J = 8 Hz) were assigned for H_2-7′. The signals at 3.63 (1H, m), 3.67 (1H, m), 3.37 (1H, m) and 3.4 (1H, m) were suggestive of methylene protons attached to an oxygen atom and were assigned for H_2-9a, H_2-9b and H_2-9′a, H_2-9′b respectively. Two methine signals at δ_H 1.76 (1H, br. m) and 1.99 (1H, br. m) were assigned for H-8 and H-8′ respectively. One benzene ring was attached in the β-orientation and evident by the chemical shift signal at δ_H 3.74 (1H, m) assigned for H-7a (axial) (Figure 2.65 and Table 2.15).

The ^{13}C NMR spectra of compound **12** exhibited signals of 20 carbons. The DEPT measurements indicated the presence of two methoxy groups, three methylene groups, eight methine groups, and seven quaternary carbons. A methoxy group signal was seen at δ_C 56.2 and was assigned for C-3-OMe and C-5′-OMe respectively. The characteristic resonances of a benzene ring were observed at δ_C 138.6 (C), 123.2 (CH), 116 (CH), 146 (C), 149 (C), 113.8 (CH), and were assigned for C-1 ~ C-6 respectively. Signals for a second benzene ring attached to a saturated aromatic ring were observed at δ_C 129 (C), 112.4 (CH), 147.2 (C), 145.3 (C), 117.4 (CH), 134.2 (C), 33.6 (CH_2), 39.9 (CH), 47.9 (CH) 65.9 (CH_2) and assigned for C-1′ ~ C-8′, C-7 and C-9 respectively. A downfield signal δ_C 65.9 and 62.2 was determined to be a methylene group bearing an oxygen atom and was assigned for C-9 and C-9′ respectively. A methylene carbon signal at δ_C 48.9 and 33.6 were assigned for C-7 and C-7′ respectively. The relatively downfield signals of methine carbon at δ_C 48.0 and 39.9 suggested they were attached to an oxygen atom and were assigned for C-8 and C-8′ respectively (Figure 2.66 and Table 2.16).

The molecular formula of compound **12** was deduced to be $C_{20}H_{24}O_6$ on the basis of the NMR spectra. The positive FAB-MS data showing a molecular ion peak at *m/z* 360 $[M]^+$ confirmed the proposed molecular formula. All spectral data were in agreement with a reference data.[120)]

Conclusion

Compound **12** was therefore assigned as (+)-isolariciresinol as shown in Figure 2.67.

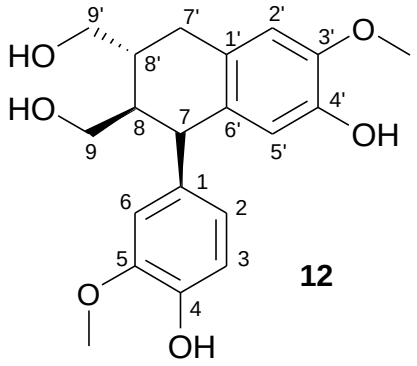

12

Figure 2.67 Structure of isolariciresinol (12)

Compound 13:

Compound **13** (18 mg) was obtained as a yellow amorphous powder from fraction E-9 showing as a single orange spot on normal phase silica gel TLC.

Spectroscopic analysis:

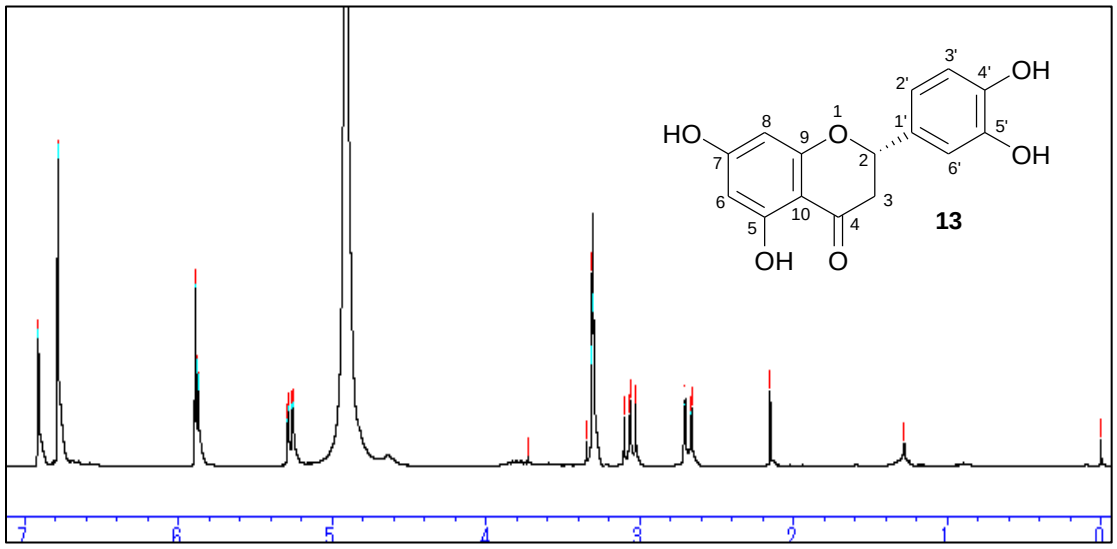

Figure 2.68 ^{1}H NMR spectrum of compound 13 (methanol-d_4, 400 MHz)

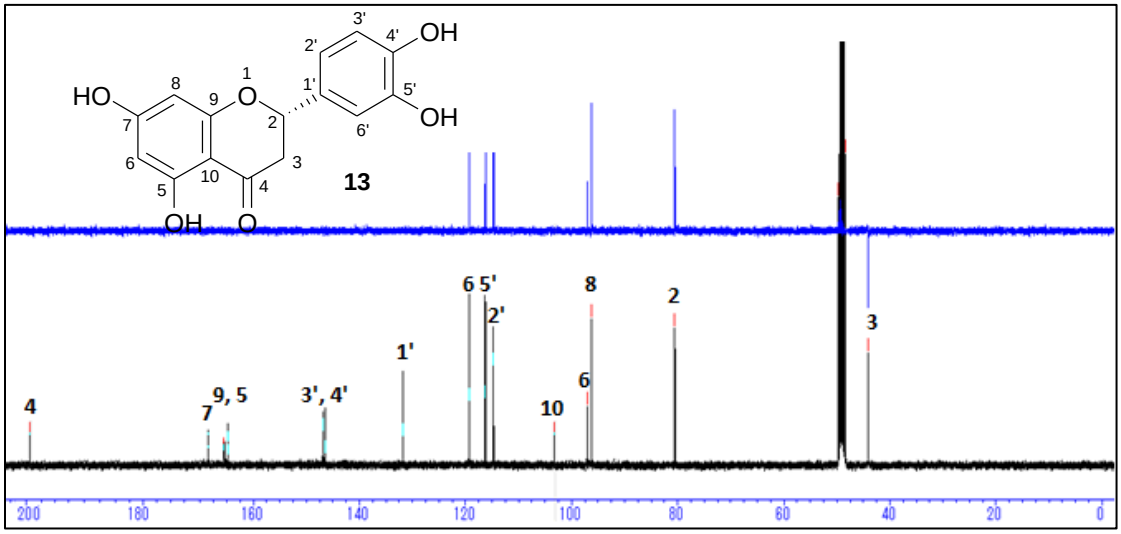

Figure 2.69 ^{13}C NMR spectrum of compound 13 (methanol-d_4, 100 MHz)

Table 2.17 ^{1}H (400 MHz) and ^{13}C NMR (100 MHz) spectroscopic data of compound 13 (methanol-d_4, δ values in ppm, J values in Hz)

Position	δ_C *(ppm)*	δ_H *(No., M,* J_{Hz}*)*	*Position*	δ_C *(ppm)*	δ_H *(No., M,* J_{Hz}*)*
2	80.5(CH)	5.26 (1H, dd, J = 12.8, 3)	1′	131.8(C)	
3a	44.1(CH_2)	2.67 (1H, dd, J = 17.2, 3)	2′	114.7(CH)	6.91 (1H, s)
3b		3.06 (1H, dd, J = 17.2, 12.8)			
4	197.8(C)		3′	146.5(CH)	6.79 (1H, br. s)
5	165.5(C)		4′	146.9(C)	
6	97.1(CH)	5.88 (1H, d, J = 2.2)	5′	116.3(C)	
7	168.5(C)		6′	119.3(CH)	6.79 (1H, br. s)
8	96.2(CH)	5.88 (1H, d, J = 2.2)			
9	164.9(C)				
10	103.4(C)				

Discussion

Compound **13** (18 mg) was obtained as a yellow amorphous powder from fraction E-9 showing as a single orange spot on normal phase silica gel TLC.

The ^{1}H NMR spectrum of compound **13** showed characteristic signals of a flavanone skeleton. The signals of a dihydroxy-substituted benzene B ring at δ_H 6.91 (1H, s, H-2′), 6.78 (2H, s, H-6′ and H-3′) were observed. The relatively downfield signals at δ_H 3.06 (1H, dd, J = 17.2, 12.8 Hz) and 2.67 (1H, dd, J = 17.2, 12.8 Hz) were suggestive of diastereotopic methylene protons bonded at C-3 and were assigned to H-3a (axial) and H-3b (equatorial) respectively. The methine signals at δ_H 5.26 (1H, dd, J = 12.8, 3 Hz) and 5.88 (2H, d, J = 2.2 Hz) were assigned for H-2, and H-6 and H-8 respectively (Figure 2.68 and Table 2.17).

The ^{13}C NMR spectra of compound **13** exhibited signals of 15 carbons. The DEPT measurements indicated the presence of one methylene, six methines, seven quaternary carbons, and one carbonyl carbon. A characteristic carbonyl resonance observed at δ_C 197.8 was assigned for C-4. Signals for the dihydroxy-substituted B ring were seen at δ_C 131.8 (C), 114.7 (CH), 146.5 (CH), 146.9 (C),

116.3 (C) and 119.3 (CH), and assigned for C-1′ ~ C-6′ respectively. The characteristic resonances of the dihydroxy-substituted A ring of the flavanone were observed at δ_C 165.5 (C), 97.1 (CH), 168.5 (C), 96.2 (CH), 164.9 (C) and 103.4 (C), and were assigned for C-5 ~ C-10 respectively. The saturated C ring signals were assigned as δ_C 80.5 (CH), 44.1 (CH_2), 197.8 (C) for C-2 ~ C-4 respectively (Figure 2.69 and Table 2.17).

The molecular formula of compound **13** was deduced to be $C_{15}H_{12}O_6$ on the basis of the NMR spectra and confirmed from the FAB-MS molecular ion peak at *m/z* 288 $[M]^+$. All spectral data were compared with a reference data and found to be matched.[123)]

Conclusion

Compound **13** was therefore assigned as (+)-eriodictyol as shown in Figure 2.70.

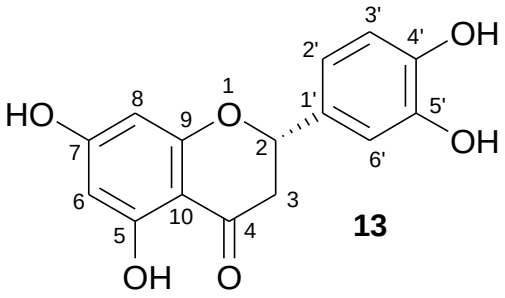

13

Figure 2.70 Structure of (+)-eriodictyol (13)

Compounds 15 ~ 17: Fatty acids from *Thonningia sanguinea*

Compounds **14** (53 mg) from H-2, **15** (40 mg) from H-4 and **16** (24 mg) and **17** (41 mg) from E-2 (Figure 2.48) were isolated as yellow oily-liquids, and each showed as a single spot on normal phase silica gel TLC.

Spectroscopic analysis:

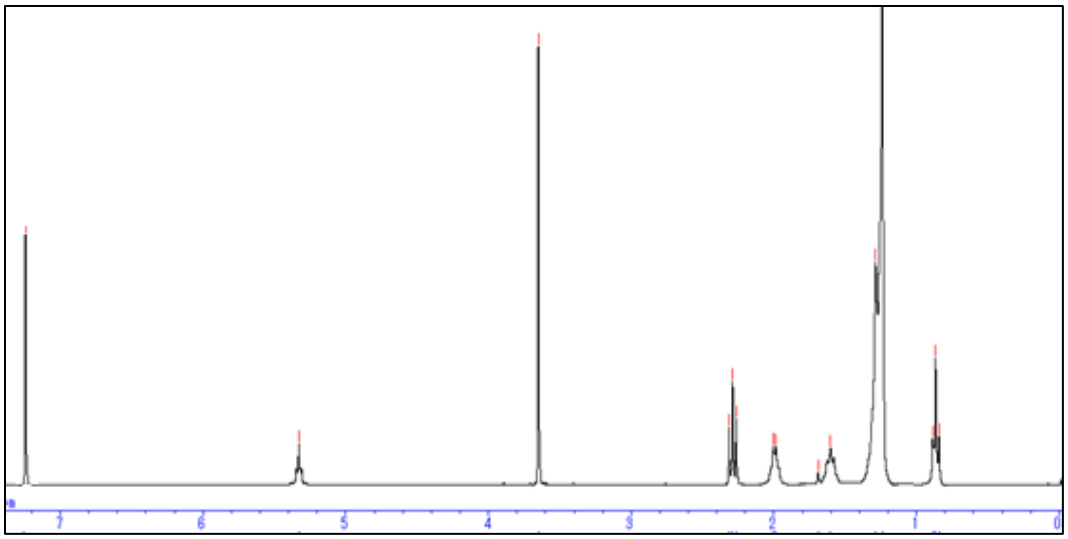

Figure 2.71 ^{1}H NMR spectrum of compound 14 (chloroform-*d*, 300 MHz)

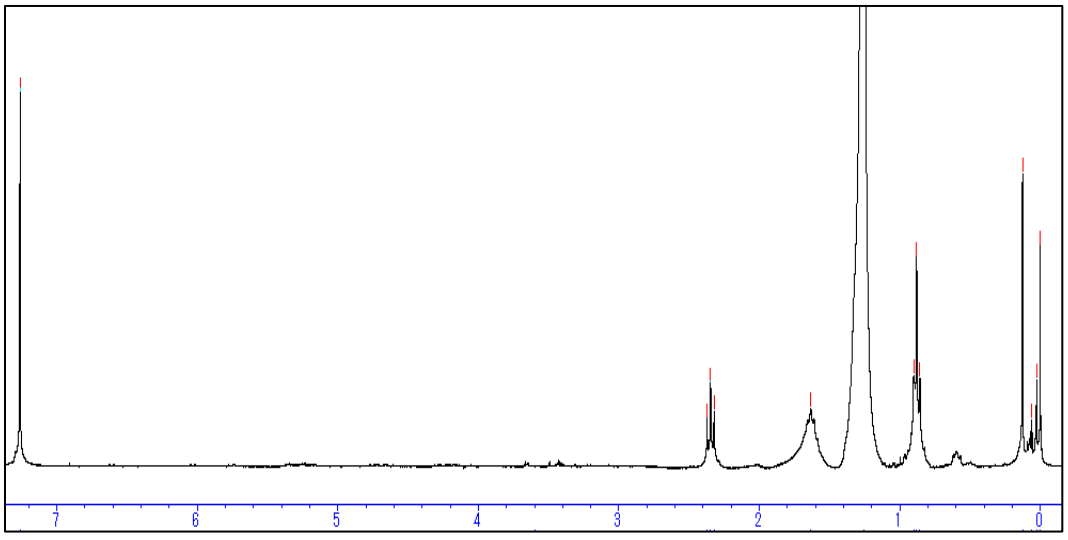

Figure 2.72 ^{1}H NMR spectrum of compound 15 (chloroform-*d*, 300 MHz)

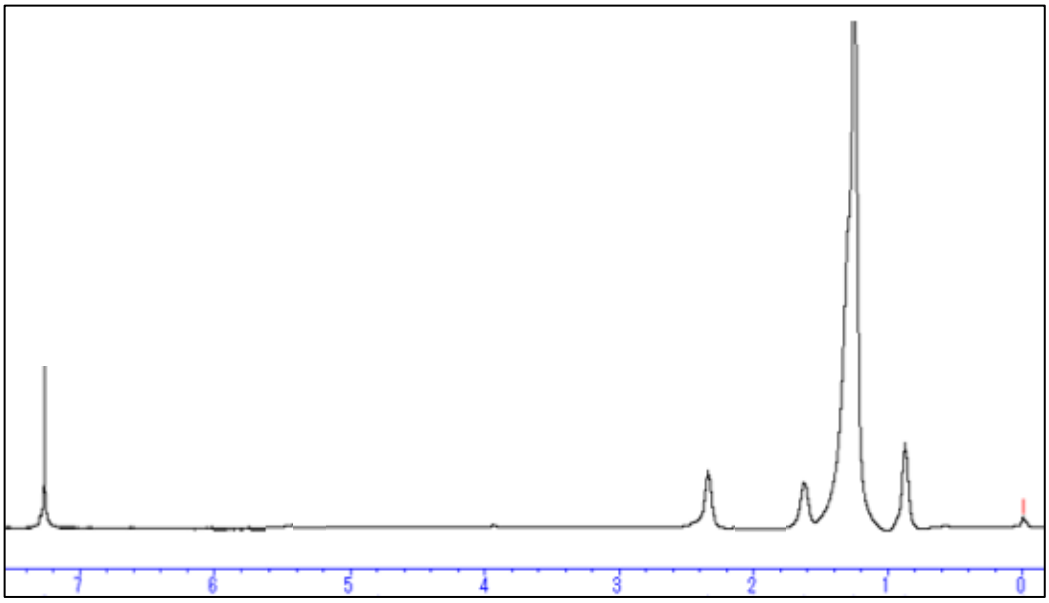

Figure 2.73 **^{1}H NMR spectrum of compound 16 (chloroform-*d*, 300 MHz**

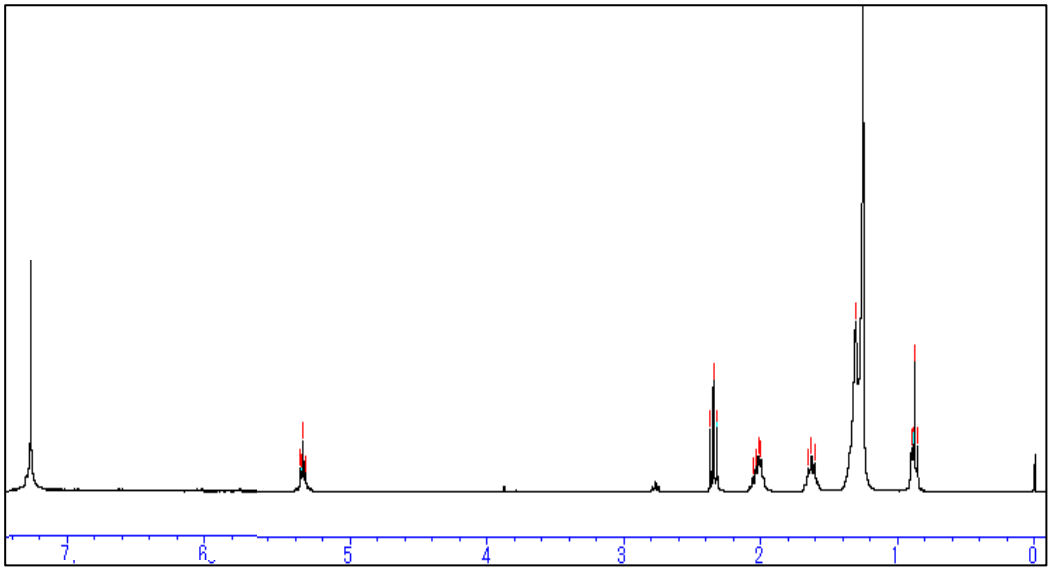

Figure 2.74 **^{1}H NMR spectrum of compound 17 (chloroform-*d*, 300 MHz)**

Table 2.18 ^{1}H (300 MHz) spectroscopic data of compounds 14 ~ 17 (chloroform-*d*, *δ* values in ppm)

Compound 14	**Compound 15**	**Compound 16**	**Compound 17**
δ$_H$ (No., M)	***δ$_H$ (No., M)***	***δ$_H$ (No., M)***	***δ$_H$ (No., M)***
(CH_2)1.24 (2H, br. s)	(CH_2)1.25 (2H, br. s)	(CH_2)1.25 (2H, br. s)	(CH_2)1.25 (2H, br. s)
(CH_2)1.29 (2H, s)		(CH_2)1.31 (2H, s)	(CH_2)1.31 (2H, s)
(CH_2)1.6 (2H, m)	(CH_2)1.63 (2H, m)	(CH_2)1.62 (2H, br. s)	(CH_2)1.61 (2H, m)
(CH_2)2.0 (2H, m)			(CH_2)2.02 (2H, m)
(CH_2)2.29 (2H, t)	(CH_2)2.35 (2H, t)	(CH_2)2.34 (2H, t)	(CH_2)2.34 (2H, t)
(OMe)3.65 (3H, s)			
(CH)5.33 (2H, m)			(CH)5.35 (2H, m)

Discussion

Compound **14** (53 mg) was obtained from fraction H-2 as a pale-yellow oily-liquid showing as a single spot on normal phase silica gel TLC.

The ^{1}H NMR spectrum of compound **14** measured in chloroform-*d,* showed resonances for methyl protons as a triplet at δ_H 0.87 (3H) and were assigned as normal type methyl terminal protons. A long methylene chain centered at δ_H 1.24 was observed as a broad singlet. Another methylene signal at δ_H 1.29 was observed. Methylene protons signals were observed at δ_H 1.60 (2H) as a broad multiplet characteristic of acyl chain signals. The more downfield signal for methylene protons were observed at δ_H 2.0 (2H, m) was also characteristic of acyl chain signals near an olefinic group. The downfield signal at δ_H 2.29 (2H, br. s) was characteristic of methylene protons attached to a carbonyl group.

The signal at δ_H 3.65 (3H) as a singlet is characteristic of methyl protons attached to an oxygen atom. The most downfield signal observed as a broad singlet at δ_H 5.33 (2H) was characteristic of olefinic protons. All these signals were suggestive of an unsaturated fatty acid methyl ester structure with normal methyl group terminal (Figure 2.71 and Table 2.18).

Conclusion

Compound **14** was therefore determined and assigned to be an unsaturated fatty acid methyl ester with a normal group methyl terminal as shown in Figure 2.75.

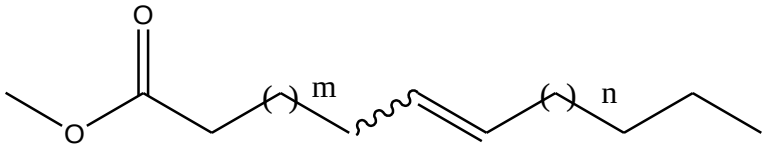

14

Figure 2.75 Structure of an unsaturated fatty acid methyl ester (14)

Compound **15** (40 mg) was obtained from fraction H-4 as a pale-yellow oily-liquid showing as a single spot on normal phase silica gel TLC.

The ^{1}H NMR spectrum of compound **15** measured in chloroform-*d*, showed similar resonances to compound **14**, with a few omissions. A signal for methyl protons as a triplet at δ_H 0.88 (3H) was observed and assigned as terminal methyl protons. A broad singlet centred at δ_H 1.25 was also observed and assigned as a long methylene chain. A signal for another methylene protons was observed at δ_H 1.63 as a multiplet was characteristic of acyl chain signals. The relatively downfield methylene signal at δ_H 2.35 observed as a triplet was characteristic of methylene protons attached to a carbonyl group. These signals were suggestive of a saturated fatty acid structure with normal methyl group terminal (Figure 2.72 and Table 2.18).

Conclusion

Compound **15** was therefore determined and assigned to be a saturated fatty acid with a normal group methyl terminal as shown in Figure 2.76.

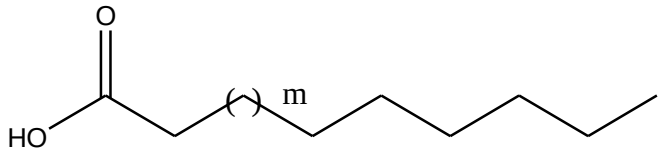

15

Figure 2.76 Structure of a saturated fatty acid (15)

Compound **16** (24 mg) was obtained from fraction E-2 as a pale-yellow oily-liquid, showing as a single spot on normal phase silica gel TLC.

The ^{1}H NMR spectrum of compound **16** measured in chloroform-*d*, showed resonances similar to that of compound **14** with a few exceptions. Methyl protons were observed as a triplet at δ_H 0.88 (3H) and assigned as normal methyl terminal. A long methylene chain centred at δ_H 1.25 was also observed as a broad singlet. Another methylene signal as a singlet was observed at δ_H 1.31. A signal for methylene protons were observed at δ_H 1.62 (2H) as a broad singlet characteristic of acyl chain signals. The signal at δ_H 2.34 (2H, t) was characteristic of methylene protons attached to a carbonyl group. All these signals were suggestive of a saturated fatty acid structure with normal methyl group terminal (Figure 2.73 and Table 2.18).

Conclusion

Compound **16** was therefore determined and assigned as a saturated fatty acid with a normal group methyl terminal as shown in Figure 2.77.

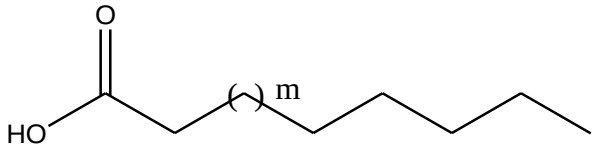

16

Figure 2.77 Structure of a saturated fatty acid (16)

Compound **17** (41 mg) was obtained from fraction E-2 as a pale-yellow oily-liquid, showing as a single spot on normal phase silica gel TLC.

The ^{1}H NMR spectrum of compound **17** measured in chloroform-*d*, showed similar resonances as compound **16**. Methyl protons at δ_H 0.88 (3H, t), methylene chain at δ_H 1.25 (br. s), methylene protons signal at δ_H 1.31 (2H, s) and two methylene protons at δ_H 1.61 (2H, m) and 2.02 (2H, m) characteristic of acyl chain signals were observed. The signal at δ_H 2.34 (2H, t) was characteristic of methylene protons attached to a carbonyl group. Signals for olefinic protons were seen as a broad multiplet at δ_H 5.32 ~ 5.38 (2H), indicative of a double bond. All these signals were suggestive of an unsaturated fatty acid structure with normal methyl group terminal (Figure 2.76 and Table 2.18).

Conclusion

Compound **17** was therefore determined and assigned as an unsaturated fatty acid with a normal group methyl terminal as shown in Figure 2.78.

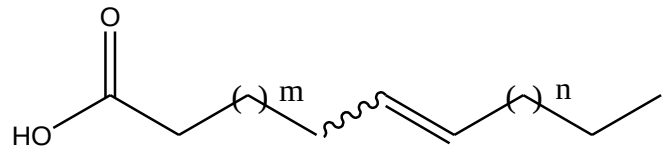

17

Figure 2.78 Structure of an unsaturated fatty acid (17)

General Discussion

It is a well-established fact that various plant metabolites have potent antimicrobial activities. All fractions except the 50% MeOH showed moderate to significant activity against *Vibrio parahaemolyticus* in the paper disc diffusion assay. Since these fractions were extracted with both polar and non-polar solvents, the compounds responsible for this action are both polar and non-polar in nature. Plant sterols and phenolic compounds such as tannins, flavonoids, lignans etc., are well known potent antimicrobial agents. All the isolated compounds in this study were from the *n*-hexane and ethyl acetate fractions. The antimicrobial activities of all these compounds may be responsible for these findings.[126-131)]

One sphingosine-type cerebroside (**TSC-1**) and one phytosphingosine-type cerebroside (**TSC-2**), with both containing mainly a 2-hydroxy fatty acid and β-D-glucopyranose moieties were isolated from the *n*-hexane fraction of *T. sanguinea* in this study. Cerebrosides and ceramides have received a lot of interest in their isolation and characterization due to their significant biological activities such as immunomodulatory antioxidant, antitumour, antiinflammatory and antiviral.[126,127)]

Six known sterols and one known triterpenoid were isolated from the *n*-hexane fraction of plant: β-sitosterol-3-*O*-β-D-glucopyranoside-6′-*O*-fatty acid ester molecular species **TSS-1**, β-sitosterol-3-*O*-β-D-(6′-*O*-palmitoyl)-glucopyranoside (**1**), β-sitosterol (**2**), β-sitosterol-3-*O*-β-D-glucopyranoside (**3**), β-stigmasterol (**4**), β-stigmasterol-3-*O*-β-D-glucopyranoside (**5**), cholesterol (**6**) and the pentacyclic triterpenoid betulinic acid (**7**). One unsaturated fatty acid methyl ester (**14**) and saturated fatty acid (**15**). Biological functions of plant sterols include antihelmintic, antidiabetic, antiinflammatory, antiapoptotic, antinociceptive, antioxidant, immunomodulatory and neuroprotective in neurodegenerative disorders like Alzheimer's disease.[128,129)]

Betulinic acid exhibits a variety of biological and medicinal properties such as inhibition of HIV, antibacterial, antimalarial, antiinflammatory, antihelmintic, antinociceptive, anti-herpes simplex virus type 1 (anti-HSV-1) and anticancer activities.[130)]

Five (5) known lignans isolated from the ethyl acetate fraction of *T. sanguinea*: (+)-epipinoresinol (**8**), (+)-pinoresinol (**9**), (+)-cycloolivil (**10**), (+)-secoisolariciresinol (**11**) and isolariciresinol (**12**), as well as one saturated fatty acid (**16**) and one unsaturated fatty acid (**17**). The isolated lignans

are reported to also have antiviral, antifungal, antimicrobial antifeedant and insecticidal properties and are probably related to plant defense against various pathogens and pests. They also have significant biological activities including antitumour, antiinflammatory, immunosuppression, cardiovascular, antioxidant and antiviral.[131] Pinoresinol and secoisolariciresinol are mammalian lignan precursors which are converted into enterodiol (END) and enterolactone (ENL) by the intestinal microflora.[119,132] These enterolignans afford protection against osteoporosis, cardiovascular diseases, liver diseases, hyperlipidemia, breast cancer, colon cancer, prostate cancer and menopausal syndrome.[112,133,134] The flavanone (+)-eriodictyol (**13**), also isolated from the ethyl acetate fraction is reported to have significant antiinflammatory, anticancer, neurotrophic, and antioxidant effects.[135]

Conclusion

In summary, the moderate to significant activity of the *n*-hexane, *n*-butanol, and aqueous fractions from *Thonningia sanguinea* against *Vibrio parahaemolyticus* in the antibacterial assay gives scientific basis for its use as an antiinfective agent. The study also led to the isolation of two glucocerebrosides **TSC-1** and **TSC-2,** one β-sitosterol-3-*O*-β-D-glucopyranoside-6′-*O*-fatty acid esters molecular species molecular species **TSS-1**, six known sterols (**1 ~ 6**), one known pentacyclic triterpenoid (**7**), five known lignans (**8 ~ 12**), one known flavanone (**13**), one fatty acid methyl ester (**14**) and three fatty acids (**15 ~ 17**) from the *n*-hexane and ethyl acetate fractions of the plant. To the best of our knowledge, all the isolated compounds in this study are being reported for the first time in this genus. These compounds have a wide range of biological activities and may act individually or in synergy to produce these biological actions. They may therefore be responsible for these biological actions, giving credence to the use of the *T. sanguinea* in Ghanaian traditional medicine.

Chapter 3

HIGH PERFORMANCE LIQUID CHROMATOGRAPY

3.1 HPLC Profiles of the crude methanolic extract of *Thonningia sanguinea* and its Herbal Medicinal Product

The HPLC fingerprints of the crude methanolic extract, fractions, isolated compounds and the herbal medicinal product from *Thonningia sanguinea* were analysed.

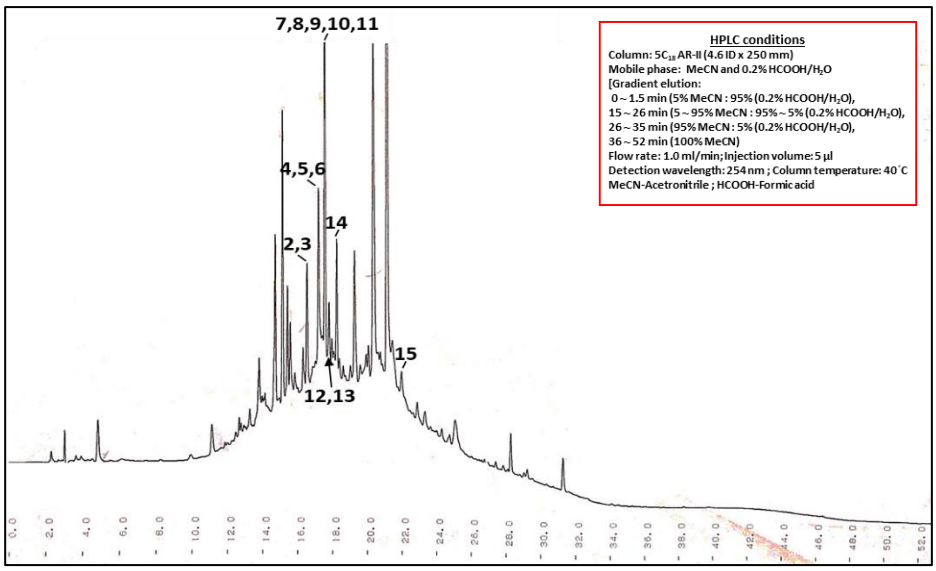

Figure 3.1 HPLC fingerprints of the crude methanolic extract of *Thonningia sanguinea* showing the isolated compounds*

*Isolated compounds: isolariciresinol (1), β-stigmasterol-3-*O*-β-D-glucopyranoside (2), β-sitosterol-3-*O*-β-D-glucopyranoside (3), cholesterol (4), TSC-1 (5), TSC-2 (6), betulinic acid (7), β-stigmasterol (8), secoisolaricirecinol (9), TSC-1 (10), β-sitosterol-3-*O*-β-D-(6′-*O*-palmitoyl)-glucopyranoside (11), β-sitosterol (12), eriodictyol (13), pinoresinol (14) and cycloolivil (15)

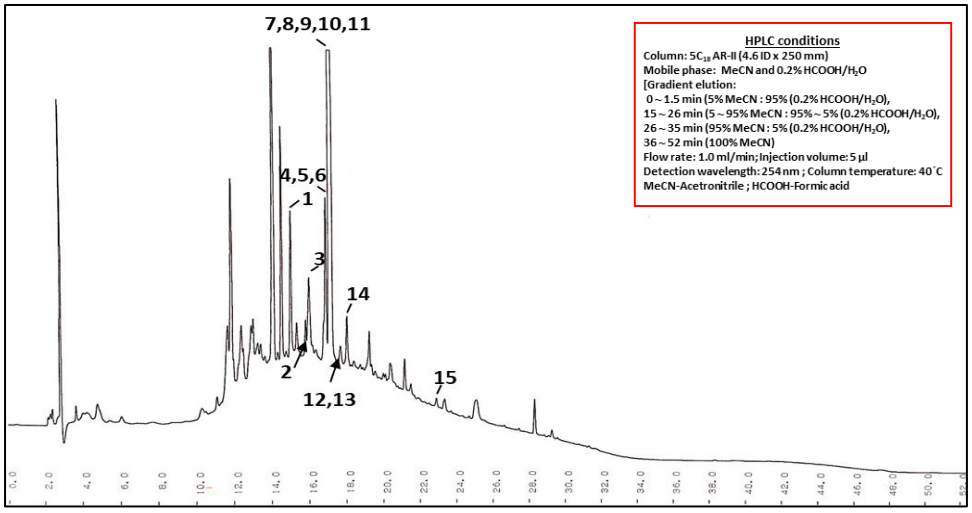

Figure 3.2 HPLC fingerprint of the Herbal Medicinal Product of *Thonningia sanguinea* showing the isolated compounds*

*Isolated compounds: isolariciresinol (1), β-stigmasterol-3-*O*-β-D-glucopyranoside (2), β-sitosterol-3-*O*-β-D-glucopyranoside (3), cholesterol (4), TSC-1 (5), TSC-2 (6), betulinic acid (7), β-stigmasterol (8), secoisolariciresinol (9), TSC-1 (10), β-sitosterol-3-*O*-β-D-(6′-*O*-palmitoyl)-glucopyranoside (11), β-sitosterol (12), eriodictyol (13), pinoresinol (14) and cycloolivil (15)

Table 3.1 Retention times (min) of isolated compounds from *Thonningia sanguinea* for HPLC chromatograms

No.	***Compound***	***Retention time (min)***
1	Isolariciresinol	15.296
2	β-Stigmasterol-3-*O*-β-D-glucopyranoside	15.897
3	β-Sitosterol-3-*O*-β-D-glucopyranoside	15.907
4	Cholesterol	17.034
5	TSC-1	17.048
6	TSC-2	17.059
7	Betulinic acid	17.064
8	β-Stigmasterol	17.067
9	Secoisolariciresinol	17.081
10	Epipinoresinol	17.086
11	β-Sitosterol-3-*O*-β-D-(6'-*O*-palmitoyl)-glucopyranoside	17.121
11	β-Sitosterol	17.440
13	Eriodictyol	17.444
14	Pinoresinol	18.235
15	Cycloolivil	22.439

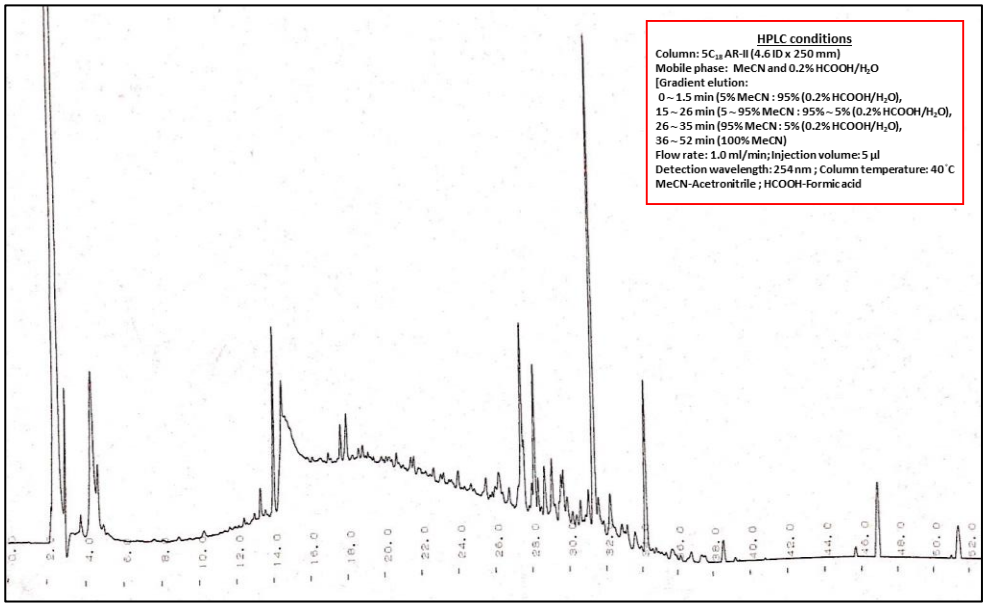

Figure 3.3 HPLC fingerprint of the *n*-hexane fraction of *Thonningia sanguinea*

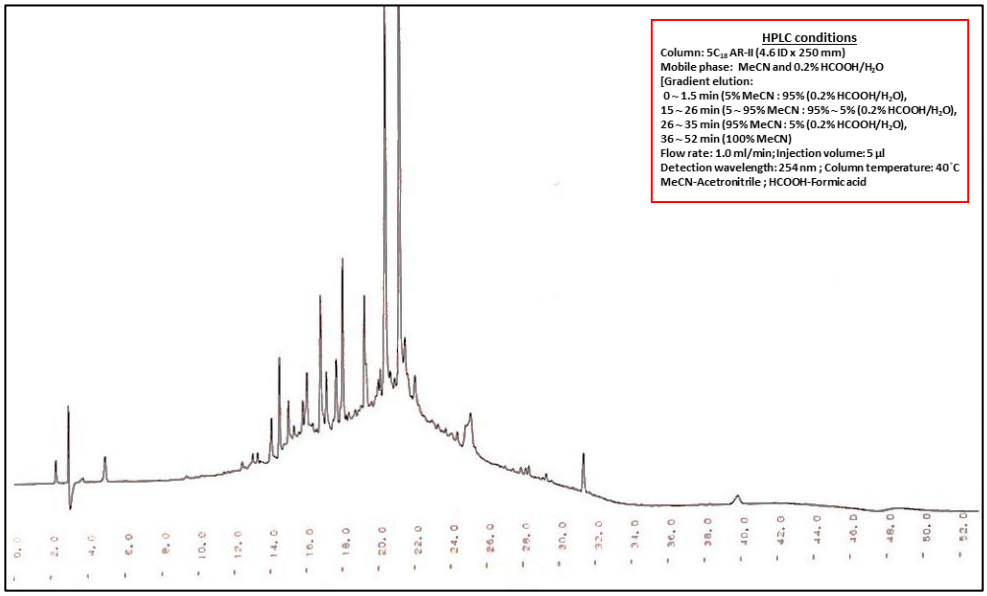

Figure 3.4 HPLC fingerprint of the EtOAc fraction of *Thonningia sanguinea*

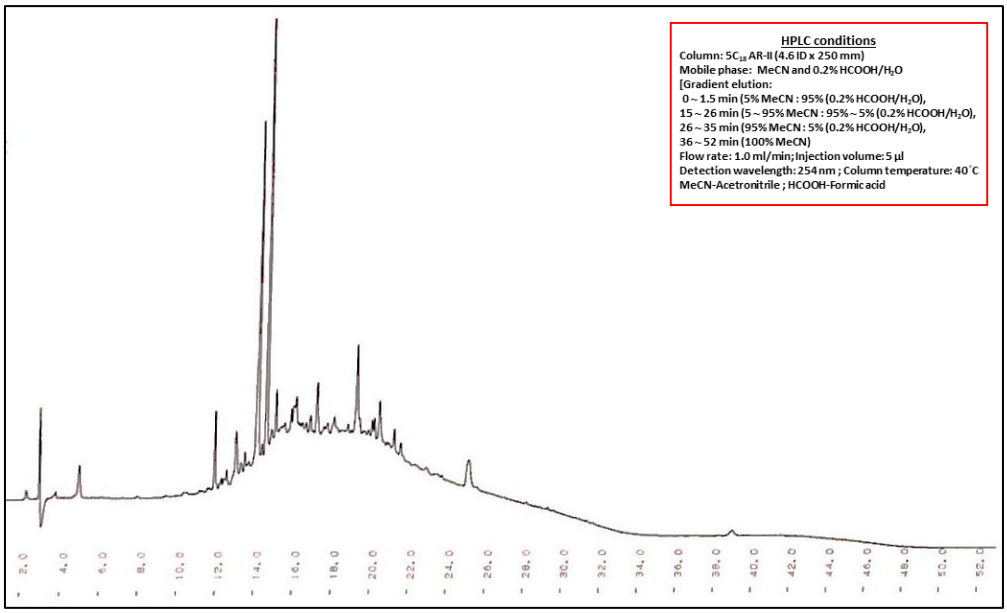

Figure 3.5 HPLC fingerprint of the *n*-BuOH fraction of *Thonningia sanguinea*

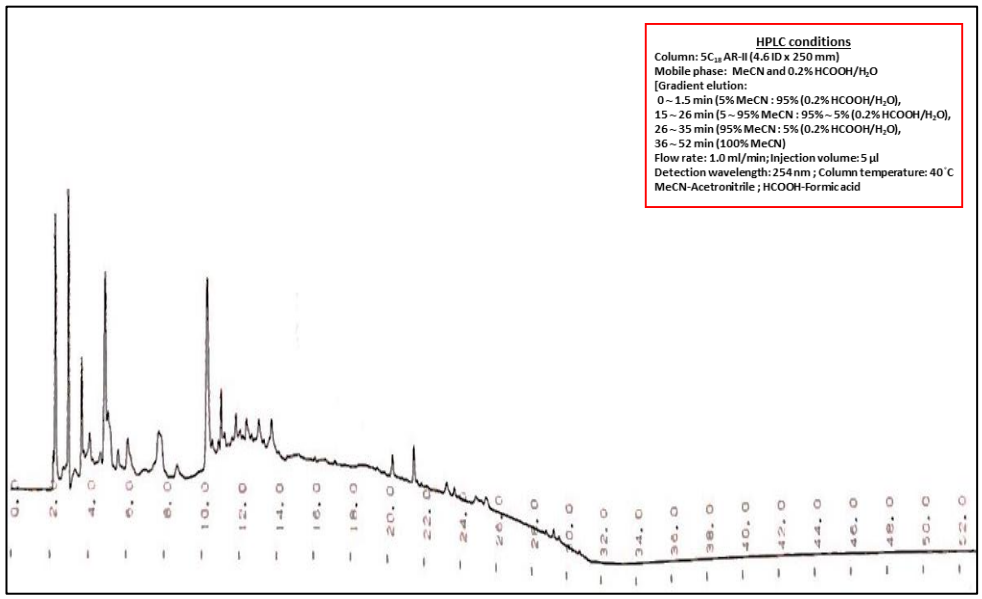

Figure 3.6 HPLC fingerprint of the 20% MeOH fraction of *Thonningia sanguinea*

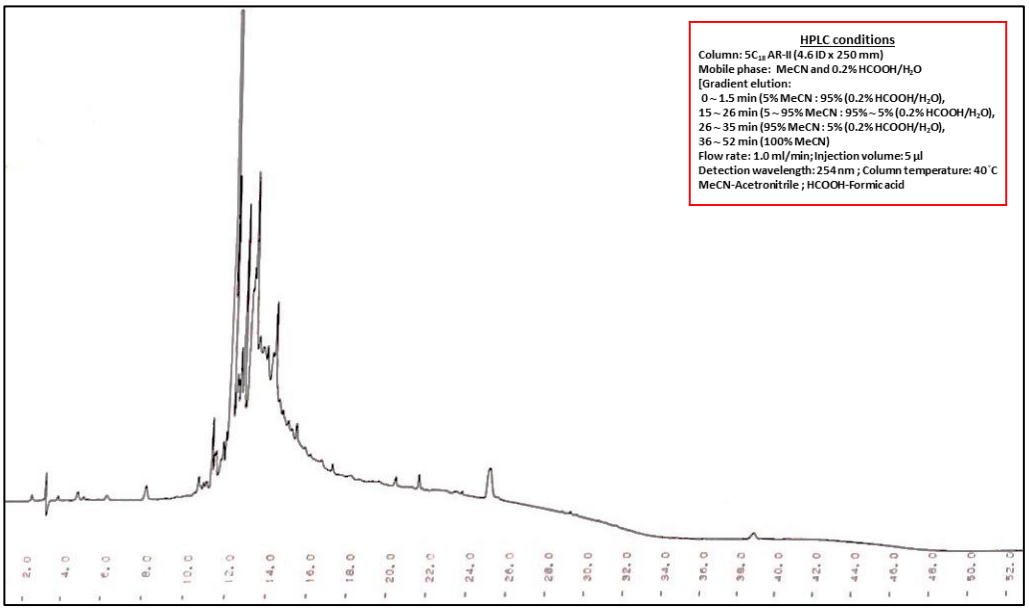

Figure 3.7 HPLC fingerprint of the 50% MeOH fraction of *Thonningia sanguinea*

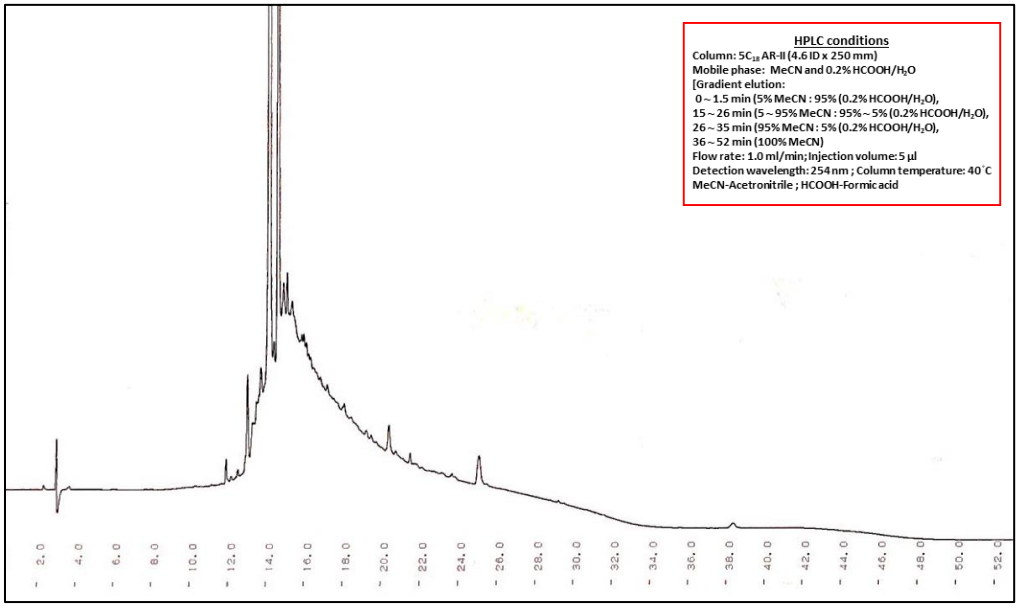

Figure 3.8 HPLC fingerprint of the 80% MeOH fraction of *Thonningia sanguinea*

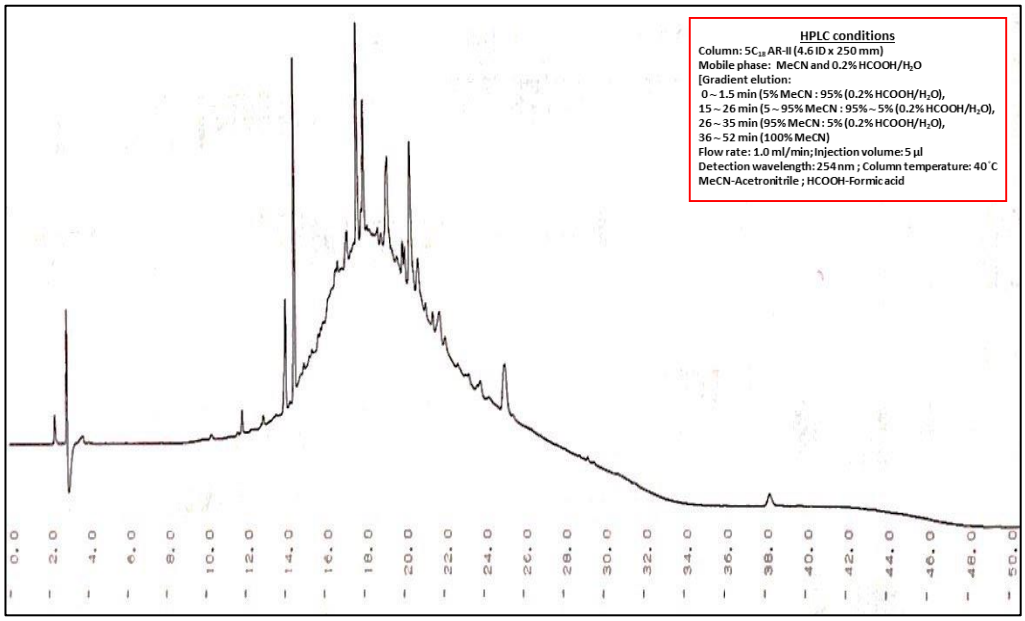

Figure 3.9 HPLC fingerprint of the 100% MeOH fraction of *Thonningia sanguinea*

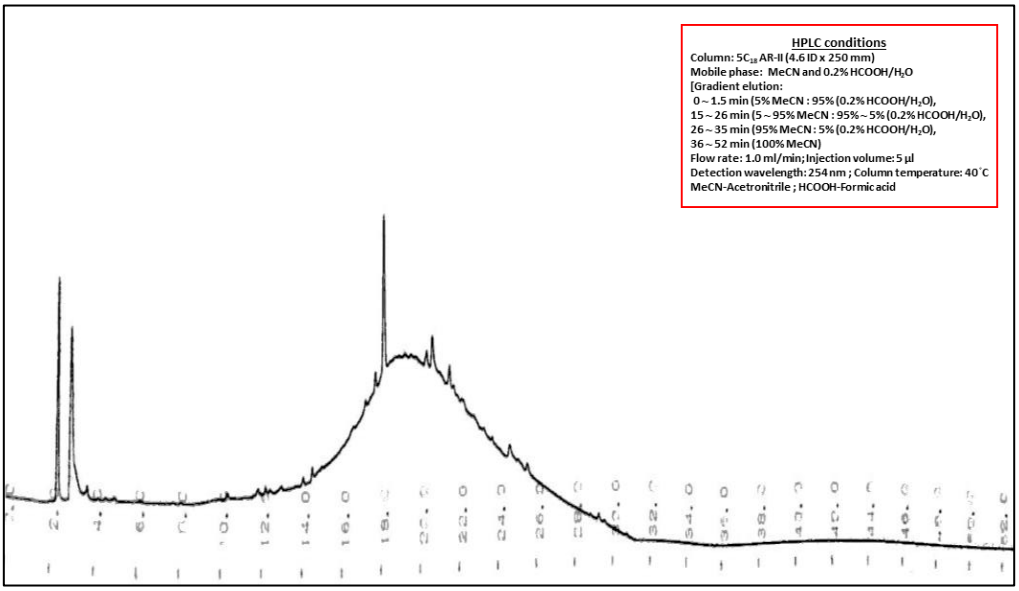

Figure 3.10 HPLC fingerprint of the 80% acetone fraction of *Thonningia sanguinea*

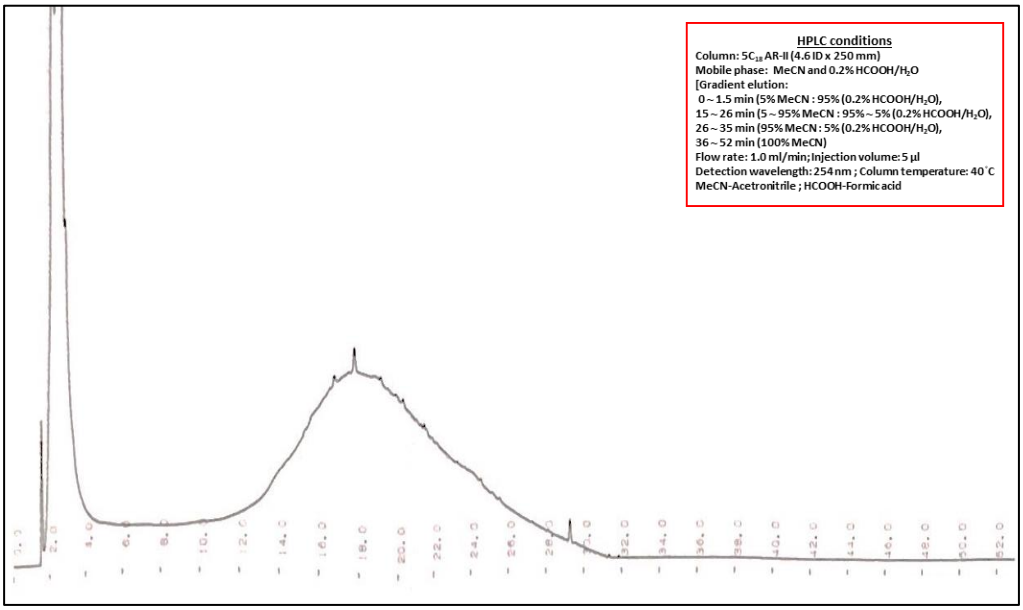

Figure 3.11 HPLC fingerprint of the 100% acetone fraction of *Thonningia sanguinea*

Discussion

Natural products continue to be a source of novel moieties for the drug development process. However, these products remain important for several societies especially those in developing countries as healthcare interventions. Such communities continue to use these products in their crude forms and therefore the provision of some quality standards for such materials is important.[136,137)] The process of developing standards for the herbal medicinal product in this study was undertaken to provide some specifications for subsequent manufacturing processes to ensure quality and provide analytical standards for the crude methanolic extract, its fractions and the herbal medicinal product from *Thonningia sanguinea*.

In the HPLC fingerprint of the crude methanolic extract (Figure 3.1 and Table 3.1), the single peaks eluting at 15.296 min (**1**), 18.235 min (**14**) and 22.439 min (**15**) were (+)-isolariciresinol, (+)-pinoresinol and (+)-cycloolivil respectively. The peaks for β-stigmasterol-3-*O*-β-D-glucopyranoside (**2**) and β-sitosterol-3-*O*-β-D-glucopyranoside (**3**) eluted at 15.897 min and 15.907 min respectively and appeared as a single peak. The peaks for cholesterol (**4**), **TSC-1** (**5**) and **TSC-2** (**6**) eluted at 17.034 min, 17.048 min, 17.059 min respectively and were also detected

as one peak. The most significant peak was comprised compounds which eluted at 17.064 min, 17.067 min, 17.081 min, 17.086 min and 17.121 min and corresponded to betulinic acid (**7**), β-stigmasterol (**8**), (+)-secoisolaricirecinol (**9**), (+)-epipinoresinol (**10**) and β-Sitosterol-3-*O*-β-D-(6′-*O*-palmitoyl)-glucopyranoside (**11**). The peaks for β-sitosterol (**12**) and (+)-eriodictyol (**13**) eluted at 17.444 min and 17.44 min respectively and also occurred superimposed as a single peak.

The HPLC fingerprints of the herbal medicinal product (Figure 3.2 and Table 3.1) and the crude methanolic extract were also compared. All fifteen (15) isolated compounds: **(1 ~ 13), TSC-1** and **TSC-2** were present in the Herbal Medicinal Product and their retention times (min) corresponded exactly with that seen in the crude methanolic extract. This information provides the first analytical study of Herbal Medicinal Product and gives a lead for manufacturers to choose these compounds for further development as analytical standards to ensure batch-to-batch consistency and ultimately improve the quality of the medicinal product.

The presence of these compounds in the herbal medicinal product and their reported biological activities therefore is an important discovery and may be able used to explain the numerous pharmacological activities that have been reported on the extracts. These important findings hence validate the usage of this *T. sanguinea* plant based-herbal medicine in primary healthcare in Ghana.

The HPLC fingerprints of the *n*-hexane, ethyl acetate, *n*-butanol and the Diaion colum-eluted fractions (20% MeOH, 50% MeOH, 80% MeOH, 100% MeOH, 80% acetone and 100% acetone) were also provided as analytical markers for the plant (Figure 3.3 ~ 11).

Conclusion

Analytical markers and chromatographic fingerprints have been provided for *T. sanguinea* and its herbal medicinal product.

Chapter 4

EXPERIMENTAL SECTION

4.1 Antimicrobial screening of the crude methanolic extract of *Thonningia sanguinea* and its fractions

The paper disc diffusion method was used for the antimicrobial assay as described in the CSLI.[139)] Briefly, a concentration of 5 mg/10 µl of the crude methanolic extract and its fractions but for the *n*-hexane which was at 2 mg/10 µl. The standard antibiotic used was ciprofloxacin. All the test agents were prepared by dissolution in $CHCl_3$: MeOH (1:1) or 20% dimethyl sulfoxide (DMSO). Thiosulfate Citrate Bile salt Sucrose (TCBS) agar was used as the media for the test microorganism *Vibrio parahaemolyticus* (NBRC No. 12711).

Agar plates were inoculated with a standardized inoculum of the test microorganism by flooding each plate with about 100 µl of the pathogenic microorganism. The plates were then kept in the refrigerator for 6 hours to allow absorption of the test agents into the media. Then, filter paper discs (about 6 mm in diameter), containing the test agents at a desired concentration were placed on the agar surface. The Petri dishes were incubated at 35 °C for 24 hr for the test organism. DMSO was used as the negative control for all test and ciprofloxacin as positive control for the bacterial organism. After the incubation period, the diameter of each zone of inhibition was graded as (-) if the test organism was not susceptible to the test agent, (+) if the diameter obtained was within 25% – 50 %, (++) if between 50% – 75 % and (+++) if between 75% – 100% when compared to the positive control ciprofloxacin. The measure of the zone of inhibition at each period of testing was compared and used as an indicator of the antibacterial potential of the test agents.

4.2 General experimental procedures for the chemical study

NMR spectra were recorded in chloroform-*d*, methanol-d_4 and Pyridine-d_5 (Nacalai Tesque, Inc., Kyoto, Japan) with Varian Unity Plus 400 spectrometer (Palo Alto, CA, USA) operating at 400 MHz for ^1H and 100 MHz for ^{13}C, and with a JEOL JNM-AL 300 spectrometer (JEOL Ltd, Tokyo, Japan) at 300 MHz for ^1H NMR. The UV spectra were recorded using a double beam Shimadzu UV-visible spectrophotometer (model UV-1601

PC, Kyoto City, Japan). IR spectra were recorded using a Jasco FT/IR-410K spectrometer (Jasco Co. Ltd., Tokyo, Japan) with a range of 400-4000 cm^{-1}. FAB-MS spectra were recorded on a JMS 700N spectrometer (JEOL Ltd., Tokyo, Japan) in positive ion mode, with glycerol or *m*-nitrobenzyl alcohol, with or without NaCl, as the matrix. The optical rotation measurements were done using a Jasco P-1020 polarimeter (Jasco Co. Ltd., Tokyo, Japan). Extraction and isolation of compounds were done the following solvents: acetone, acetonitrile, *n*-butanol, chloroform, ethyl acetate, *n*-hexane and methanol (Nacalai Tesque, Inc., Kyoto, Japan). Column chromatography (CC) was performed using Sephadex LH-20 (25-100 mm, GE Healthcare UK Ltd., Buckinghamshire HP7 9NA, UK), Silica gel Purasil 60Å, 230-400 mesh (Whatman, Sanford, ME, USA) and Cosmosil 140 C_{18}-PREP Silica gel 90Å, 40-63 mesh (Nacalai Tesque, Inc., Kyoto, Japan). TLC was performed on 0.25 mm thick, precoated silica gel 60 F_{254} and Silica gel RP-18 F_{254} plates (Merck, Darmstadt, Germany). Prep. TLC was performed on 2 mm thick PLC Silica gel 60 F_{254} glass plates (Merck, Darmstadt, Germany). Spots were developed with 5% H_2SO_4 : MeOH and detected by illumination under a short wavelength UV (254 nm). Analytical HPLC was performed on a Cosmosil 5C_{18}-AR-II 4.6 mm x 250 mm column (Nacalai Tesque, Inc., Kyoto, Japan) with methanol and acetonitrile in 0.2% formic acid (Nacalai Tesque, Inc., Kyoto, Japan) at a flow rate of 0.8 mL min^{-1} and 1.0 mL min^{-1} respectively and Cosmosil-sugar-D, 4.6 ID x 250 mm, 1 mL min^{-1}, Refractive Index (RI) detector using 95% acetonitrile). Preparative HPLC was performed on a Develosil 5C_{18} 4.6 mm x 150 mm column (Nacalai Tesque, Inc., Kyoto, Japan) using 100% MeOH as solvent, at a flow rate of 0.5 mL min^{-1} on a Jasco DG-2080-53 Plus degasser, Jasco PU-2080 Plus pump, Jasco AS-2055 Plus auto sampler, Jasco CO-2065 Plus column oven (maintained at 35 °C) and Jasco MD-2018 Plus PDA detector (Jasco Co. Ltd., Tokyo, Japan).

4.3 Plant collection and identification

Thonningia sanguinea was collected by the staff of the Centre for Plant Medicine Research from the Eastern region of Ghana in the month of January 2015 and authenticated by the curator of their Herbarium. A voucher specimen with the number CSRPM No: 140 was assigned to the sample.

4.4 Extraction and isolation

The whole plant of *Thonningia sanguinea* was shade-dried for seven days and pulverized. The dried powdered plant material (3.5 Kg) was extracted by cold maceration with MeOH (3 x 10 L for 3 days), followed by MeOH : $CHCl_3$ (1:1; 3 x 10 L for 3 days). The filtrates were pooled together and concentrated *in vacuo* using the rotary evaporator. The methanol/chloroform crude extract (423 g) was dissolved in distilled water and serially partitioned between *n*-hexane, ethyl acetate, *n*-butanol solvents to obtain the *n*-hexane (20 g), ethyl acetate (260 g), *n*-butanol (88 g) and aqueous (30 g) fractions. The volume of aqueous fraction (30 g) was adjusted with distilled H_2O, applied on a Diaion HP-20 column and eluted serially with appropriate solvents to yield the corresponding fractions: 20% MeOH (7.9 g), 50% MeOH (9.5 g), 80% MeOH (7.6 g), 100% MeOH (1.3 g), 80% acetone (2.3 g) and 100% acetone (1.3 g) (Figure 2.1).

The *n*-hexane fraction (20 g) was subjected to silica gel CC (800 g) using *n*-hexane : EtOAc (9:1 – 1:9), $CHCl_3$: MeOH (8:2 ~ 6:4) and 80% acetone to give sixteen sub-fractions (H-1 ~ H-16). Fraction H-2 (1.29 g) was subjected to repeated silica gel CC using *n*-hexane : EtOAc (97:3 ~ 2:8) to afford (**14**) [unsaturated fatty acid methyl ester, 53 mg). Fraction H-4 (500 mg) was subjected to repeated silica gel CC using *n*-hexane : EtOAc (85:15 ~ 1:1) to afford compound **6** (200 mg) and **(15)** [saturated fatty acid, 40 mg). Fraction H-5 (330 mg) was subjected to repeated silica gel CC using $CHCl_3$: MeOH (1:0 ~ 1:1) to afford seven fractions. Fraction H-5-6 (138 mg) was further chromatographed on a C_{18} RP silica gel column (10 g) using MeOH : H_2O (8:2 ~ 1:0) and acetone : H_2O (1:1 ~ 1:0) to afford compound **7** (22 mg). Fraction H-10 ~ H-11 (630 mg) was chromatographed on silica gel (20 g) using $CHCl_3$: MeOH (98:2 ~ 1:1) to afford eleven sub-fractions (H-10-1 ~ H-10-11). Fraction H-10-4 (350 mg) was further chromatographed on a C_{18} RP silica gel column (10 g) using 100% MeOH to afford (**1**) [β-sitosteryl-3-*O*-β-D-(6′-*O*-palmitoyl)-glucopyranoside, 28 mg), **TSS-1** (94 mg) and a mixture purified by preparative HPLC using 100% MeOH to afford (**2**) [β-sitosterol, 40 mg] and (**4**) [stigmasterol, 15 mg]. Fraction H-13 (2.3 g) was chromatographed on silica gel (100 g) using $CHCl_3$: MeOH (98:2 ~ 2:8) to afford five sub-fractions H-13-1 ~ H-13-5. Fraction H-13-4 (340 mg) was subjected to repeated silica gel CC using $CHCl_3$: MeOH (95:5 ~ 1:1) to afford **TSC-1** (37 mg) and

TSC-2 (68 mg). Fraction H-14 ~ H-16 (1.4 g) was chromatographed on silica gel (60 g) using $CHCl_3$: MeOH (98:2 ~ 2:8) to afford eight sub-fractions H-14-1 ~ H-14-8. Fraction H-14-4 (30 mg), a mixture was purified by preparative HPLC using 100% MeOH to afford (**3**) [β-sitosterol glucoside, 13 mg] and (**5**) [stigmasterol glucoside, 8 mg). Fraction H-14-6 (79 mg) was chromatographed on silica gel (10 g) using $CHCl_3$: MeOH (98:2 ~ 2:8) to afford **TSC-1** (6 mg) and **TSC-2** (22 mg).

The ethyl acetate fraction (70 g) was subjected to silica gel CC (240 g) using $CHCl_3$: MeOH (98:2 ~ 3:7) and 80% acetone to afford twenty two sub-fractions (E-1 ~ E-22). Fraction E-2 (1.08 g) was subjected to silica gel CC (10 g) using *n*-hexane : EtOAc (8:2 ~ 2:8) to give fourteen sub-fractions (E-2-1 ~ E-2-14) which afforded (**8**) [(+)-epipinoresinol, 100 mg], (**9**) [(+)-pinoresinol, 200 mg], (**16**) [saturated fatty acid**,** 24 mg] and (**17**) [unsaturated fatty acid, 41 mg]. Fraction E-9 (500 mg) was subjected to silica gel CC (15 g) using $CHCl_3$: MeOH (99:1 ~ 96:4) to give sixteen sub-fractions (E-9-1 ~ E-9-16). Fraction E-9-7 (175 mg) was subjected to repeated silica gel CC (10 g) using *n*-hexane : EtOAc (8:2 ~ 1:1) and $CHCl_3$: MeOH (97:3 ~ 1:1) to afford (**10**) [(+)-cycloolivil, 14 mg] and (**11**) [(+)-secolariciresinol, 23 mg]. Fraction E-9-8 (168 mg) was chromatographed on a C_{18} RP silica gel column (10 g) using MeOH : H_2O (3:7 ~ 4:6) to afford (**12**) [(+)Isolariciresinol, 117 mg) and (**13**) [(+)-eriodictyol, 18 mg] (Figure 2.48).

TSS-1. White amorphous powder. IR ν_{max}/cm^{-1}: 3350 (hydroxy), 1720 (carbonyl). Positive-ion FAB-MS: *m/z* 837, 851, 865, 879, 893, 806, 907, 921, 935, 949, 963 and 977 $[M + Na]^+$ series. ^1H NMR (chloroform-*d*) δ_H: 0.68 ~ 0.93 (3H, t), 1.25 (2H, s, *n*CH_2), 4.37 (1H, d, *J* = 8 Hz, glucose H-1′). ^{13}C NMR: Table 2.2.

TSC-1. White amorphous powder. IR ν_{max}/cm^{-1}: 3422 (hydroxy), 1640 and 1540 (amide). $[\alpha]_D^{20}$ = +31.3 (*c* 0.1 in MeOH). Positive-ion FAB-MS: *m/z* 736, 764, 778, 792, 806, 820, 834, 848 and 862 $[M + Na]^+$ series. ^1H NMR (pyridine-d_5) δ_H: 0.86 (6H, br. t), 4.89 (1H, d, *J* = 8 Hz, glucose H-1′′). ^{13}C NMR: Table 2.3.

TSC-2. White amorphous powder. IR ν_{max}/cm^{-1}: 3289 (hydroxy), 1640, 1540 (amide). $[\alpha]_D^{22}$ = +29 (*c* 0.1 in MeOH). Positive-ion FAB-MS: *m*/z 810, 824, 838, 852, 866 and 880

$[M + Na]^+$ series. ^1H NMR (pyridine-d_5) δ_H: 0.83 (6H, br. t), 4.93 (1H, d, J = 8 Hz, glucose H-1''). ^{13}C NMR: Table 2.3.

Methanolysis of TSC-1. TSC-1 (5 mg) was heated with 5% HCl in MeOH (0.5 mL) at 70 °C for 8 h in a sealed small-volume vial. The reaction mixture was extracted with *n*-hexane and the extract was concentrated *in vacuo* to yield a mixture of fatty acid methyl ester (FAME) products. The methanolic layer was neutralized with Silver nitrate (Ag_2CO_3), filtered, and the filtrate was concentrated *in vacuo* to give a mixture of long chain base (LCB) and methyl glycoside products. The mixture was further evaporated and reacted with acetic anhydride/pyridine (1:1) (0.2 mL) at 70 °C for 8 h in a sealed small-volume vial followed by evaporation *in vacuo* to dryness. The mixture was separated using preparative TLC to afford the LCB, LCB acetates and LCB glucoacetates. The ^1H, ^{13}C NMR and FAB-MS analyses were performed on the FAMEs and the LCB products (Figure 2.14).

Methanolysis of TSC-2. In the same manner as described for **TSC-1**, **TSC-2** (5 mg) was methanolized and the reaction mixture was worked up to give the FAMEs, LCB, LCB acetates and LCB glucoacetates. The ^1H, ^{13}C NMR and FAB-MS analyses were performed on the FAMEs and the LCB products (Figure 2.23).

FAB-MS analysis of the FAME mixture from TSC-1. Positive molecular ion peaks at 287, 315, 329, 343, 357, 371, 385, 399 and 413 $[M + H]^+$ indicated the presence of C-16, C-18 ~ C-25 fatty acid methyl esters in **TSC-1** (Figure 2.8).

FAB-MS analysis of the LCB products from TSC-1. Positive ion FAB-MS analysis showed molecular ion peaks at 395 $[M]^+$ (LCB) and 424 $[M + H]^+$ (LCB acetate) indicating the presence of a C-16 LCB, while 652 $[M + Na]^+$ (LCB glucoacetate) indicated the presence of a C-18 LCB in **TSC-1** (Figure 2.9 ~ 10).

FAB-MS analysis of the FAME mixture from TSC-2. Positive molecular ion peaks at 343, 357, 371, 385, 399 and 413 $[M + H]^+$ indicated the presence of C-20 ~ C-25 fatty acid methyl esters in **TSC-2** (Figure 2.17).

FAB-MS analysis of the LCB products from TSC-2. Positive ion FAB-MS analysis showed molecular ion peaks at 455 $[M]^+$ (LCB acetate) and 484 $[M + H]^+$ (LCB acetate) indicating the presence of a C-16 and C-18 LCB respectively in **TSC-2** (Figure 2.18 ~ 19)

Identification of the sugar moiety in TSC-1. TSC-1 (5 mg) was heated with 5% HCl in MeOH (0.5 mL) at 70 °C for 8 h in a sealed small-volume vial. The reaction mixture was extracted with *n*-hexane to remove the release fatty acid. The methanolic was neutralized with Ag_2CO_3 to give the methylated glucoside followed by HPLC analysis (Cosmosil-sugar-D, 4.6 ID x 250 mm, 1 mL min^{-1}, RI detector, 95% acetonitrile) against standard glucose and galactose. **TSC-1** showed a retention time identical to glucose (glucose t_R = 14.11 min, galactose t_R = 13.27 min). In the same way, the sugar moiety was identified as glucose for **TSC-2** and **TSS-1.**

Determination of the Absolute Configuration of the Glucose Moiety in TSC-1. (Tanaka *et al*., 2007).[115)] The glycosidic bond in **TSC-1** (2 mg, 1.1 x 10^6 mol) was hydrolysed by heating in 0.5 M HCl (0.1 mL) and neutralized with Amberlite IRA400. After drying *in vacuo*, the residue was dissolved in pyridine (0.1 mL) containing L-cysteine methyl ester hydrochloride (0.5 mg) and heated at 60 °C for 1 h. A 0.1 mL solution of *o*-toryl isothiocyanate (0.5 mg) in pyridine was added to the mixture, which was heated at 60 °C for 1 h. The reaction mixture was directly analysed by reversed-phase HPLC.

4.5 Development of HPLC Profiles for the crude methanolic extract, fractions and the Herbal Medicinal Product from *Thonningia sanguinea*

Solvents and Chemicals

Solvents used: acetonitrile (MeCN), chloroform ($CHCl_3$), dimethyl sulfoxide (DMSO), formic acid (HCOOH) and methanol (MEOH), of HPLC grade (Sigma Aldrich). Deionised water was prepared by a Milli-Q Water purification system (Millipore, MA, USA).

Development of Chromatographic Conditions

A $5C_{18}$ AR-II (4.6 ID x 250 mm) column was used in this experiment. Mobile phase for the detection of the fifteen compounds was developed by varying solvents: acetonitrile (MeCN) and 0.2% formic acid (HCOOH) in H_2O in different ratios. The solvent system of MeCN (Solution A) and 0.2% HCOOH in H_2O (Solution B) [Gradient elution: 0 ~ 1.5 min (5% Solution A : 95% Solution B), 15 min ~ 26 min (5% ~ 95% Solution A : 95% ~ 5% Solution B), 26 min ~ 35 min (95% Solution A : 5% Solution B), 36 min ~ 52 min (100% Solution A) was settled upon based on the separation and retention time (resolution), height of the peak and the area produced. Detection wavelength for the samples was selected after analysing fingerprints produced using a UV-VIS detector at 210 and 254 nm. Flow rate and injection volume were set at 1.0 ml min^{-1} and 5 µl respectively. Column temperature was also kept at ambient temperature of 40 ˚C.

Preparation of Standard Solutions

The lyophilised fractions, the crude methanolic extract and the herbal product were each reconstituted in methanol/ DMSO to achieve a concentration of 10 mg/ml and then sonicated for 20 minutes. The isolated compounds were prepared in the same manner, at a stock solution of 1 mg/ml. They were then filtered through 0.45 µm PTFE membrane syringe filters (Thermo Fischer Scientific, USA) prior to injection. From the stock solutions, a 2.5 mg/ml solution was prepared for the crude methanolic extract, fractions and the herbal medicinal product. The injection volume of all test agents was 5 µl per cycle. Samples were then injected in triplicates.

ACKNOWLEDGEMENTS

The Lord is my light and my salvation, He leads me in the path of righteousness. He is my comfort and my strength. Bless the Lord oh my soul, bless His Holy name, may I never forget your goodness toward me, Amen.

This work was fully funded by the Ministry of Science, Culture, Technology and Sports (MEXT) Japan, which is gratefully acknowledged. I am grateful for the investment I have received in this training. I hope to work tirelessly to improve on humanity in my own little way, and with humility to promote Japanese culture and quality research everywhere I go.

My sincere gratitude goes to my supervisor, Professor Koji Yamada for his critique and guidance during this study. I wish him well in all his endeavours and pray for good health and sustained strength for the work ahead. I hope we can continue to work together to impact our field of study.

I appreciate the support of Professor Takashi Tanaka, Professor Masakazu Tanaka and Professor Jun Ishihara of the thesis committee for their time, and Associate Professor Yoshinori Saitou and Assistant Professor Yosuke Matsuo of the School of Pharmaceutical Sciences, Graduate School of Biomedical Sciences, Nagasaki University for their input during my training period.

I am grateful to the Centre for Plant Medicine Research (CPMR), Ghana, for providing the plant material for this study and grateful for the support of the staff of the Department of Biomedical Sciences, University of Cape Coast, Ghana.

I am thankful to members of the Laboratory in Medicinal Plants Garden and all my friends at Nagasaki University, who were present during my study period for their friendship and support.

My deepest appreciation goes to my family: the Thomfords and Amoh-Barimahs in Ghana and across the Globe, the Setoguchis of Nagasaki, the Kinji Babas of Kobe, and the International Christians Fellowship at Nagasaki Baptist Church, Japan. Your prayers, encouragement, emotional support and kind-heartedness toward me during this study has been indispensable.

Finally to my husband Kwesi: Thank you for cheering me on, for being patient and supporting my professional and academic commitments. Your unwavering confidence in me is God's lovely way of reaching out to me in time of great need. Only you know how much work has gone into this.

DEDICATION

This dissertation is dedicated to my parents Yaw Amoh and Ekua Aso, my siblings Ewuraekua, Paapa, Effie, Baaba and my dearest husband Paa Kwesi.

REFERENCES

1. Cragg M. A, Newman D. J. *Biochim. Biophys. Acta,* **1830**, 3670-3695 (2013).

2. World Health Organization (WHO) Fact sheet No:**134**, 2008). (http://www.who.int/mediacentre/factsheets/2003/fs134/en/

3. Gurib-Fakim A. *Mol. Aspects Med.,* **27,** 1-93 (2006).

4. WHO Traditional Medicine Strategy 2002-2005., *World Health Organisation,* EDM/TRM (2002).

5. Sandhya B., Thomas S., Isabel W., Shenbagarathai R. *Afr. J. Trad. CAM,* **3,** 101-114 (2006).

6. Mposhi A., Manyeruke C., Hamauswa S. *Int J Human & Soc. Sci.,* **3,** 236-246 (2013).

7. Thomford K. P, Mensah M. L. K. Dickson R. A., Sarfo B. S., Edoh D. A., Mills-Robertson F. C., Annan K. *J Herb Med,* **5,** 140-146 (2015).

8. Nichols R. L. *J Antimicrob Chemother,* **44,** 9-23 (1999).

9. Senekal M. *CME*, **28,** 54-57 (2010).

10. World Bank, Indigenous Knowledge, In Local Pathways to Global Development (2004) http://worldbank.org/afr/ik/default.htm

11. Mahomoodally, M. F. *Evid Based Complement Alternat Med,* **2013**, Article ID 617459, 14 pages, (2013).https://doi.org/10.1155/2013/617459.

12. Tan A. C., Konczak I. L G., Roufogalis B. D., Sekhon B., Sze-Daniel M.-Y. *J. Comp. Integ. Med.,* **12,** 245-249 (2015).

13. Farnsworth N. R., Akerele O., Bingel A. S., Soejarto D. D., Guo Z. *Bull. World Health Organ.* **63,** 965-981 (1985).

14. Fabricant D. S., Farnsworth N. R. *Environ Health Perspect.,* **109,** 69-75 (2001).

15. Atanasov A. G., Waltenberger B., Pferschy-Wenzig E-M., Linder T., Christoph W. *Biotechnol Adv.,* **33**, 1582-1614 (2015).

16. Yaseen G., Ahmad M., Sultana S., Alharrasi A. S., Hussain J., Zafar M., Ur-Rehman S. *J Ethnopharmacol,* **163,** 43-59 (2015).

17. Fauzi F. M., Koutsoukas A., Lowe R., Joshi K., Fan T. P., Glen R. C., Bender A. *J Ayur. Integ. Med.,* **4,** 117-119 (2013).

18. Donia M. S., Fricke F., Ravel J., Schmidt E.W. *PLoS ONE,* **6,** e17897 (2011). *doi:10.1371/journal.pone.0017897*

19. Conforti F., Ioele G., Statti G.A., Marrelli M., Ragno G., Menichini F. *Food Chem. Toxicol*. **46,** 3325-3332 (2008).

20. Moloney M. G. *Trends Pharm. Sci*., **37**, 1689-1701 (2016).

21. Bezerra R. J. S., Calheiros A. S., Ferreira N. C. S., Frutuoso V. D. S., Alves L. A. *Pharmaceuticals,* **6,** 650-658 (2013).

22. Das S., Sasmal D., Basu S. P. *Int. J. Pharm. Sci. Res.,* **6,** 51-55 (2010).

23. Mali R. G., Mehta A. A. *Nat. Prod. Rad.,* **7,** 466-475 (2008).

24. Zhu J., Huang X., Gao H., Bao Q., Zhao Y., Hu J.-F., Xia G. *J. Peptide Sci.*, **19,** 598-605 (2013).

25. Kinghorn A. D., Young-Won C., Swanson S. M. *Curr. Opin. Drug Discov. Devel.*, **12,** 189-196 (2009).

26. Khan R. A. *Saudi Pharm J,* (2018), https://doi.org/10.1016/j.jsps.2018.02.015.

27. Chin Y. W, Balunas M. J., Chai H. B., Kinghom A. D. *AAPS J,* **8**, 239-242 (2006).

28. Mathur S., Hoskins C. *Biomed Rep,* **6,** 612-614 (2017).

29. Butler M. S. *J Nat Prod*, **67,** 2141-2153 (2004).

30. Li J., Larregieu C. A., Benet L. Z. *Chin J Nat Med*, **14,** 888-897 (2016).

31. Miller L. H., Su X. *Cell*, **146**, 855-858 (2011).

32. Gerwick W.H. Plant sources of drugs and chemicals. In: *Encyclopedia of Biodiversity*. 2nd ed. Elsevier Inc., 129-139 (2013).

33. Vakil R. J. *Br. Heart J.*, **11**, 350-355 (1949).

34. Kufe D. W., Pollock R. E., Weichselbaum R. R., Bast R. C., Gansler T. S., Holland J. F. eds. *Holland-Frei Cancer Medicine.* 6th ed. Hamilton (ON): BC Decker; (2003). Available from: https://www.ncbi.nlm.nih.gov/books/NBK12354/

35. Malik A., Rasool R., Khan S. R., Waquar S., Iqbal J., *J Carcinog Mutagen,* **8,** 291 (2017).

36. Rowinsky E. K., Donehower R. C. *N Engl J Med.,* **332,** 1004-1014 (1995).

37. World Health Organization. 19th WHO model list of essential medicines. http://www.who.int/medicines/publications/essentialmedicines/EML20158-May-15.pdf. accessed 26 March 2017.

38. Himes R. H. *Pharmacol Ther.*, **51**, 257-267 (1991).

39. Moudi M., Go R., Yien C. Y. S., Nazre M. *Int J Prev Med.*, **4,** 1231-1235 (2013).

40. Anitha S. *JPRPC*, **4**, 27-34 (2016).

41. Kantarjian H. M., Talpaz M., Santini V., Murgo A., Cheson B., O'Brien S. M. *Cancer,* **92**, 1591-1605 (2001).

42. Grem J. L., Cheson B. D., King S. A., Leyland-Jones B., Suffness M. *J Natl Cancer Inst,* **80**, 1095-1103 (1988).

43. Fresno M., Jimenez A., Vazquez D. *Eur J Biochem*, **72**, 323-330 (1977).

44. Huang M. T. *Mol Pharmacol*, **11**, 511-519 (1975).

45. Lu S., Wang J. *J Hematol Oncol*, **7**, 2, (2014). 10.1186/1756-8722-7-2.

46. Discovery: Natural Compound Offers Hope - National Cancer Institute https://www.cancer.gov/research/progress/discovery/taxol. (accessed on January 15th, 2018).

47. Schiff P. B., Fant J., Horwitz S. B. *Nature,* **277**, 665-667 (1979).

48. Schiff P. B., Horwitz S. B. *Proc. Natl. Acad. Sci. U.S.A.,* **77,** 1561-1565 (1980).

49. Yardley D. A. *J Control Release*, **170**, 365-372 (2013).

50. Wall M., Wani M. *Ann N Y Acad Sci*, **803**, 1-12 (1996).

51. Bomgaars L, Berg S. L., Blaney S. M. *The Oncologist*, **6**, 506-516 (2001).

52. Jardine, I. Podophyllotoxins. In Anticancer Agents Based on Natural Products Models; Cassady, J. M., Douros, J. Eds.; Academic Press: New York, 319-351 (1980).

53. Issell B. F. *Cancer Chemother. Pharmacol.*, **7**, 73-80 (1982).

54. Xiao Z, Xiao Y-D., Feng J., Golbraikh A., Tropsha A., Lee K. H. *J. Med. Chem.,* **45**, 11, 2294-2309 (2002).

55. Calixto J. B., Otuki M. F., Santos A. R. S. *Planta Med*, **69**, 973-983 (2003).

56. Furst R., Zündorf I., *Mediators Inflamm.,* **146832**, 1-9 (2014).

57. Hong J., Sang S., Park H. J., Kwon S. J., Suh N., Huang M. T., Ho C. T., Yang C. S. *Carcinogenesis*. **25**, 1671-1679 (2004).

58. Kim G-Y, Kim K-H, Lee S.-H., Yoon M-S., Lee H-J., Moon D-O., Lee C-M., Ahn S-C., Park Y. C., Park, Y. M. *J Immunol.* **174**, 8116-8124, (2005).

59. Shah V.O., Ferguson J.E, Hunsaker L.A, Deck L.M, Jagt D. L. V. *Nat Prod Res,* **24**, 177-1188, (2010).

60. Kumar A., Dhawan S., Hardegen N. J., Aggarwal B. B. *Biochem Pharmacol*, **55**, 775-783, (1998).

61. de la Lastra C.A., Villegas I. *Mol Nut. & Food Res,* **49**, 405-430, (2005).

62. Kundu J.K., Shin Y.K., Surh Y-K. *Biochem Pharmacol*, **72**, 1506-1515, (2006).

63. Surh Y-J., Chun K-S, Cha H-H. *Mutation Res*, **480481**, 243-268, (2001).

64. Chung S., Yao H., Caito S., Hwang J-W., Arunachalam G., Rahman I. *Archives Biochem and Biophys,* **501**, 79-90, (2010).

65. Knutson M.D., Leeuwenburgh C. *Nutr Rev,* **66**, 591-596, (2008).

66. Nakata R., Takahashi S., Inoue H. *Bio & Pharm Bulletin*, **35**, 273-279, (2012).

67. Schmitt C.A, Dirsch V.M., *Nitric Oxide*, **21**, 77-91, (2009)

68. Caterina M. J., Schumacher M.A., Tominaga M., Rosen T.A., Levine J. D., Julius D. *Nature*, **389**, 816–824, (1997).

69. O'Neill J., Brock C., Olesen A. E., Andresen T., Nilsson M., Dickenson A. H., *Pharmacol Rev*, **64**, 939–971, (2012).

70. Haanpaa M., Treede R-D., *Eur Neurology*, **68**, 264–275, (2012).

71. Joe B., Rao U. J., Lokesh B. R. *Mol and Cellular Biochem*, **169**, 125–134, (1997).

72. Park J-S., Choi M-A., Kim B-S., Han I-S., Kurata T., Yu R. *Life Sciences*, **67**, 3087-3093, (2000).

73. Kim C-S., Kawada T., Kim B-S. *Cellular Signalling*, **15**, 299-306, (2003).

74. Singh B. N, Shankar S., Srivastava R.K. *Biochem Pharmacol,* **82**, 1807–1821, (2011).

75. Domingo D. S., Camouse M. M., Hsia A. H. *Int J. Clin Exp Path*, **3**, 705–709, (2010).

76. Riegsecker S., Wiczynski D., Kaplan M. J., Ahmed S. *Life Sciences*, **93**, 307–312, (2013).

77. Steinmann J., Buer J., Pietschmann T., Steinmann E. *Bri J Pharmacol*, **168**, 1059–1073, (2013).

78. Yang C. S., Wang H., Li G. X., Yang Z., Guan F., Jin H. *Pharmacol Res*, **64**, 113–122, (2011).

79. Chen L., Zhang H-Y., *Molecules*, **12**, 946–957 (2007).

80. Nam, N.-H. *Mini Rev Med Chem*. **6**, 945–951 (2006).

81. Khan N., Afaq F.,Saleem M., Ahmad N., Mukhtar H., *Cancer Res.* **66**, 2500–2505 (2006).

82. Yang H., K. Landis-Piwowar K., Chan T. H., Dou Q. P. *Curr Cancer Drug Targets.* **11**, 296–306 (2011).

83. Adachi, S., Nagao T., Ingolfsson H. I., Maxfield F. R., Andersen, O. S., Kopelovich L., Weinstein I. B. *Cancer Res.* **67,** 6493–6501 (2007).

84. Masuda, M., Wakasaki, T., Toh, S., Shimizu, M., Adachi, S. *J Oncol.* 540148. doi:10.1155/2011/540148 (2011).

85. Patra, S. K., Rizzi, F., Silva, A., Rugina, D. O., Bettuzzi, *S. J. Physiol. Pharmacol.***59**, 217– 235 (2008).

86. Kim H. P., Mani I., Iversen L., Ziboh V. A. *Prostaglandins Leukot Essent Fatty Acids.* **5**, 17-24 (1998).

87. Lee K. M., Hwang M. K., Lee D. E., Lee K. W., Lee H. J. *J Agric Food Chem.* **58**, 5815-20 (2012).

88. Geraets L., Moonen H. J., Brauers K., Wouters E. F., Bast A., Hageman G. J., *J Nutr*. **137**, 2190-2195 (2007).

89. Bureau G., Longpré F., Martinoli M. G. *J Neurosci Res*, **86**, 403-10, (2008).

90. Endale M., Park S. C., Kim S., Kim S. H., Yang Y., Cho J. Y., Rhee M. H. *Immunobiology*, **218**, 1452-67 (2013).

91. Anand David, A. V., Radhakrishnan A., Subramani P. *Pharmacognosy Reviews* **10**, 84–89 (2016).

92. Cynthia R.L., Hepatobiliary Cytoprotective Agents. Webster, in Canine and Feline Gastroenterology, (2013).

93. Imazio M., Brucato A., Cemin R. *The New England Journal of Medicine*, **369,** 1522–1528, (2013).

94. Imazio M., Bobbio M., Cecchi E. *Archives of Int Med.* **165**, 1987–1991, (2005).

95. Imazio M., Brucato A., Cemin R. *Annals of Int Med.* **155**, 409–414, (2011).

96. Deftereos S., Giannopoulos G., Kossyvakis C. *J Amer Col of Cardio*. **60**, 1790–1796, (2012).

97. Imazio M., Trinchero R., Brucato A. *Eur Heart J.* **31**, 2749–2754, (2012).

98. Jigam A. A., Abdulrazaq U. T., Mahmud H. A., Tijani F. O. *J Appl. Pharm. Sci.,* **2**, 47-51 (2012).

99. Gyamfi M. A., Aniya Y. *Hum Exp Toxicol.,* **17**, 418-423 (1998).

100. N'guessan J. D., Dinzedi M. R., Guessennd N., Coulibaly A., Dosso M., Djaman A. J., Guede-Guina, F. *Trop J Pharm Res.,* **6**, 779-83 (2007).

101. Ohiri F. C., Uzodinma V. C. *Fitoterapia,* **71,** 176-178 (2000).

102. Kouakou A. V., N'guessan J. D., Kra A. K. M., Guede-Guina F. *J Soc Ouest-Afr chim.,* **22**, 21-25 (2006).

103. N'guessan J. D., Bidie A. P., Lenta B. N., Weniger B., Andre P., Guede-Guina F. *Afr. J. Biotechnol.,* **6**, 1685-1689 (2007).

104. Ohtani I. I., Gotoh N., Tanaka J., Higa T., Gyamfi M. A., Aniya Y. *J. Nat. Prod.,* **63**, 676-679 (2000).

105. Chang C. C., Lien Y. C., Liu K. C. S. C., Lee S. S. *Phytochem.,* **63**, 825-833 (2003).

106. Gyamfi M. A., Aniya Y. *Toxicol.,* **164**, 171 (2001).

107. Zhang T-T., Yang L., Jiang J-G. *Food Funct.,* **6**, 2588-2597 (2015).

108. Gyamfi M. A., Ohtani I. I., Shinno E., Aniya Y. *Food Chem. Toxicol.,* **42**, 1401-1408 (2004).

109. Nyarko A. K., Addy M. E. *J Ethnopharmacol.,* **41**, 45-51 (1994).

110. Konan K. S., Toure A., Ouattara K., Djaman A. J., N'guessan J. D. *Afr. J. Microbiol. Res.*, **6**, 6247-6251 (2012).

111. Etkins N. L., *Trop. Doct.*, **27**, 12-16 (1997).

112. Gyamfi M. A., Yonamine M., Aniya Y. *Gen. Pharmacol.*, **32**, 661-667 (1999).

113. Gyamfi M. A., Tanaka T., Aniya Y. *Life Sc.*, **74**, 1723-1737 (2004).

114. Gyamfi M. A., Hokama N., Oppong-Boachie K., Aniya Y. *Human Exp Toxicol.*, **19**, 623-631 (2000).

115. Tanaka T., Nakashima T., Ueda K., Tomii K., Kouno I. *Chem. Pharm. Bull.*, **55**, 899-901 (2007).

116. Ng V. A. S., Agoo E. M. G., Shen C.C., Ragasa C. Y. *Int J Pharm Clin Res.*, **7**, 643-646 (2015).

117. Arora M., Kalia A.N. *Int J Pharm Pharm Sci.*, **5**, 245-249 (2013).

118. Sawan S.P., James T.L., Gruenke L.D., Craig J.C. *J. Magn. Reson.*, **35**, 409-413 (1979).

119. Ikuta A., Itokawa H. *Phytochem.*, **27**, 2813-2815 (1988).

120. Okuyama E., Suzumura K., Yamazaki M. Chem. Pharm. Bull., **43**, 2200-2204 (1995).

121. Ghogomu-Tih B., Bodo B., Nyasse B., Sondengam B.L. **45**, 464 (1985).

122. Banskota A.H., Usia T., Tezuka Y., Kouda K., Nguyen N.T., Kadota S.J. *J Nat Prod.*, **65**, 1700-1702 (2002).

123. da Silva L. A. L., Faqueti L. G., Reginatto F. H., dos Santos A. D. C., Barison A., Biavatti M. W. *Revista Brasileira de Farmacognosia*, **25**, 375-381 (2015).

124. Higuchi R., Inagaki M., Togawa K., Miyamoto K. T., Komori T. *Liebigs Ann. Chem.*, 635-658 (1994).

125. Higuchi R., Jhou J. X., Inukai K., Komori T. *Liebigs Ann. Chem.*, 745-752 (1991).

126. Yamada K., Matsubara R., Kaneko M., Miyamoto T., Higuchi R. *Chem. Pharm. Bull.*, **49**, 447-452 (2001).

127. Abdelhameed R., Elgawish M. S., Mira A., Ibrahim A.K., Ahmed S. A., Shimizu K., Yamada K. *RSC Adv.*, **6**, 20422-20430 (2016).

128. Shi C., Wu F., Zhu X., Xu J. *Biochim Biophysic Acta*, **1830**, 2538-2544 (2013).

129. Saeidnia S., Manayi A., Gohari A.R., Abdollahi M. *Eur. J. Med. Plants*, **4**, 590-609 (2014).

130. Moghaddam G. M., Faujan B. H. A., Alireza S-K. *Pharmacol. Pharm*., **3**, 119-123 (2012).

131. Pan J-Y., Chen S-L., Yang M-H., Wu J., Sinkkonen J., Zoud K. *Nat. Prod. Rep*., **26**, 1251-1292 (2009).

132. Heinonen S., Nurmi T., Liukkonen K., Poutanen K., Wahala K., Deyama T., Nishibe S., Adlercreutz H. *J. Agric. Food Chem*., **49**, 3178-3186 (2001).

133. Adlercreutz H., *Crit. Rev. Clin. Lab Sci*., **44**, 483-525 (2007).

134. Landete J. M., *Food Res Int.*, **46**, 410-424 (2012).

135. Lee S. E., Yang H., Son G. W., Park H. R., Park C-S., Jin Y-H., Park Y.S. *Int. J. Mol. Sci*. **16**, 14526-14539 (2015).

136. Yi-Zeng L., Peishan X., Kelvin, C. *J Chromatography B*, **812**, 53-70 (2004).

137. Songlin L., Quanbin H., Chunfeng Q., Jingzheng S., Chuen L., Cheng X. and Hongxi X. *Chin Med*, **3**, 7-23 (2008).

138. Drake S. L., DePaola A., Jaykus L-A. *Compr Rev Food Sci Food Saf*, **6**, 120-144 (2007).

139. CLSI, Performance Standards for Antimicrobial Disk Susceptibility Tests, Approved Standard, 7th ed., CLSI document M02-A11. Clinical and Laboratory Standards Institute, 950 West Valley Road, Suite 2500, Wayne, Pennsylvania 19087, USA, (2012).